João Filipe da Costa Martins

MODULATION OF RETINAL GANGLION CELL FUNCTION AND IMPLICATIONS FOR NEUROPROTECTION

Doctoral Thesis in Health Sciences (Biomedical Sciences), supervised by Doctor António Francisco Ambrósio, and Doctor Miguel de Sá e Sousa Castelo-Branco, and presented to the Faculty of Medicine of the University of Coimbra.

2014

· U C ·

UNIVERSIDADE DE COIMBRA

Cover:

Neuropeptide Y (red) in the rat retina. Cell nuclei in grey.

João Filipe da Costa Martins

MODULATION OF RETINAL GANGLION CELL FUNCTION AND
IMPLICATIONS FOR NEUROPROTECTION

MODULAÇÃO DA FUNÇÃO DAS CÉLULAS GANGLIONARES DA
RETINA E IMPLICAÇÕES PARA A NEUROPROTEÇÃO

2014

· U C ·

UNIVERSIDADE DE COIMBRA

Publications

The results presented in this study have been submitted for publication in international peer-reviewed journals.

Martins J, Elvas F, Brudzewsky D, Martins T, Kolomiets B, Tralhão P, Cavadas C, Castelo-Branco M, Woldbye D, Picaud, S, Santiago AR, and Ambrósio AF. (2014) Neuropeptide Y receptors are present and functional active in the rat retina, modulate retinal ganglion cell $[Ca^{2+}]_i$ and spiking activity, and exert neuroprotective actions *in vitro*. Submitted to *The Journal of Neuroscience*.

Martins J, Kolomiets B, Caplette R, Sahel JA, Castelo-Branco M, Ambrósio AF, and Picaud S. (2014) Sildenafil acutely decreases light responses in retinal ganglion cells. Submitted to *Neurobiology of Disease*.

Acknowledgements / Agradecimentos

Aos meus pais e minha irmã, pelo apoio e dedicação sem o qual eu não poderia ter realizado este trabalho. À Luísa e à Letícia pela ajuda em Paris. Aos meus avós, em especial ao meu avô Laudemiro pelo exemplo de trabalho e dedicação.

A todos os meus amigos, em especial aos colegas da "Banda Khaos", pela persistência na manutenção do grupo durante a minha ausência. Aos meus amigos também na Casa de Portugal em Paris, pelo apoio e boa disposição.

Em especial à Rita pela paciência, ajuda e incentivo quando me faltou a motivação, principalmente na fase final deste trabalho. Por tudo.

João Martins

CONTENTS

Abbreviations

AC, adenylate cyclase

AF, Alexa Fluor

Akt, protein kinase B

AM, acetoxymethyl

AMPA, α-amino-3-hydroxy-5-methyl-4-isoxazolepropionic acid

ANOVA, analysis of variance

ATCC, american type culture collection

ATP, adenosine 5'-triphosphate

bp, base pairs

BRB, blood-retinal barrier

BSA, bovine serum albumin

$[Ca^{2+}]_i$, intracellular free calcium concentration

CA3, *cornu ammonis* area 3

cAMP, cyclic adenosine monophosphate

cDNA, complementary deoxyribonucleic acid

cGMP, cyclic guanosine monophosphate

CGR, células ganglionares da retina

Ci, Curie

CNG channel, cyclic nucleotide gated channel

CNS, central nervous system

CPON, C-terminal peptide of neuropeptide Y

DAPI, 4',6-diamidino-2-phenylindole dihydrochloride

DARPP, dopamine and cyclic adenosine monophosphate-regulated phosphoprotein

dATP, 2'-deoxyadenosine, 5'-triphosphate

DIV, days in vitro

DMEM, Dulbecco's modified medium

DNA, deoxyribonucleic acid

DNase, deoxyribonuclease

DPBS, Dulbecco's phosphate buffered saline

DPCPX, 1,3-dipropyl-8-cyclopentylxanthine

DPPIV, dipeptidyl peptidase IV

dUTP, 2'-deoxyuridine, 5'-triphosphate

EBSS, Earle's balanced salt solution

EDTA, ethylenediaminetetraacetic acid

EGTA, ethylene glycol-bis(2-aminoethylether)-*N,N,N',N'*-tetraacetic acid

ERG, electroretinogram

ERK1/2, extracellular-signal-regulated kinase 1 and 2

FRET, fluorescence resonance energy transfer

GABA, γ-aminobutyric acid

GC, guanylate cyclase

GCAP, guanylate cyclase-activating protein

GCL, ganglion cell layer

GDP, guanosine 5'-diphosphate

GFAP, glial fibrillary acidic protein

GIRK channels, G-protein-coupled inwardly-rectifying potassium channels

$(Gly^1, …Aib^{32})$-PP, $(Gly^1, Ser^{3,22}, Gln^{4,34}, Thr^6, Arg^{19}, Tyr^{21}, Ala^{23,31}, Aib^{32})$-pancreatic polypeptide

5'-GMP, guanosine 5'-monophosphate

GPCR, G protein-coupled receptor

GTP, guanosine 5'-triphosphate

GTPγS, guanosine 5'-[γ-thio]triphosphate

HBSS, Hank's balanced salt solution

HEPES, (4-(2-hydroxyethyl)-1-piperazineethanesulfonic acid)

icv, intracerebroventricular

INL, inner nuclear layer

IOP, intraocular pressure

ip, intraperitoneal

IPL, inner plexiform layer

ipRGCs, intrinsically photosensitive retinal ganglion cells

ir, immunoreactivity

I-R, ischemia reperfusion

L-cones, long wavelength sensitive cones

LED, light-emitting diodes

2

M-cones, middle wavelength sensitive cones

MAPKs, mitogen-activated protein kinases

MDMA, 3,4-methylenedioxy-*N*-methylamphetamine

MEA, multi-electrode array

mGluR6, metabotropic glutamate receptor 6

mRNA, messenger ribonucleic acid

NCKX, sodium/calcium, potassium (Na^+/Ca^{2+}, K^+) exchanger

NFL, nerve fibre layer

NMDA, *N*-Methyl-D-aspartic acid

NMR, nuclear magnetic resonance

NO, nitric oxide

NPY, neuropeptide Y

NSB, non-specific binding

nt, nucleotides

ONL, outer nuclear layer

OPL, outer plexiform layer

P3-4, Post-natal day 3 or 4

PBS, phosphate buffered saline

PDE, phosphodiesterase

PET, positron emission tomography

PFA, paraformaldehyde

PKG, protein kinase G

PI, propidium iodide

PLC, phospholipase C

PP, pancreatic polypeptide

PSTH, peri-stimulus time histogram

PYY, peptide YY

R*, metarhodopsin II

RGC, retinal ganglion cell

RNA, ribonucleic acid

RPE, retinal pigmented epithelium

RT, room temperature

RT-PCR, reverse-transcription polymerase chain reaction

S-cones, short wavelength sensitive cones

SCN, suprachiasmatic nucleus

SD, standard deviation

SEM, standard error of the mean

SVZ, subventricular zone

TdT, terminal deoxynucleotidyl transferase

TUNEL, TdT-mediated dUTP nick-end labelling

UTR, untranslated region

VDCC, voltage-dependent calcium channel

Abstract

Neuropeptide Y (NPY) is a neuromodulator in central nervous system (CNS) that can exert neuroprotective effects. NPY is expressed in mammalian retina but the location and potential modulatory effects of NPY receptor activation remains largely unknown. Retinal ganglion cell (RGC) death is a hallmark of several retinal degenerative diseases, particularly glaucoma. In purified RGCs, we detected immunoreactivity and mRNA for NPY and NPY receptors in these cells. Using cultured purified RGCs and *ex vivo* retinal preparations we have evaluated the effect of NPY receptor activation on changes in RGC intracellular free calcium concentration – $[Ca^{2+}]_i$ and RGC spiking activity. RGC spike recordings were performed by a multi-electrode array (MEA). We found that NPY application attenuated the increase in the $[Ca^{2+}]_i$ triggered by glutamate in purified RGCs, possibly via Y_1 receptor activation. Moreover, Y_1/Y_5 receptor activation increased the initial burst response of OFF-type RGCs, though no effect was observed in the RGC spontaneous spiking activity. The Y_1 receptor activation was able to modulate directly RGC responses by attenuating the *N*-Methyl-D-aspartic acid (NMDA)-induced increase in RGC spiking activity. These results suggest that Y_1 receptor activation at the level of inner or outer plexiform layers leads to modulation of RGC receptive field properties. Using *in vitro* culture of retinal explants exposed to NMDA, we found that NPY pre-treatment prevented NMDA-induced cell death through activation of Y_1 and Y_5 receptors. In an animal model of retinal ischemia-reperfusion (I-R) injury, pre-treatment with NPY was not able to prevent cell death or rescue RGCs. In summary, we found clear modulatory effects of NPY at the level of RGCs, and Y_1 receptor appears to have a predominant role. However, further studies are needed to evaluate whether NPY neuroprotective action translates to *in vivo* models of retinal degenerative diseases.

Sildenafil (Viagra™), a cyclic guanosine monophosphate (cGMP)-specific phosphodiesterase type 5 inhibitor, is widely used for the treatment of erectile dysfunction and pulmonary arterial hypertension. Clinical studies reported transient visual impairments in patients after a single dose sildenafil ingestion, suggesting the implication of RGCs, since these cells convey visual information to the brain centres of visual processing. However, the effect of sildenafil on the RGC light responses is not fully understood. Using a MEA technique, in the second part of this study, we evaluated the effect of sildenafil on RGC light responses in *ex vivo* retinas. Under continuous perfusion, sildenafil citrate (0.3 to 30 µM) was applied to

Abstract

retinal preparations during 10 to 60 min followed by sildenafil washout. High concentration (30 µM) of sildenafil reversibly decreased the magnitudes of both ON- and OFF-type RGC light responses, and in 50% of RGCs, light responses were completely supressed. Sildenafil also greatly increased the latency of ON- and OFF-types of light responses. We provide the evidence that extended exposure to sildenafil and repeated light stimulation potentiates drug effects and delays recovery.

In conclusion, we show that MEA recordings in *ex vivo* retinas might be a valuable method to understand how RGC circuitry can be affected by different drug treatments. This understanding is relevant to the development of neuroprotective strategies needed for retinal degenerative diseases, namely glaucoma, where no available treatment can effectively stop the progression of RGC death.

Resumo

O neuropeptídeo Y (NPY) é um neuromodulador no sistema nervoso central, capaz de exercer efeitos neuroprotetores. O NPY é expresso na retina de mamíferos mas a sua localização, e dos seus recetores, e o seu potencial efeito neuromodulador na retina continua pouco estudado. A morte das células ganglionares da retina (CGR) é uma das principais caraterísticas de doenças degenerativas da retina, particularmente do glaucoma. Neste trabalho, verficámos a presença de mRNA e immunoreatividade para o NPY e os recetores do NPY em preparações purificadas de CGR. Também avaliámos o efeito da ativação de recetores do NPY nos níveis intracelulares de cálcio livre – $[Ca^{2+}]_i$, e na formação de potenciais de ação, utilizando culturas purificadas de CGR e em preparações de retina *ex vivo*. Os potenciais de ação gerados pelas CGR foram registados com uma matriz de elétrodos. A aplicação de NPY atenuou o aumento da $[Ca^{2+}]_i$ induzido por glutamato via ativação do recetor Y_1. Além disso, a ativação dos recetores Y_1/Y_5 induziu um aumento da resposta inicial das CGR tipo-OFF após estimulação luminosa, embora não tenha alterado a atividade espontânea das CGR. A ativação dos recetores Y_1 inibiu o aumento da formação de potenciais de ação pelas CGR após estimulação com *N*-metil-D-aspartato (NMDA). Estes resultados sugerem que a ativação dos recetores Y_1, ao nível da camada plexiforme interna ou da camada plexiforme externa da retina modula as propriedades do campo recetivo das CGR. Ao expor explantes de retina *in vitro* a NMDA verificámos que o pré-tratamento com NPY foi capaz de prevenir a morte celular induzida pelo NMDA através da ativação dos recetores Y_1 e Y_5. Num modelo animal de isquémia-reperfusão, o pré-tratamento com NPY não preveniu a morte das CGR. Em resumo, identificámos efeitos modulatórios do NPY ao nível das CGR, em que a ativação dos recetores Y_1 parece ter um papel central. Contudo, são necessários mais estudos com a finalidade de avaliar o potencial neuroprotetor do NPY *in vivo* em modelos de doenças degenerativas da retina.

O sildenafil (Viagra™) é um inibidor da fosfodiesterase tipo 5, amplamente usado no tratamento da disfunção erétil e na hipertensão arterial pulmonar. Alguns estudos clínicos reportaram deficiências visuais temporárias em doentes que utilizavam sildenafil, o que sugere o possível envolvimento das CGR, uma vez que são estas células que transmitem a informação visual para centros cerebrais responsáveis pelo processamento da visão. Contudo, o efeito do sildenafil nas respostas das CGR a estímulos luminosos está pouco esclarecido. Na

segunda parte deste estudo, utilizámos uma matriz de elétrodos para avaliar o efeito do sildenafil nas respostas das CGR à luz em retinas *ex vivo*. Com perfusão constante, aplicámos concentrações crescentes de sildenafil (0,3 – 30 µM) durante períodos de 10 ou 60 minutos, seguidos de solução de lavagem. Uma concentração elevada de sildenafil (30 µM), provocou um decréscimo reversível na magnitude das respostas das CGR à luz, do tipo ON ou OFF das CGR, sendo que em 50% das CGR as respostas à luz foram completamente inibidas, embora reversivelmente. Além disso, o sildenafil provocou um aumento das latências das respostas do tipo ON e OFF. Também verificámos que a exposição prolongada a sildenafil, simultaneamente com estimulação luminosa, potencia os efeitos do fármaco e dificulta a recuperação das respostas das CGR à luz.

Assim, concluímos que o registo da atividade das CGR com uma matriz de elétrodos em retinas *ex vivo* é um método eficiente para estudar o modo como as CGR poderão ser afetadas por diferentes fármacos. Esta avaliação é importante para o desenvolvimento de estratégias neuroprotetoras necessárias para o tratamento de doenças degenerativas da retina, nomeadamente o glaucoma, para o qual não existe um tratamento eficaz, capaz de impedir a morte das CGR.

CHAPTER 1

General Introduction

1.1 – The retina

1.1.1 – Anatomy of the retina

The retina is a thin tissue composed of a highly organized neuronal network inside of the eyeball (Fig. 1.1 A). It is part of the CNS and is responsible for transforming outside world natural scenes into meaningful information to the brain. The retina is basically formed by three main layers of neurons (Fig. 1.1 B), which cell somas are packed into three nuclear layers: outer nuclear layer (ONL), inner nuclear layer (INL), and ganglion cell layer (GCL). These retinal neurons communicate through chemical and electrical synapses forming two tightly organized plexiform layers: outer plexiform layer (OPL) and inner plexiform layer (IPL). The ONL is composed of cell somas of photoreceptors: rods and cones. The rods operate mainly in dim light conditions and cones in daylight, being responsible for coloured and fine resolution vision. The INL is composed of cell somas of bipolar cells, horizontal cells, and amacrine cells. The GCL comprise the cell somas of displaced amacrine cells and retinal ganglion cells (RGCs) whose axons compose the nerve fibre layer (NFL), leaving the eyeball and forming the optic nerve that conveys the information from the retina to the brain visual centres. Within the OPL the photoreceptor terminals synapse with bipolar cell and horizontal cell dendrites. The IPL is a complex layer of synaptic connections, organized in five strata. In this layer, different sub-types of bipolar cells, amacrine cells, and RGCs form synapses in specific strata. This complex plexiform layer is responsible for the final tuning of output visual information which is coded in the form of action potential patterns (spiking activity) by RGCs. In addition to neurons, other cell types compose and support the retina. An epithelial cell layer in the outermost part, the retinal pigmented epithelium (RPE), is responsible for recycling outer segments of photoreceptors, among other important functions such as absorbing excessive light and transporting nutrients and ions from choriocappilaries. Retinal glial cells, namely microglia, astrocytes, and Müller cells (Fig. 1.1 C) exert an important role in supporting and regulating retinal physiology.

The photoreceptors are supplied by the choroidal blood vessels while inner retina is nourished by the retinal artery, which then branches into three capillary networks throughout the retina. An important feature of retinal vascular network is the presence of tight junctions

between endothelial cells of the retinal capillaries. In addition, epithelial cells of RPE also exhibit tight junctions. Therefore, the RPE and retinal capillaries form a blood-retinal barrier (BRB) that tightly regulates the transport of molecules into the retina. The RPE forms the outer BRB, while retinal capillaries form the inner BRB. The BRB is an important player in the retinal defence mechanisms against circulating toxins (Siu et al., 2008).
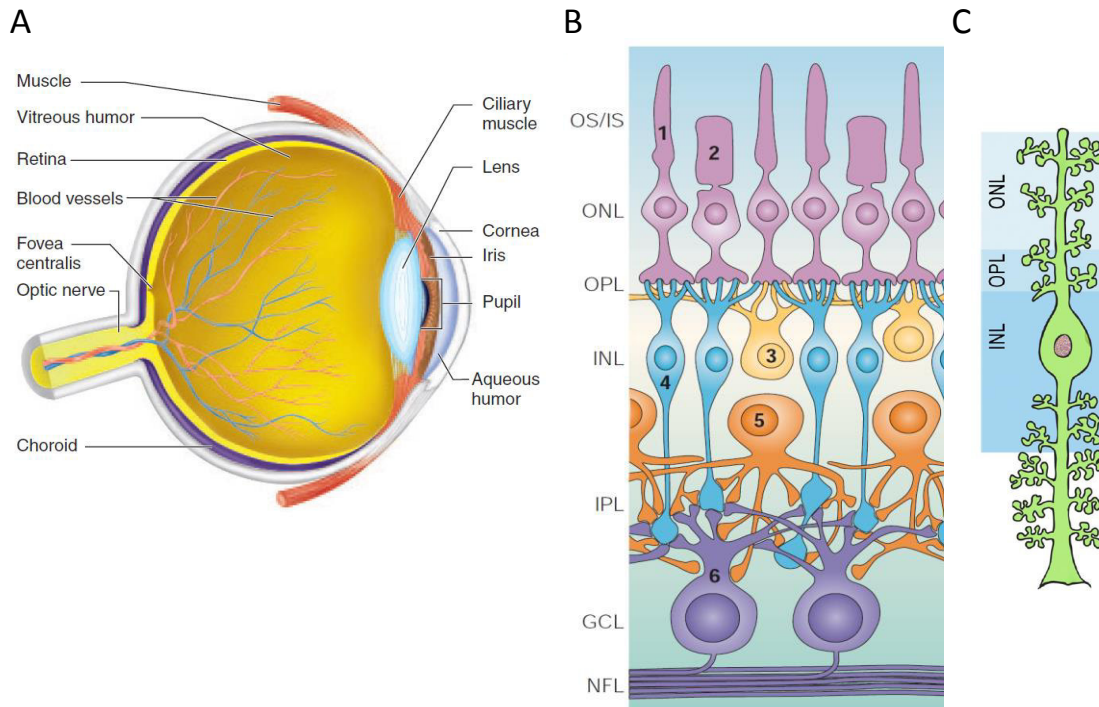
Figure 1.1. Anatomy of the retina. (A) The retina is a thin tissue inside the eyeball (Widmaier et al., 2004). (B) There are six types of neurons in the mammalian retina: 1 – rods, 2 – cones, 3 – horizontal cells, 4 – bipolar cells, 5 – amacrine cells, 6 – retinal ganglion cells (RGCs). OS/IS, outer and inner segments of rods and cones; ONL, outer nuclear layer; OPL, outer plexiform layer; INL, inner nuclear layer; IPL, inner plexiform layer; GCL, ganglion cell layer; NFL, nerve fibre layer. Adapted from Wassle (2004). Müller glial cells (C) extend throughout the retinal thickness Adapted from Ahmad et al. (2011).

1.1.2 – Phototransduction

Phototransduction is the process by which photoreceptors convert photons absorbed by photopigments into synaptic response at photoreceptor terminals (Fig. 1.2). The presence of photopigments in photoreceptor outer segments allows these cells responding to light. Photopigments consists of an opsin isoform and a covalently attached chromophore derived from vitamin A (11-*cis* retinal).
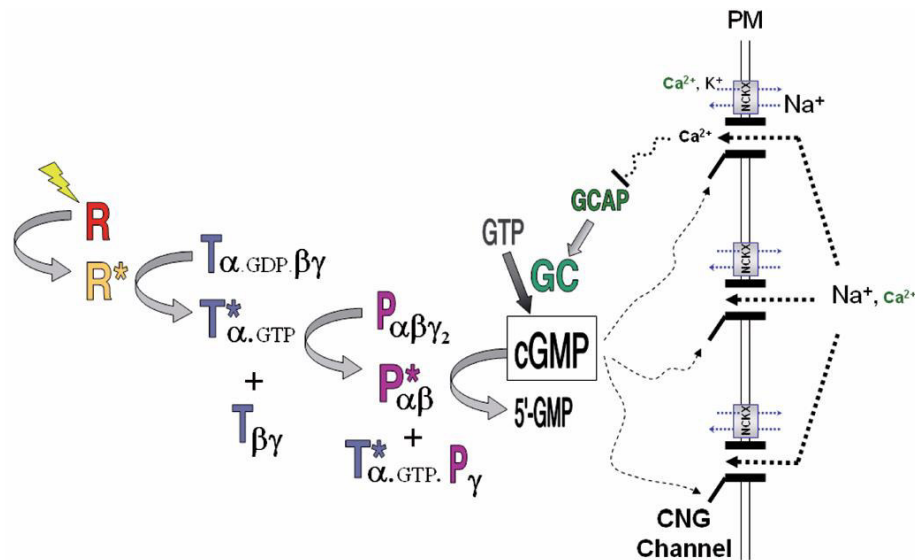
Figure 1.2. Phototransduction cascade. After rhodopsin (R) activation by light, the subsequent transducin (T) and phosphodiesterase (P) activation triggers cGMP hydrolysis. The drop in cGMP leads to the closure of cyclic nucleotide-gated (CNG) channels which results in membrane hyperpolarization. Then, the activation of guanylate cyclase-activating protein (GCAP) and guanylate cyclase (GC) restores the cGMP levels and membrane depolarizes. NCKX, Na^+/Ca^{2+}, K^+ exchanger; PM, plasma membrane (Chen, 2005).

In the dark, the photoreceptor cell membrane is depolarized and the neurotransmitter glutamate is being released. The first step of phototransduction occurs when light isomerizes the 11-*cis* bond of the retinal to the all-*trans* configuration. This isomerization triggers a conformational change in rhodopsin (R) which becomes active in a conformation state called metarhodopsin II (R*). R* catalyses the exchange of guanosine 5'-triphosphate (GTP) for guanosine 5'-diphosphate (GDP) on the α-subunit of the heteromeric G protein transducin ($T_{\alpha GDP\beta\gamma}$). Activated transducin α-subunit ($T^*_{\alpha GTP}$) dissociates from transducin $\beta\gamma$-subunits ($T_{\beta\gamma}$) and binds to the inhibitory γ-subunit of the tetrameric phosphodiesterase - PDE - ($P_{\alpha\beta\gamma2}$). The uninhibited catalytic subunit of PDE ($P^*_{\alpha\beta}$) hydrolyzes cGMP into guanosine 5'-monophosphate (5'-GMP). The drop of intracellular cGMP concentration closes the cyclic

nucleotide-gated (CNG) channel located at the plasma membrane, blocking the entry of Na^+ and Ca^{2+}, which results in membrane hyperpolarization and glutamate release decrease. Since the Na^+/Ca^{2+}, K^+ exchanger (NCKX) at the cell membrane is not light sensitive and Ca^{2+} extrusion continues while Ca^{2+} entry through the CNG channel is blocked, the phototransduction leads to a decline in intracellular Ca^{2+} concentration $[Ca^{2+}]_i$. The drop in $[Ca^{2+}]_i$ leads to the interaction between guanylate cyclase-activating protein (GCAP) and guanylate cyclase (GC) resulting in GC activation. This restores the levels of cGMP, so CNG channels open and the membrane depolarization is restored (Chen, 2005).

1.1.3 – Retinal circuitry and transmission of visual signals

A simple representation of signal flow in the retina is the division in the vertical pathway (photoreceptor – bipolar cell – RGC), using the excitatory neurotransmitter glutamate, and in the lateral pathway, associated with horizontal cell and amacrine cell activity, which provide lateral inhibition using mainly γ-aminobutyric acid (GABA). However, multiple pathways operate simultaneously extending the understanding of the retinal circuitry, and will be detailed below.

Rod photoreceptors contain only one type of photopigment - rhodopsin - most sensitive to wavelengths around 505 nm. In cone photoreceptors, different photopigments (photopsins) are found, based on their spectral sensitivity (Fig. 1.3 A). The type of pigment gives the name to the cone photoreceptor. Most mammals contain two types of cones, namely middle wavelength sensitive (green, M-cones) and short wavelength sensitive (blue, S-cones). In addition to M- and S-cones, primates also contain long wavelength sensitive cones (red, L-cones). The processing of visual information in the retina starts at the OPL where photoreceptors synapse with bipolar cells and horizontal cells through special synapses called pedicles for cones and spherules for rods. Is at this level that the two major functional visual pathways, ON and OFF, are generated and run in parallel towards brain visual centres. This dichotomy, ON and OFF, is based on two different types of bipolar cells.

OFF-type bipolar cells that respond to light with the same polarity as the photoreceptor, i.e. bipolar cells are depolarized in the dark and hyperpolarize upon light stimulation. This connection is named sign conserving synapse. In contrast, ON-type bipolar cells respond to light with an inverted polarity, i.e. bipolar cells are hyperpolarized in the dark

and depolarized upon light stimulation – sign inverting synapses. The presence of different glutamate receptors at bipolar dendritic terminals determines the type of bipolar cell. In the OFF-type bipolar cells the glutamate released by photoreceptors in the dark activates excitatory ionotropic glutamate receptors (α-amino-3-hydroxy-5-methyl-4-isoxazolepropionic acid (AMPA)-Kainate type), resulting in membrane depolarization.

In contrast, in the ON-type bipolar cells, the glutamate released by photoreceptors in the dark activates inhibitory metabotropic glutamate receptor 6 (mGluR6), which results in membrane hyperpolarization (Nakajima et al., 1993). Since each bipolar cell contact many photoreceptors, the relative amount and location of ON- and OFF- connections determine the centre-surround organization of the receptive field and, thus, define the respective cell type: ON-centre or OFF-centre bipolar cell. The ON and OFF dichotomy and the centre-surround organization of the receptive fields are maintained at IPL resulting in ON-centre and OFF-centre RGC types.
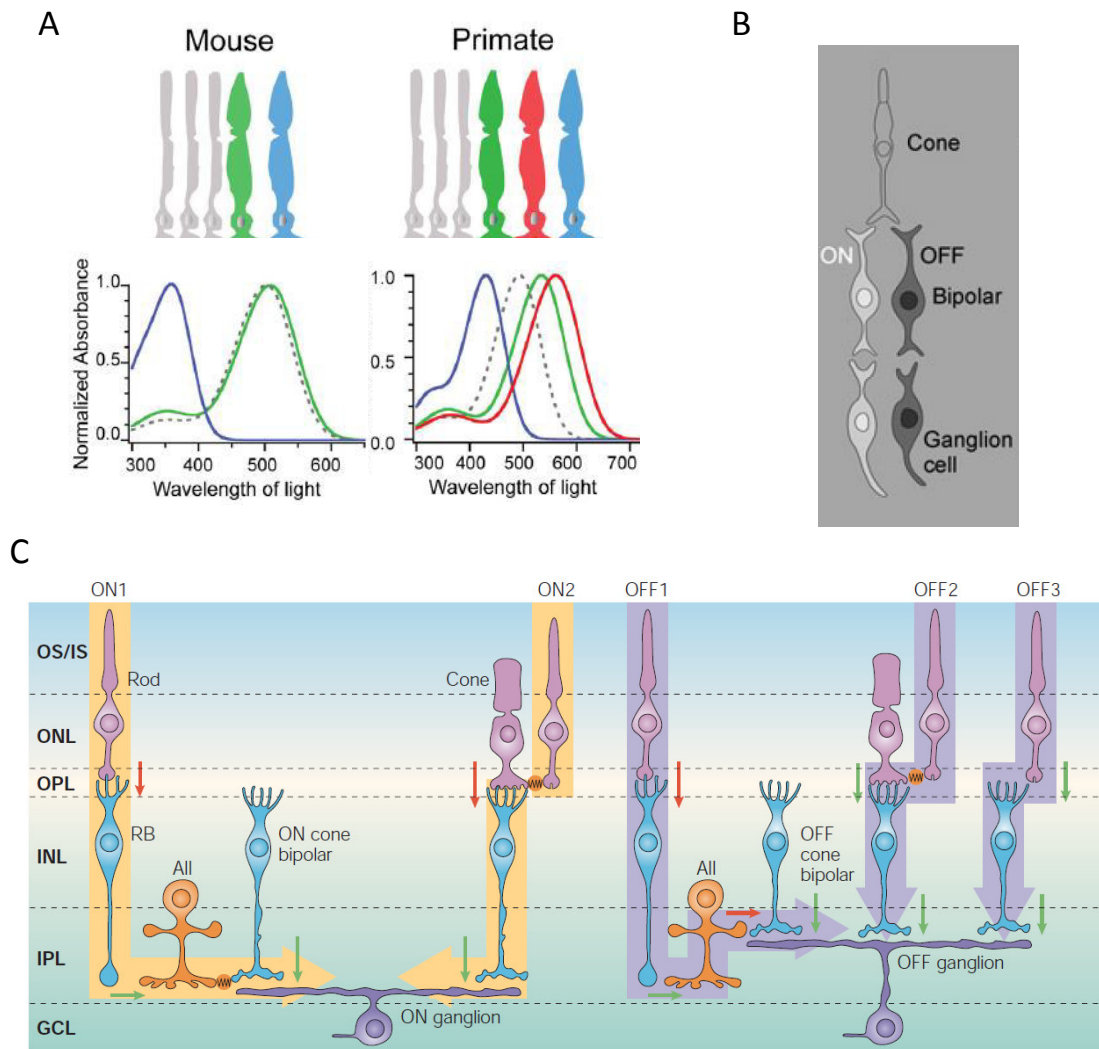
Figure 1.3. Cone and rod pathways. (A) Cone photoreceptor types are determined by their photopigment spectral sensitivities. The absorption spectrum is shown for each photopigment. Adapted from Hoon et al. (2014). Dashed trace represents rhodopsin. In addition to M-cones (middle wavelength, green) and S-cones (short wavelength, blue), primates also contain L-cones (long wavelength, red). (B) Two major cone pathways, ON and OFF, run in parallel to RGCs. Adapted from Balasubramanian and Sterling (2009). OFF bipolar cells make sign conserving contacts with cone photoreceptors whereas ON bipolar cells make sign inverting contacts with cone photoreceptors. Then, both bipolar cell types synapse with ON or OFF RGCs. (C) Rod photoreceptor signals reach ON and OFF channels at RGC level through multiple pathways. Adapted from Wassle (2004). ON1 and OFF1 represent classical pathways. Rods make sign inverting synapses (red arrows) with invaginating dendrites of rod bipolar cells (RB), which then contact AII amacrine cells through sign conserving synapses (green arrows). AII amacrine cells access simultaneously ON and OFF channels. They make gap junctions (electrical synapses) with ON cone bipolar cells, which in turn synapse with ON RGCs (ON1), and at the same time they make inverting synapses with the axons of OFF cone bipolar cells, which in turn synapse with OFF RGCs (OFF1). In the ON2 and OFF2 pathways, the rod signals are transmitted to cones through gap junctions and then follow cone pathways to either ON or OFF RGCs, respectively. In the OFF3 pathway, OFF cone bipolar cells make direct synaptic contacts with the base of rod spherules and transfer this signal directly onto OFF RGCs.

The way photoreceptor signals access RGCs involves various pathways. Cone photoreceptors connect ON and OFF cone bipolar cells which in turn contact RGCs (Fig 1.3 B), whereas rod photoreceptors contact mainly ON rod bipolar cells that do not contact directly RGCs but instead use a particular type of amacrine cell – AII amacrine cell – which in turn contact ON and OFF cone bipolar cells and thus access RGCs (Fig. 1.3 C).

However, in the last decades, alternative pathways have been identified (Fig. 1.3 C) broadening the knowledge of retinal complex circuitry (Wassle, 2004). Of special interest are the electrical synapses various retinal neurons are able to establish through gap junctions. The rod and cone photoreceptors contact via gap junctions allowing rod signals to access cone pathways (DeVries and Baylor, 1995). In addition, some OFF-cone bipolar cells make direct synaptic contacts with the base of rod spherules transferring this signal directly onto OFF RGCs (Soucy et al., 1998; Hack et al., 1999).

Taking into account the neuronal diversity found in the mammalian retina (Fig. 1.4), one may anticipate the complexity of this neural structure in terms of anatomical arrangement and physiological interactions. In fact, more than different 50 neuronal types have been identified by structural criteria and many remain to be assigned to a specific visual function (Masland, 2001). In the circuitry depicted in Figure 1.3 C, it is clear that the processing of visual information in the retina involves mainly two stages, one at the OPL and the other at the IPL. At the OPL, horizontal cells make sign conserving synaptic contacts with photoreceptors, thus maintaining a relatively depolarized potential in the dark and then hyperpolarizing upon light. Horizontal cells mainly release GABA providing a negative feedback signal to photoreceptors. They play an important role in the generation of receptive field surrounds in bipolar cells (Dacey, 1999) adding an opponent signal that is spatially constrictive. Moreover, horizontal cell activity is regulated by signals from the IPL, which are transmitted via various molecules such as dopamine, nitric oxide, and retinoic acid. These signals contribute to the regulation of horizontal cells under different light conditions (Twig et al., 2003).
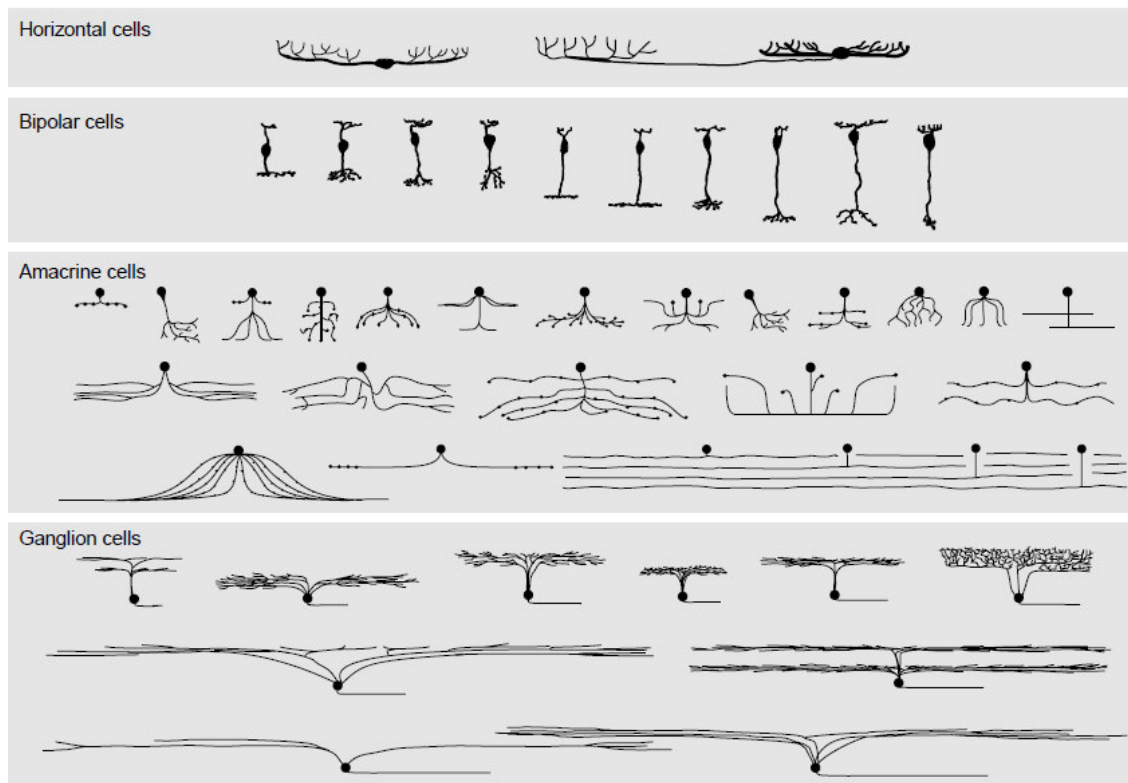
Figure 1.4. Neuronal diversity of mammalian retina. Based on receptive field size and dendritic stratification various neuronal classes are identified. The retina is composed of wide-field cells and narrow-field cells, though wide-field are less numerous. The numbers of cells are distributed uniformly among the different classes. Note that amacrine cells and RGC dendritic terminals exhibit various stratification modalities in IPL, e.g. monostratified and bistratified (Masland, 2001).

At the second stage of image processing at the IPL, bipolar cell terminals, RGC dendrites, and amacrine cells establish contacts. At the RGC level, visual information is computed in the form of spike trains, and, as abovementioned, two basic channels, ON and OFF, form the major retina output to the brain. ON-centre RGCs are maximally activated when a spot of light is presented to the centre of their receptive field, and they are maximally inhibited when light stimulation is presented on the receptive field periphery. OFF-centre RGCs respond to light stimulation in an opposite way. Because the contacts between bipolar cell and RGCs are sign conserving, the ON- and OFF-response origin is essentially determined by the bipolar cell types contacting with each individual RGC (Westheimer, 2007). Amacrine cells convey additional information to IPL circuitry. Several neurotransmitter molecules are used by amacrine cells, such as GABA, glycine, acetylcholine, dopamine, and serotonin (Kolb, 1995). Using specific markers for each neurotransmitter-containing amacrine cell, it is possible to identify specific strata on IPL, since their dendrites ramify in narrow bands (Haverkamp and Wassle, 2000). Within these different strata, specific aspects of light signals are processed,

where amacrine cells play a predominant role (Wassle, 2004). In fact, to extract meaningful features from natural scenes by the brain, part of the necessary neuronal computation of visual information is performed by the retina. As above mentioned, different retinal neurons are involved in this process, though the output signal is carried out only by RGC spiking activity. In Figure 1.5 are exemplified various specific visual tasks performed by retinal circuitry, such as detection of dim light flashes, sensitivity to texture motion, detection of differential motion and approaching motion, the rapid encoding of spatial structures, and the ability to switch circuits (Gollisch and Meister, 2010). These tasks might be understood as answers to particular challenges shared by many animals, such as the need to detect dim lights and the need to detect moving objects.
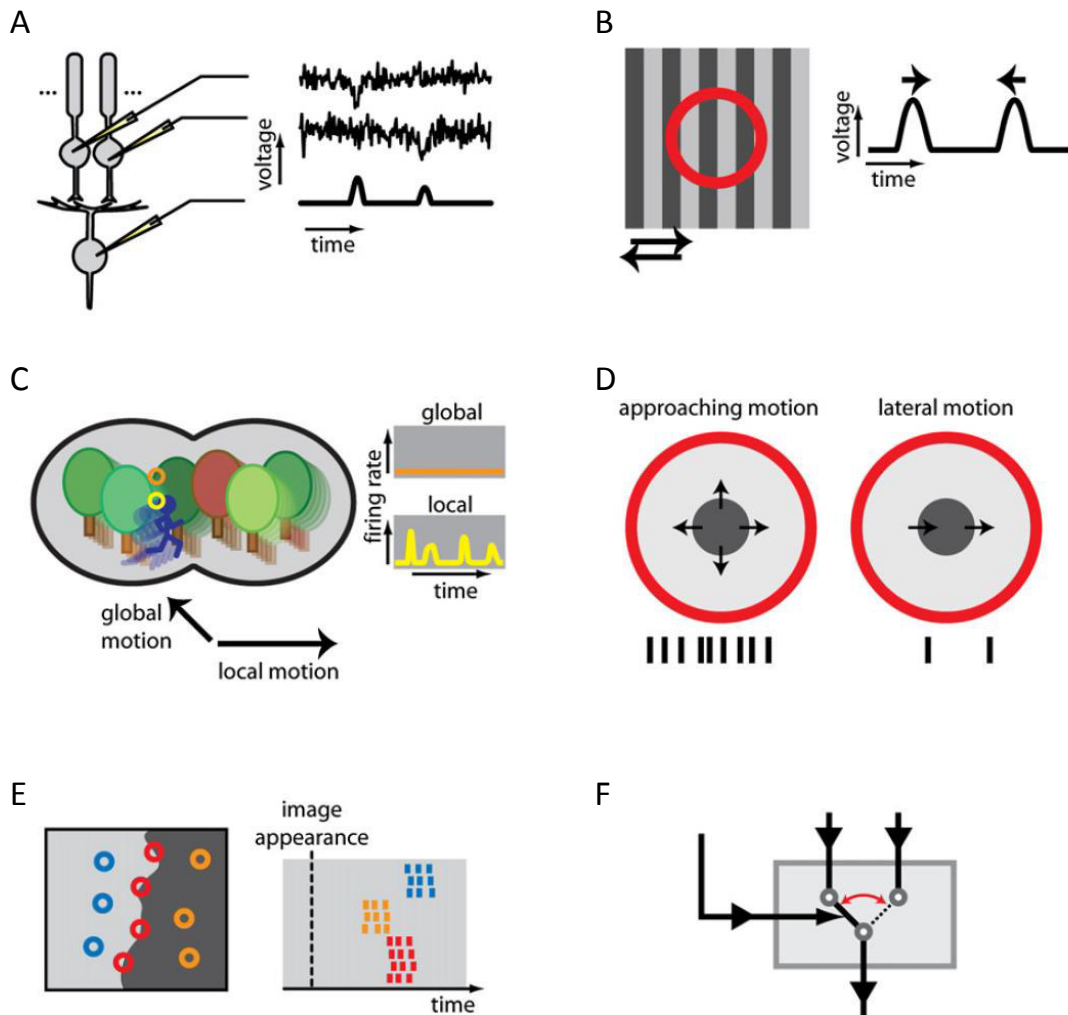
Figure 1.5. Neural computations in retinal circuitry. All computations within retinal circuitry involves different retinal cell types, namely bipolar cells, amacrine cells, and RGCs, though the output signal is carried out by RGC spiking activity. (A) Detection of dim light flashes originates in rod-to-rod bipolar pathway. Rod bipolar cells pool over many rod photoreceptors. (B) Sensitivity to texture motion results from the selective activation of a particular RGC when a fine grating shifts in either direction within the RGC receptive field (circle). (C) The detection of differential motion is attributed to an object-motion-sensitive RGC that remains silent under global motion of the entire image, but fires when the image patch in its receptive field moves differently from the background. (D) The detection of approaching motion is assigned to a certain type of RGC that responds strongly to the visual pattern of an approaching dark object. (E) The rapid encoding of spatial structures is based on spike latencies of specific RGCs. RGCs with receptive fields (circles) in a dark region fire early, and those in a bright region fire late. (F) The ability to switch between circuits is driven by a certain type of wide-field amacrine cell, activated during rapid image shifts in the periphery, which selectively gates one of two potential input signals. Adapted from Gollisch and Meister (2010).

1.1.4 – Circadian visual system

In mammals, in addition to classical rod and cone photoreceptors, a third type of photosensitive neuron is present and define a particular type of intrinsically photosensitive RGCs (ipRGCs), which mediate non-image-forming visual functions such as pupillary light reflex and circadian photoentrainment. The photosensitivity of ipRGCs requires the expression of melanopsin, a photopigment with peak absorbance around 484 nm (Berson et al., 2002). The ipRGCs project predominantly to the suprachiasmatic nuclei (SCN) of the hypothalamus (Hattar et al., 2002), which is the primary circadian oscillator in mammals. Indeed, ipRGCs play an important role in photoentrainment, a process by which the light/dark cycle synchronizes the SCN central oscillator (Morin and Allen, 2006). This central oscillator then synchronizes peripheral circadian clocks distributed in other mammalian tissues, such as the retina (Tosini et al., 2008), multiple brain regions (Abe et al., 2002), and many peripheral tissues (Damiola et al., 2000). The retinal intrinsic circadian oscillator is involved in circadian rhythms of the inner retinal circuitry (Storch et al., 2007). The retinal circadian pacemaker property is assured by the expression in multiple types of retinal neurons of key elements of the circadian autoregulatory gene network "clock genes" like *Period 1* and *2*, *Cryptochrome 1* and *2*, and *Clock* and *Bmal 1* (Ruan et al., 2006).

1.1.5 – Glaucoma and retinal ganglion cell death

Pathologies of the neural retina represent a major cause of visual impairment and blindness worldwide and the development of effective neuroprotective strategies is an important challenge in ophthalmology research. In order to evaluate the effectiveness of putative neuroprotective compounds, various *in vitro* and animal models of neurotoxicity, such as retinal ischemia, exposure to glutamate or NDMA, optic nerve crush, and glaucoma models characterized by increased intraocular pressure (IOP) have been used (Barkana and Belkin, 2004).

In particular, glaucoma is the major cause of irreversible blindness worldwide, estimated to affect approximately 80 million people by 2020 (Quigley and Broman, 2006), and the search for neuroprotective strategies to prevent RGC death is an important challenge (Baltmr et al., 2010). Glaucoma is a multifactorial disease characterized mainly by the

progressive degeneration of RGCs and their axons. Clinically, a characteristic cup excavation due to alterations of the connective tissue at the optic disc are coincident with the initial abnormalities in both human and experimental glaucoma (Quigley et al., 1981). Although increased IOP is a major risk factor, several pathophysiological mechanisms have been associated with the progression of the disease (Cheung et al., 2008). These include excitotoxicity, protein misfolding, mitochondrial dysfunction, oxidative stress, inflammation, and neurotrophin deprivation. Currently, the medical management of glaucoma is based in lowering IOP, but although effective control of IOP is many times achieved, the progression of RGC loss is not prevented (Geringer and Imami, 2008). Therefore, pharmacological therapies targeting pathophysiological mechanisms, others than elevated IOP, as above mentioned, have been extensively evaluated in *in vitro* and animal models of RGC degeneration (Chidlow et al., 2007; Baltmr et al., 2010). The *in vitro* studies include mainly cultured RGCs and cultured retinal explants exposed to different stimuli, such as NMDA or glutamate (Pang et al., 1999; Dun et al., 2007), neurotrophic withdrawal (Johnson et al., 1986; Hu et al., 2010), and elevated hydrostatic pressure (Sappington et al., 2006; Ishikawa et al., 2010). The different stimuli used in *in vitro* studies aimed to mimic isolated characteristics of glaucoma pathophysiology. In addition, various animal models have been used to evaluate the potential neuroprotective effects of different drug treatments against RGC death. These include animal models where IOP is chronically elevated by blocking the aqueous humour outflow. This has been achieved by injecting a hypertonic saline solution into the episcleral veins (Morrison et al., 1997), cauterization of episcleral veins (Shareef et al., 1995; Hernandez et al., 2008), or injection of polystyrene microbeads into the anterior chamber (Sappington et al., 2010) among other techniques. Other animal models include mainly optic nerve crush (Schuettauf et al., 2000) or optic nerve transection (Kikuchi et al., 2000), injection of NMDA or glutamate directly into vitreous humour (Nash et al., 2000; Santos-Carvalho et al., 2013b), and retinal I-R injury (Kapin et al., 1999; Chidlow et al., 2002).

Although these studies have contributed to significant advances in understanding both the pathogenic and neuroprotective mechanisms involved in glaucoma and its treatment, translating experimental drug treatments to glaucoma patients has not been successfully achieved. In fact, the clinical trial of memantine (a NMDA receptor antagonist, anti-excitotoxic) in glaucoma patients have failed, likely due to the multifactorial nature of glaucoma (Osborne, 2009). This finding suggests that neuroprotective compounds with multiple modes of action might be more efficient.

1.2 – Neuropeptide Y

1.2.1 – Structure and biosynthesis

Neuropeptide Y (NPY) is a 36 amino acid peptide that was first isolated from porcine brain (Tatemoto, 1982; Tatemoto et al., 1982). NPY is widely expressed in the CNS and acts as a neurotransmitter/neuromodulator or neurohormone. In the periphery it is mainly found in sympathetic nerve terminals where is co-released with norepinephrine and adenosine 5'-triphosphate (ATP) (Morris, 1999; Wier et al., 2009). During the last three decades NPY has been associated with a multitude of physiological functions such as feeding behaviour and energy homeostasis (Chambers and Woods, 2012; Sohn et al., 2013), regulation of emotionality and behavioural stress responses including drug addiction (Heilig, 2004; Koob, 2008; Hirsch and Zukowska, 2012), regulation of circadian rhythm (Moore and Card, 1990; Yannielli and Harrington, 2004), bone physiology (Lee and Herzog, 2009; Khor and Baldock, 2012), neurogenesis (Hansel et al., 2001; Malva et al., 2012), and immune response (Prod'homme et al., 2006; Bedoui et al., 2007; Wheway et al., 2007; Dimitrijevic and Stanojevic, 2013). NPY belongs to a family of highly conserved peptides which includes also pancreatic polypeptide (PP), and peptide YY (PYY), all with 36 amino acid residues (Fig. 1.6 A, B) (Michel et al., 1998), which bind to seven transmembrane G protein-coupled receptors (GPCRs) named NPY receptors, Y_1, Y_2, Y_4, and Y_5 in humans.

A

pPYY   pNPY   bPP

B

Peptide	Sequence
pNPY	YPSKPDNPGEDAPAEDLARYYSALRHYINLITRQRY-NH$_2$
hPYY	YPIKPEAPGEDASPEELNRYYASLRHYLNLVTRQRY-NH$_2$
hPP	APLEPVYPGDNATPEQMAQYAADLRRYINMLTRPRY-NH$_2$
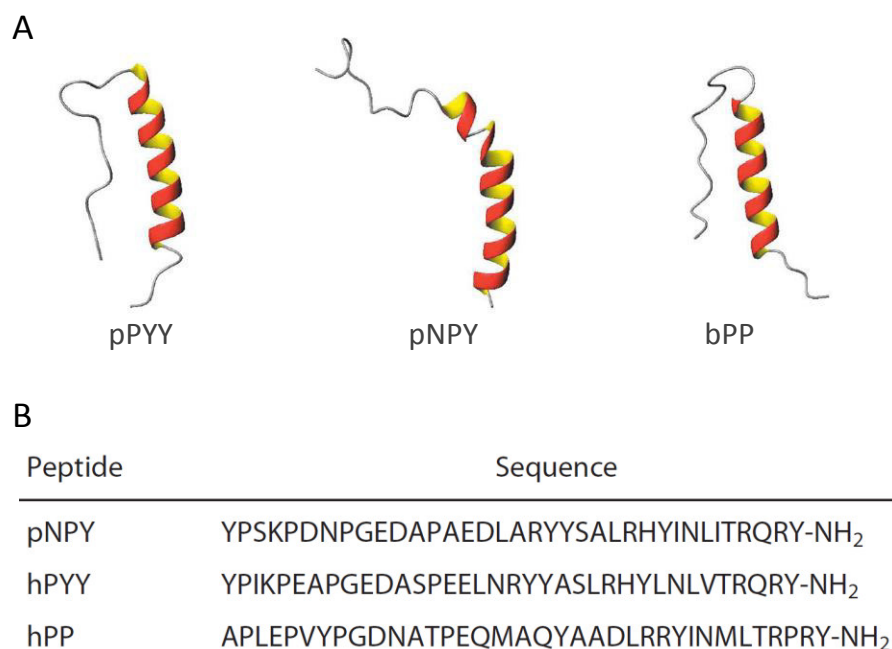
Figure 1.6. NPY family of peptides. (A) Structure of porcine PYY (pPYY), porcine NPY (pNPY), and bovine PP (bPP). Adapted from Lerch et al. (2004). (B) Amino acid sequences of porcine NPY (pNPY), human PYY (hPYY), and human PP (hPP) (Walther et al., 2011).

The high homology between these peptides results from whole genome and individual gene duplication events occurred early in vertebrate evolution, a common feature for other peptides (Larhammar et al., 2009). The first duplication is believed to have generated NPY and PYY, and a second duplication generated PP from PYY (Cerda-Reverter and Larhammar, 2000; Conlon and Larhammar, 2005). These peptides have been associated with a hairpin-like spatial arrangement called "PP-fold", consisting of an N-terminal polyproline helix (residues 1-8), a consecutive turn and a C-terminal α-helix (residues 14-31) arranged in a U-shape tertiary structure (Blundell et al., 1981). However, nuclear magnetic resonance (NMR) studies found that the N-terminal is flexible and does not form hairpin-like fold under physiological conditions (Bader et al., 2001; Lerch et al., 2002; Lerch et al., 2004). Particularly, for NPY, fluorescence resonance energy transfer (FRET) studies confirmed that the N-terminal does not fold back onto C-terminal α-helix in solution (Bettio et al., 2002; Haack and Beck-Sickinger, 2009).

The NPY gene is located on human chromosome 7p15.1. It is composed of four exons and results in the synthesis of a 97-amino-acid pre-pro-NPY (Fig. 1.7) (Minth et al., 1984). The signal peptide of pre-pro-NPY is cleaved in the endoplasmic reticulum by a signal peptidase, a common feature to most pre-pro-peptides (Dores et al., 1996). In the following step, pro-NPY

is proteolytically processed at a dibasic site by prohormone convertases into the C-terminal peptide of NPY (CPON) and NPY_{1-39} (Hook et al., 1996; Funkelstein et al., 2008; Funkelstein et al., 2012). This is further processed by carboxypeptidase to NPY_{1-37}. The processing and C-terminal amidation of NPY is accomplished by peptidylglycine α-amidating monooxygenase. The amidation of NPY is essential for biological activity and prevents degradation by carboxypeptidases. Mature NPY (NPY_{1-36}) is rapidly cleaved in serum into three main fragments: NPY_{3-36}, NPY_{3-35}, and NPY_{2-36} (Medeiros and Turner, 1996; Abid et al., 2009). NPY_{1-36} is predominantly cleaved into NPY_{3-36} by dipeptidyl peptidase IV (DPPIV), and through a slower process by aminopeptidase P into NPY_{2-36}. Both of these peptides loose the affinity for Y_1 receptor, retaining high affinity for Y_2 and Y_5 receptors. In addition, a fraction of NPY_{3-36} is further degraded by plasma kallikrein into NPY_{3-35}. This later peptide does not bind to any of NPY receptors, thus representing a possible major metabolic clearance product of NPY_{3-36}.
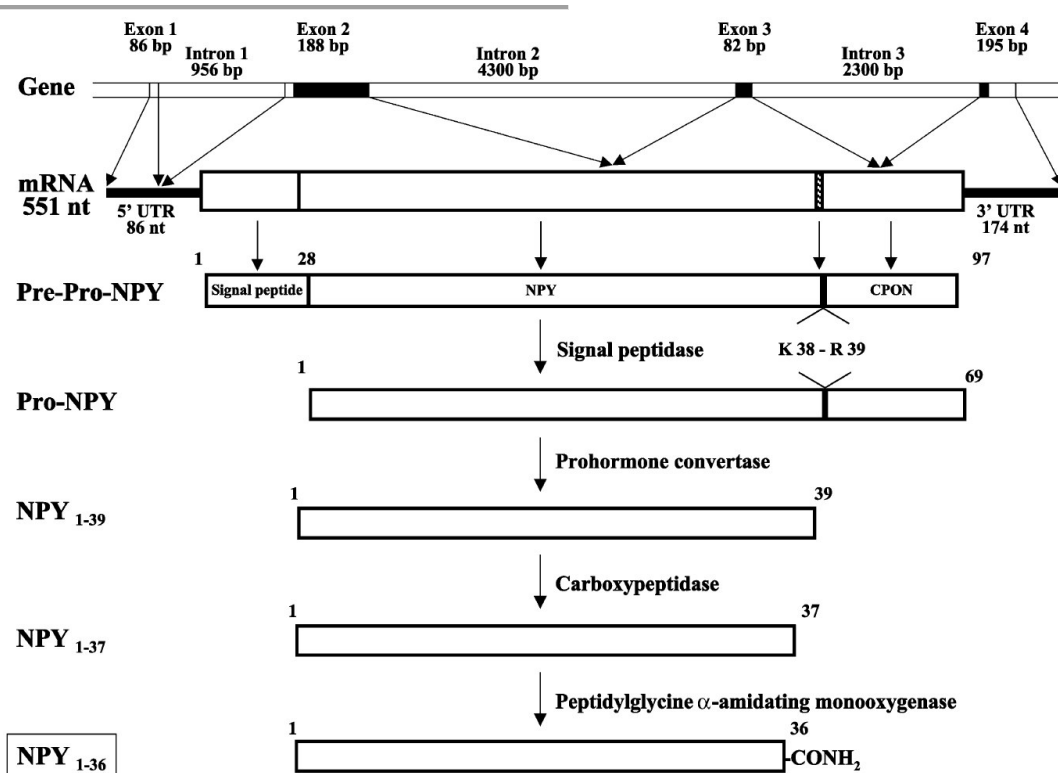
Figure 1.7. Biosynthesis of NPY. NPY gene is composed of four exons and results in the synthesis of a 97-amino-acid pre-pro-NPY. After a series of proteolytic steps and final C-terminal amidation, the mature and biological active NPY_{1-36} is formed. bp, base pairs; nt, nucleotides; UTR, untranslated region; CPON, C-terminal peptide of NPY (Silva et al., 2002).

1.2.2 – Neuropeptide Y receptors

Similarly to the ligand peptides NPY, PYY, and PP, the various NPY receptors result from chromosomal and gene duplication events during evolution (Larhammar and Salaneck, 2004). Interestingly, mammals have lost some NPY receptors, namely Y_7 (Fredriksson et al., 2004) and Y_8 (Lundell et al., 1997; Larsson et al., 2008), which have arisen in the ancestor of the jaw vertebrates (Larhammar and Bergqvist, 2013). Functional active NPY receptors, Y_1, Y_2, Y_4, and Y_5, in humans and rats, as for all GPCRs, consist of an extracellular N-terminus, seven transmembrane α-helices connected by three intracellular and three extracellular loops, and an intracellular C-terminus. The mRNA presence evaluated by *in situ* hybridization for different NPY receptors, Y_1, Y_2, Y_4, and Y_5, together with functional autoradiography, show that all the receptors are widely distributed throughout the rat brain, especially in regions such as hypothalamus, hippocampus, and amygdala (Lynch et al., 1989; Parker and Herzog, 1999).

The Y_1 receptor was first cloned from rat brain in 1990 (Eva et al., 1990). In humans, Y_1 receptor gene is located on chromosome 4q31.3-q32 (Herzog et al., 1993). The following agonist order of potency of NPY ≥ PYY ≥ [Pro^{34}]substituted analogue >> C-terminal fragment > PP has been found for Y_1 receptor was reported (Michel et al., 1998). Functional autoradiography and immunohistochemistry experiments revealed an abundant presence of Y_1 receptor in several brain regions such as cerebral cortex, hippocampus, hypothalamus, thalamus, amygdala, and brainstem (Shaw et al., 2003; Wolak et al., 2003).

The Y_2 receptor was first cloned from human SMS-KAN cells (Rose et al., 1995). In humans, Y_2 receptor gene is located on chromosome 4q31 (Ammar et al., 1996). The following agonist order of potency of NPY ≈ PYY ≥ C-terminal fragment >> [Pro^{34}]substituted analogue > PP was reported (Michel et al., 1998). Positron emission tomography (PET) neuroimaging in pig brain showed the presence of Y_2 receptor mainly in thalamus, caudate nucleus, hippocampus, and cerebellum (Winterdahl et al., 2014).

In various systems and organs such as rat CNS (Grundemar et al., 1991), lung (Hirabayashi et al., 1996), and adrenals (Bernet et al., 1994), it was reported the presence of binding sites or responses where NPY is considerably more potent than PYY, and these sites has been referred as *Y_3*. However, since no receptor has been cloned and no specific agonist or antagonist has been described so far, this receptor might not exist, and these sites or responses were proposed to be referred as "putative *Y_3*" (Michel et al., 1998).

The Y_4 receptor was first cloned from a human genomic library and named as "PP1" due to the high affinity (13.8 pM, *K_i*) to PP (Lundell et al., 1995), while NPY and PYY binds with 9.9 and 1.44 nM affinity, respectively. In humans, the gene encoding for Y_4 receptor is located on chromosome 10q11.2 (Darby et al., 1997). Although in the periphery Y_4 receptor is highly expressed in colon, small intestine, pancreas, and prostate (Lundell et al., 1995), in the brain low levels are detected, and restricted to brain stem, hypothalamus, and hippocampus (Parker and Herzog, 1999).

The Y_5 receptor was initially cloned from rat hypothalamus (Gerald et al., 1996; Hu et al., 1996) and the corresponding gene in human localized on chromosome 4q31, in the same location as human Y_1 receptor gene, but in opposite orientation (Gerald et al., 1996; Borowsky et al., 1998). The following agonist order of potency of NPY ≥ PYY ≈ [Pro^{34}]substituted analogue ≈ NPY$_{2-36}$ ≈ PYY$_{3-36}$ >> NPY$_{13-36}$ was reported in *in vitro* functional assays. Since this pharmacological profile was consistent with *in vivo* food intake assays and mRNA for Y_5 receptor was localized in areas of hypothalamus known to regulate food intake, the Y_5

receptor was soon suggested as the primary mediator of NPY-induced feeding (Gerald et al., 1996). In rat brain, autoradiographic assays revealed Y_5 receptor binding sites in olfactory bulb, lateral septum, anteroventral thalamic nucleus, hippocampal CA3, nucleus tractus solitarius, and area postrema (Dumont et al., 1998). Using immunohistochemistry, the presence of Y_5 receptor imunoreactivity was found in cerebral cortex, hippocampus, hypothalamus, thalamus, amygdala, and brainstem (Wolak et al., 2003).

The y_6 was first cloned from mouse genomic DNA (Weinberg et al., 1996). The homologous gene in humans was localized in chromosome 5q31 (Gregor et al., 1996). However, compared to mouse, the human sequence differs by a frame shift mutation which causes a stop codon predicting a truncated protein, though this later has not been successfully expressed (Gregor et al., 1996). Several sequences from primate species contain this stop codon suggesting the receptor function has been inactivated early in primate evolution (Matsumoto et al., 1996). In fact, no physiological correlate has been reported for the cloned y_6 receptor (Michel et al., 1998).

1.2.3 – Intracellular signalling pathways

NPY receptors are all coupled to heterotrimeric G-proteins, mainly $G_{i/0}$ family, and their activation leads mainly to the inhibition of adenylate cyclase (Fig. 1.8), regulation of K^+ and Ca^{2+} channels, and the activation of extracellular-signal-regulated kinase 1 and 2 (ERK1/2) (Shimada et al., 2012). The inhibition of adenylate cyclase, which results in decreased intracellular cyclic adenosine monophosphate (cAMP) levels, is found in most tissues and cell types studied, and also in all cloned NPY receptors upon heterologous expression (Gerald et al., 1996; Weinberg et al., 1996).
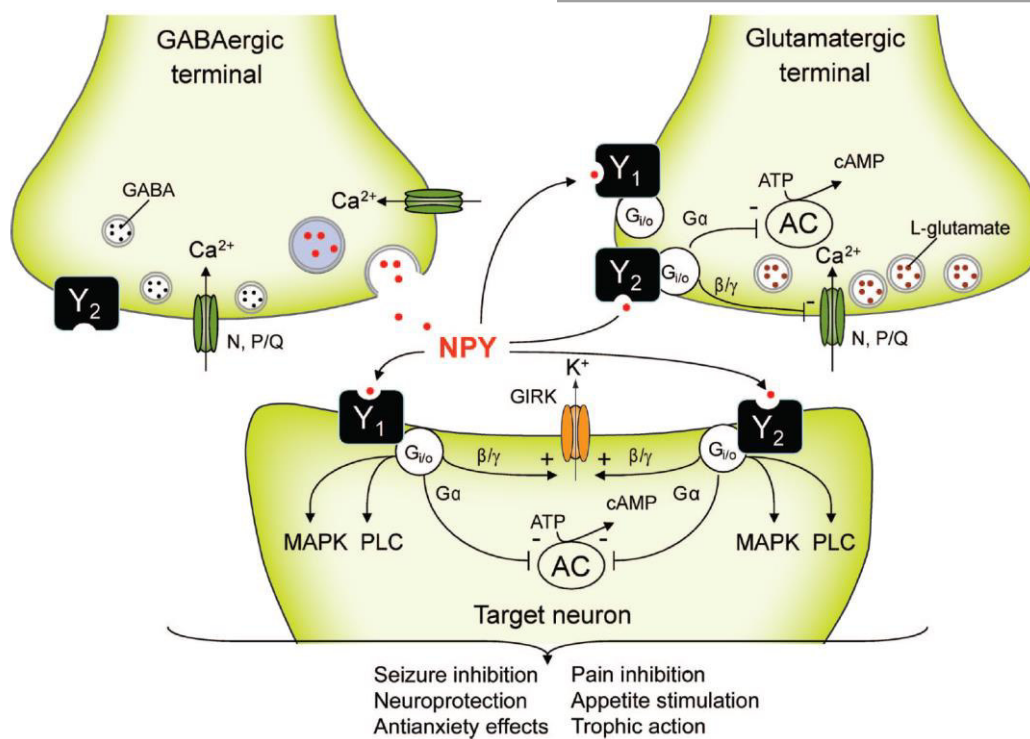
Figure 1.8. Examples of NPY receptor-mediated transduction cascades. NPY is frequently present in neurons synthesizing GABA. Y_1 receptors are located mainly postsynaptically, and Y_2 receptors are located both presynaptically and postsynaptically. NPY receptor activation, via $G\alpha$ subunit, leads to inhibition of adenylate cyclase (AC), and via $G\beta\gamma$ subunits leads to inhibition of presynaptic N- and P/Q-type Ca^{2+} channels involved in the release of glutamate and other neurotransmitters. Postsynaptically, NPY receptor activation, via $G\beta\gamma$ subunits, leads to activation of G-protein-coupled inwardly-rectifying K^+ channels (GIRKs). Other pathways include activation of mitogen-activated protein kinases (MAPKs) and phospholipase C (PLC) (Benarroch, 2009).

NPY-mediated regulation of Ca^{2+} includes the activation or inhibition of Ca^{2+} channels (Ewald et al., 1988; Michel and Rascher, 1995). In particular, facilitation of L-type voltage-dependent Ca^{2+} channels (VDCCs) via $G\alpha_s$-protein and inhibition of N- and P/Q-VDCCs via $G\alpha_i$-protein has been reported in submandibular ganglion neurons (Endoh et al., 2012). The control of Ca^{2+} channels, especially the inhibition of VDCC, has been reported to regulate neurotransmitter release in sympathetic nerve terminals (Toth et al., 1993), cortical nerve terminals (Wang, 2005), and hippocampus (Silva et al., 2001). In some cell types, NPY receptor activation can mobilize Ca^{2+} from intracellular stores, which involve inositol triphosphate in some cells (Perney and Miller, 1989), but not in other cell types (Motulsky and Michel, 1988). The activation or inhibition of K^+ channels has also been reported (Millar et al., 1991; Xiong and Cheung, 1995). Indeed, the activation of G-protein-coupled inwardly-rectifying K^+ channels (GIRKs) has been reported in several brain regions such as hippocampus (Paredes et

al., 2003), thalamus (Sun et al., 2001; Sun et al., 2003), arcuate nucleus (Acuna-Goycolea et al., 2005), and amygdala (Sosulina et al., 2008). Activation of mitogen-activated protein kinase (MAPK) family members have also been reported in various cell types, such as cell lines expressing NPY receptors (Nie and Selbie, 1998), erythroleukemia cells (Keffel et al., 1999), adrenal chromaffin cells (Rosmaninho-Salgado et al., 2007; Rosmaninho-Salgado et al., 2009), adipocytes (Rosmaninho-Salgado et al., 2012), vascular cells (Shimada et al., 2012), neuroblastoma cells (Lu et al., 2010), and in retinal neural cells (Alvaro et al., 2008a) and retinal glial cells (Milenkovic et al., 2004). Furthermore, each NPY receptor has a distinct molecular mechanism responsible for the receptor trafficking processes, such as anterograde transport, internalization, and recycling, which contributes to receptor response and signalling (Babilon et al., 2013). In particular, internalization experiments showed that Y_1, Y_2, and Y_4 receptor internalize at comparable rates, whereas the Y_5 receptor internalized much slower upon agonist binding (Bohme et al., 2008).

1.2.4 – Neuropeptide Y and neuropeptide Y receptors in the retina

The presence of NPY in the retina has been extensively studied in various species, revealing a conserved pattern of NPY-immunoreactivity (ir) (Santos-Carvalho et al., 2014). After NPY discovery in 1982, immunohistochemistry studies assessing the presence and localization of NPY soon reported the existence of NPY-ir in the retina of trout, carp, goldfish, zebrafish, gilthead seabream, killifish, frog, pigeon, chicken, guinea-pig, rat, rabbit, pig, cat, dolphin, and baboon (Fig. 1.9) (Bruun et al., 1984; Osborne et al., 1985; Bruun et al., 1986; Verstappen et al., 1986; Muske et al., 1987; Bruun et al., 1991; Subhedar et al., 1996; Chen et al., 1999; Kang et al., 2001; Le Rouëdec et al., 2002; Mathieu et al., 2002; Pirone et al., 2008). In these species, a common pattern was found. NPY-ir was localized mainly to amacrine cells, with cell bodies in the innermost row of INL, which processes ramified in the IPL forming up to three distinct layers.
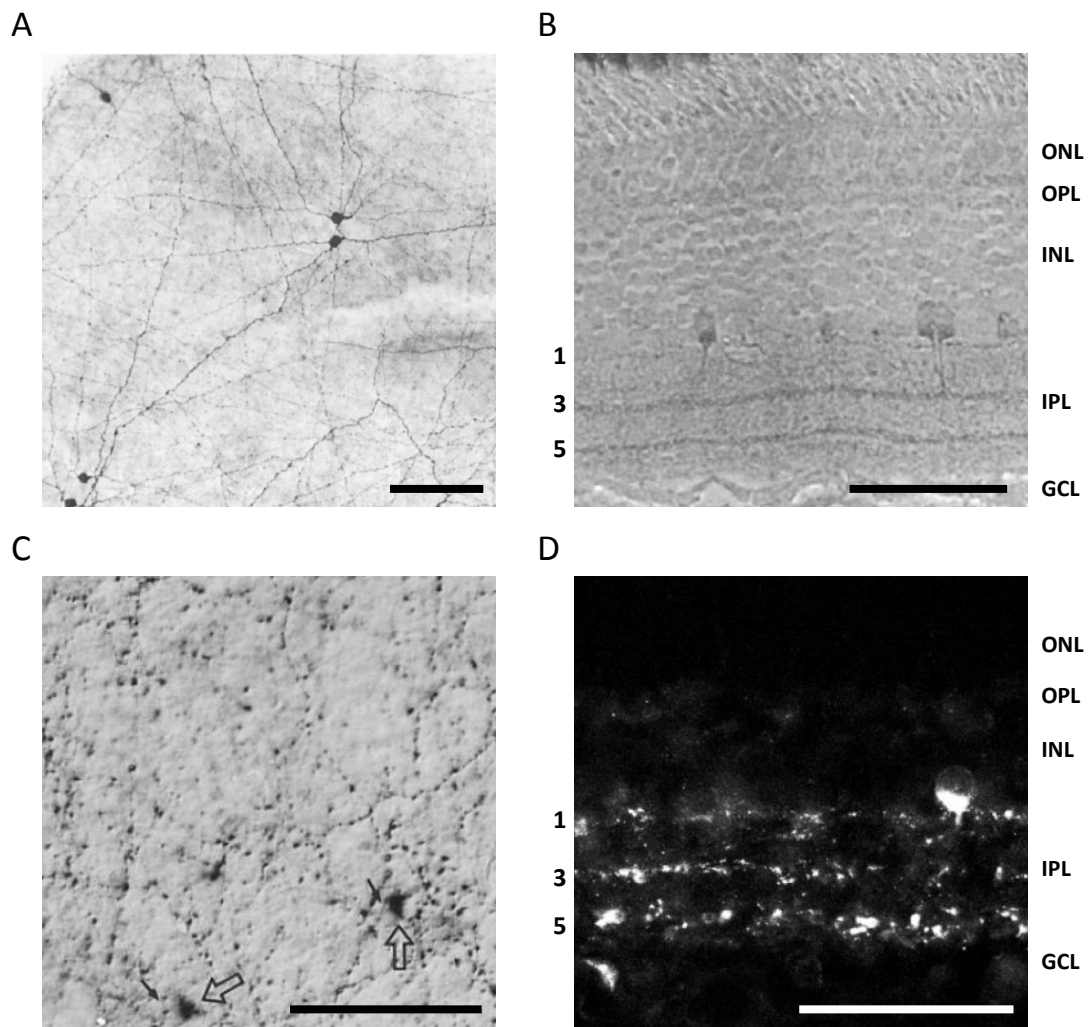
Figure 1.9. NPY immunoreactivity in the retina. Examples of NPY-ir in the frog retina (A, B) and rat retina (C, D). (A) Wholemount of frog retina showing NPY-ir cells and their dendrites. Adapted from Hiscock and Straznicky (1989). (B) Section of frog retina. NPY-ir dendrites ramify in strata 1, 3, and 5 of IPL. Adapted from Bruun et al. (1986). (C) Wholemount of rat retina showing NPY-ir in emerging processes (fine arrows) from cell somas (open arrows) of amacrine cells. Adapted from Oh et al. (2002). (D) Section of rat retina. NPY-ir dendrites ramify in strata 1, 3, and 5 of IPL. Adapted from Oh et al. (2002). Scale bar: 100 µm in A and B, 50 µm in C and D.

The NPY-ir has been studied in various species of frogs (Fig. 1.9 A, B) and it has been reported to appear during early larval life (Hiscock and Straznicky, 1989, 1990; Zhu and Gibbins, 1995). The NPY-ir is found in amacrine cells that co-localize with GABA (Main et al., 1993), and a single report also demonstrated that NPY-ir can be found in Müller cells (Zhu and Gibbins, 1996). Interestingly, NPY-ir exhibit seasonal variations with higher concentration in the autumn and lower in the spring, and NPY release is increased upon light stimulation or depolarization (Bruun et al., 1991). In the cat retina, NPY-ir is found not only in amacrine cells but also in RGCs (Hutsler et al., 1993; Hutsler and Chalupa, 1994, 1995).

In mouse and rat retina, NPY-ir was reported to localize in cell bodies of amacrine cells in INL and displaced amacrine cells in GCL (Fig. 1.9 C, D), co-localizing mainly with GABA (Ferriero and Sagar, 1989; Sinclair and Nirenberg, 2001; Oh et al., 2002). The corresponding cell processes extended and ramified mainly in strata 1, 3, and 5 of IPL, and very occasionally in OPL (Oh et al., 2002). In human retina, NPY-ir was shown to be confined to a subset of amacrine cells and RGCs, which processes extend mainly in IPL and occasionally in OPL (Tornqvist and Ehinger, 1988; Straznicky and Hiscock, 1989; Jen et al., 1994; Jotwani et al., 1994). Moreover, in primary cultures of rat retinal cells, NPY-ir is found in different rat retinal cells, namely neurons, endothelial cells, microglial cells, and in Müller cells (Alvaro et al., 2007). Regarding NPY receptor localization in the retina, there are only a few studies addressing this issue. In human retina, transcripts for Y_1, Y_2, and Y_5 receptors were detected in RPE (Ammar et al., 1998). The presence of mRNA for both NPY and NPY receptors (Y_1, Y_2, Y_4, and Y_5) has also been demonstrated in the rat retina (D'Angelo and Brecha, 2004; Alvaro et al., 2007) and NPY, Y_1, and Y_2 mRNA was detected in mouse retina (Yoon et al., 2002). Y_1 receptor-ir was detected in horizontal and amacrine cells of rat retina and in glial cells of diseased human retina (Canto Soler et al., 2002; D'Angelo et al., 2002), and immunoreactivity for Y_1 and Y_2 receptors was found in neurons and glial cells in cultured rat retinal cells (Santos-Carvalho et al., 2013a).

Besides these studies addressing the presence of NPY and NPY receptors in the retina, the role of NPY in this neural tissue remains unclear. NPY application was found to regulate neurotransmitter release of rabbit and chicken retinas (Bruun and Ehinger, 1993). Also, NPY attenuates depolarization-induced increase in intracellular free calcium concentration – $[Ca^{2+}]_i$ – in primary retinal cell cultures (Alvaro et al., 2009). Moreover, NPY decreased depolarization-dependent Ca^{2+} influx into bipolar cells via activation of Y_2 receptors (D'Angelo and Brecha, 2004), and in retinas with selective ablation of NPY-expressing amacrine cells, alterations on receptive field properties of RGCs were reported, though a direct effect of NPY was not demonstrated (Sinclair et al., 2004). In addition, other studies have suggested the involvement of NPY and Y_1 receptor activation in the regulation of osmotic Müller glial cell swelling in the rat retina (Uckermann et al., 2006; Linnertz et al., 2011).

1.2.5 – Neuroprotective actions of neuropeptide Y

Targeting NPY receptors has been reported to exert neuroprotective actions in several systems. In fact, NPY receptors have been regarded as potential therapeutic targets in the brain, namely for epilepsy (Xapelli et al., 2006). Several studies have evaluated the neuroprotective potential of NPY or NPY receptor activation after exposure to glutamatergic agonists which have been used to induce an excitotoxic insult *in vitro* or *in vivo*. Using organotypic hippocampal slice cultures, the activation of Y_1, Y_2, or Y_5 receptor was found to prevent kainate or AMPA-induced neuronal cell death measured by propidium iodide incorporation (Silva et al., 2003; Xapelli et al., 2007; Xapelli et al., 2008). However, the contribution of individual NPY receptor activation depends on the subregion analysed. In neocortical and hippocampal neuronal cultures, the application of NPY before or after kainate exposure was able to attenuate neurotoxicity assessed by lactate dehydrogenase efflux and caspase-3 activity (Domin et al., 2006). In agreement with this result, Y_1 or Y_2 receptor activation, 30 min after the excitotoxic insult, prevented kainate-induced cell death in organotypic hippocampal slice cultures (Xapelli et al., 2007), and NPY applied 6 h after kainate treatment decreased cell death in cortical and hippocampal neuronal cultures (Smialowska et al., 2009). When NPY, Y_2 or Y_5 receptor agonist was injected into the hippocampus it was also able to reduce the extent of kainate-induced cell death (Smialowska et al., 2003; Smialowska et al., 2009). Similarly, NPY, or Y_2 or Y_5 receptor agonists infused icv reduced kainate-induced hippocampal cell death (Wu and Li, 2005). The modulation of hippocampal synaptic transmission by NPY system has long been studied (Colmers, 1990; Nadler et al., 2007; Sperk et al., 2007). Accordingly, the protective effect of NPY observed in hippocampus is in agreement with studies suggesting NPY as an endogenous antiepileptic peptide, and targeting NPY system as an antiepileptic strategy by reducing glutamate release and excitability (Vezzani and Sperk, 2004; Woldbye and Kokaia, 2004; Silva et al., 2005).

In various models of neurodegenerative diseases, NPY system is affected by the disease (Beal et al., 1986; Minthon et al., 1990; Cannizzaro et al., 2003). This evidence, together with the accumulating findings showing protective actions exerted by exogenous NPY or NPY receptor agonist application in animal models of neurodegenerative diseases such as Parkinson's disease (Fig. 1.10) (Decressac et al., 2012), and Alzheimer's disease (Rose et al., 2009; Croce et al., 2011; Croce et al., 2012) indicates that NPY system may respond to neuronal injury in order to counteract the progressive neuronal loss (Decressac and Barker, 2012). For

example, the icv injection of NPY increases striatal dopamine release (Kerkerian-Le Goff et al., 1992) and protects dopaminergic neurons, an effect mediated by Y_2 receptor activation and ERK1/2 and protein kinase B (Akt) pathways (Decressac et al., 2012).

In the retina, NPY also exerts neuroprotective actions. In primary rat retinal cell cultures, NPY pre-treatment inhibited both 3,4-methylenedioxy-*N*-methylamphetamine (MDMA)- and glutamate-induced increased cell death (Alvaro et al., 2008b; Santos-Carvalho et al., 2013b). Moreover, in an animal model of excitotoxicity-induced retinal injury by using intravitreal injection of glutamate, NPY prevented the injury-induced increase in cell death and RGC loss (Santos-Carvalho et al., 2013b).
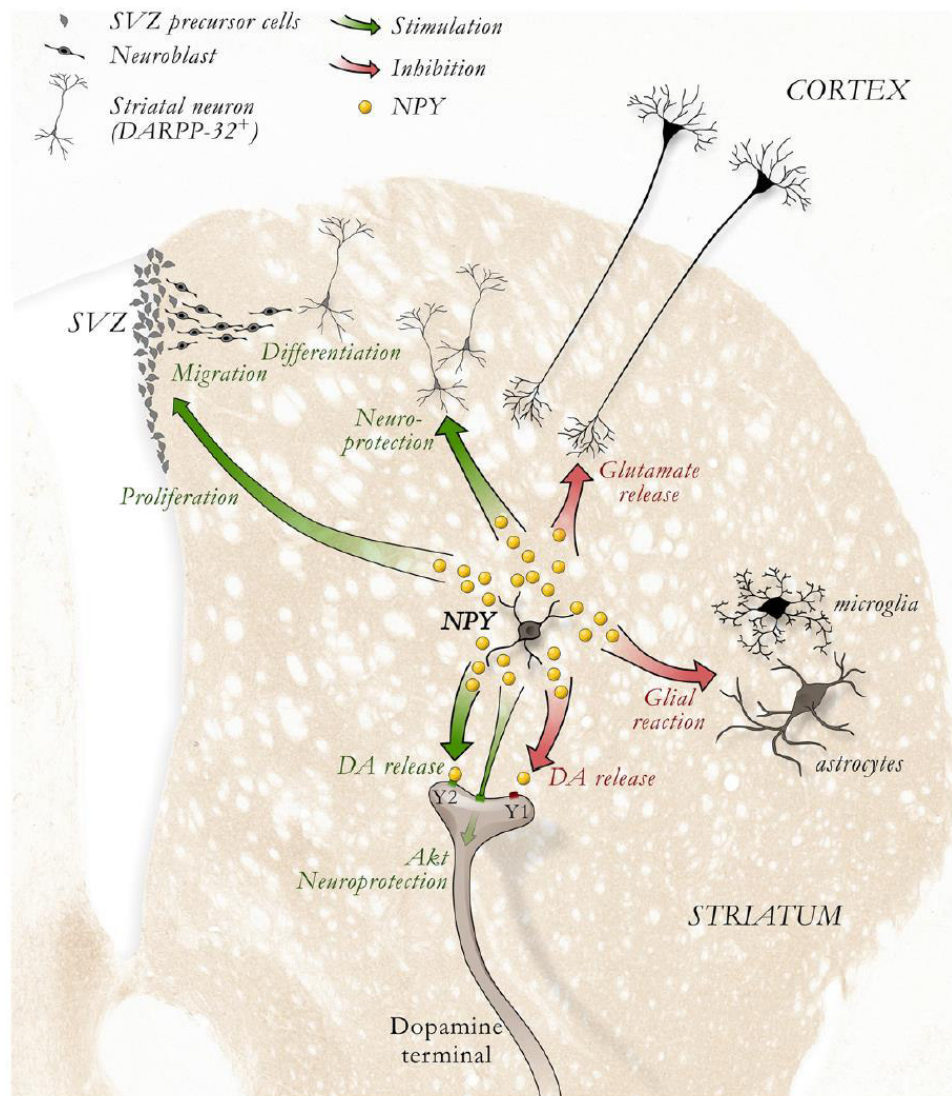
Figure 1.10. Examples of possible neuroprotective effects of NPY in the diseased brain. In the striatum, NPY is present in GABAergic neurons that receive inputs from cortical glutamatergic and nigral dopaminergic neurons. NPY inhibits glutamate release, thus reducing excitotoxicity in Parkinson's disease. NPY ability to inhibit glial reactivity has been also reported (Ferreira et al., 2010; Ferreira et al., 2011). NPY has a pro-neurogenic effect on SVZ neural stem cells (Agasse et al., 2008), and by recruiting the endogenous pool of progenitors NPY might promote the self-repair capacity of the adult brain. SVZ, subventricular zone; DA, dopamine; Akt, protein kinase B; DARPP, dopamine and cAMP-regulated phosphoprotein (Decressac and Barker, 2012).

1.3 – Sildenafil

1.3.1 – Mechanism of action

Sildenafil is an orally active inhibitor of PDE type 5 (Fig. 1.11). Sildenafil was initially manufactured by Pfizer, as Viagra™, and used for the treatment of male erectile dysfunction (Boolell et al., 1996).
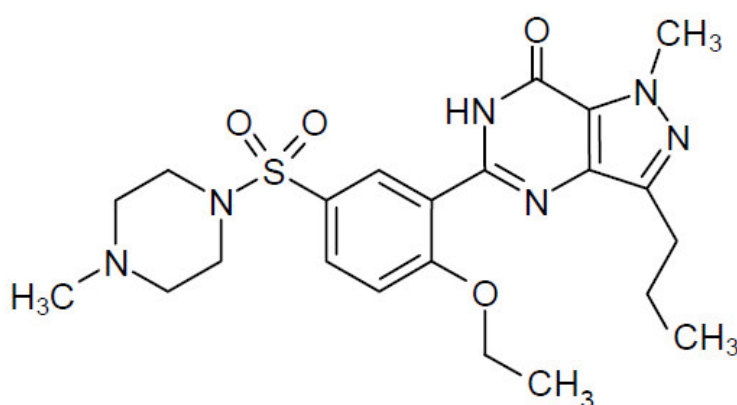
Figure 1.11. Structure of sildenafil citrate. (Salonia et al., 2003).

Since its launch in 1998 sildenafil has been distributed worldwide (Salonia et al., 2003), and it has also been used for the treatment of pulmonary arterial hypertension under the trade name Revatio™ (Montani et al., 2013). Recommended doses for the treatment of erectile dysfunction are 25, 50, and 100 mg to be administered 1 h before sexual activity (Salonia et al., 2003), whereas for pulmonary arterial hypertension is usually up to 20 mg three times a day (Montani et al., 2013). Concerning erectile dysfunction, sildenafil enhances the relaxant effect of NO on the penile corpus cavernosum by inhibiting PDE5 which is responsible for degradation of cGMP in this tissue (Fig. 1.12). When sexual stimulation causes local release of NO, inhibition of PDE5 by sildenafil increases cGMP concentration causing smooth muscle relaxation and subsequent increase in blood flow. Smooth muscle relaxation is partly mediated by protein kinase G (PKG) activation leading to a decrease in intracellular Ca^{2+} levels. A similar mechanism is responsible for pulmonary arterial vasodilatation (Ghofrani et al., 2006).
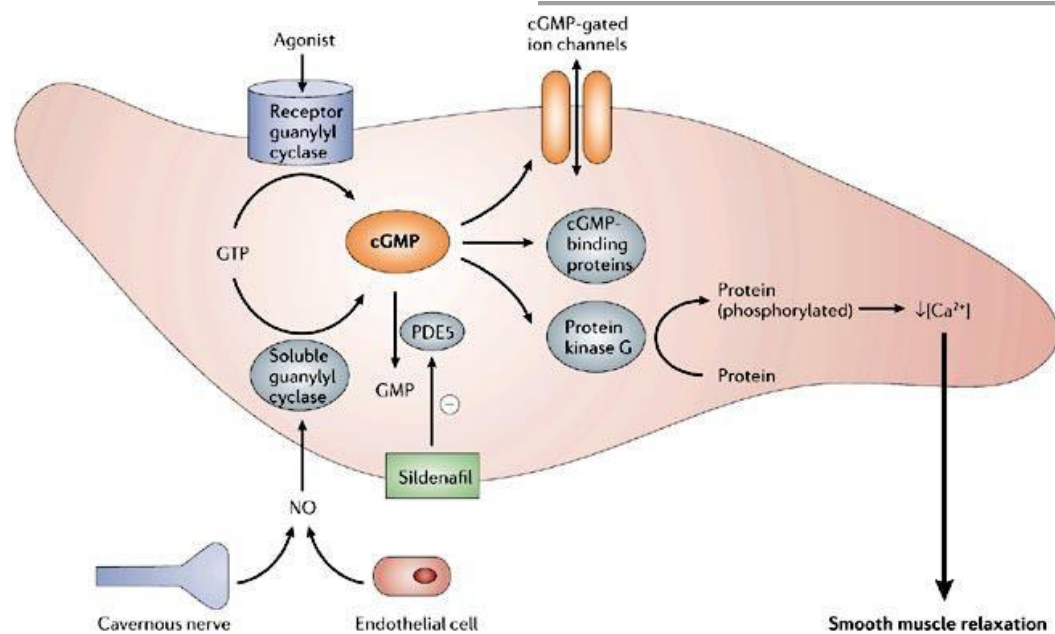
Figure 1.12. Mechanism of action of sildenafil. The figure shows the pathway mediating relaxation of vascular smooth muscle and penile erection (only upon sexual stimulation) and pulmonary vasodilatation (continuously). Local release of NO from cavernous nerve or endothelial cells regulates positively the concentration of cGMP which is then reduced by PDE5. The inhibition of PDE5 by sildenafil results in increased cGMP concentration causing smooth muscle relaxation and subsequent increase in blood flow. Smooth muscle relaxation is partly mediated by protein kinase G activation leading to a decrease in $[Ca^{2+}]_i$. PDE5, phosphodiesterase 5; cGMP, cyclic guanosine monophosphate; GMP, guanosine 5'-monophosphate; GTP, guanosine 5'-triphosphate; NO, nitric oxide (Ghofrani et al., 2006).

1.3.2 – Ocular side effects

Patients with erectile dysfunction have experienced transient and mild impairments of colour discrimination, which are occur at the peak of the drug action (Laties and Zrenner, 2002). Moreover, sildenafil was found to decrease visual performance, particularly the temporal response, in S-cone isolating conditions (Stockman et al., 2007), and, in rare cases, transient blindness was reported (Montastruc et al., 2006). It has also been suggested that sildenafil might be a possible, but not yet certain, cause of anterior ischaemic optic neuropathy (Carter, 2007). However, other studies reported no visual toxic effects in both human patients and laboratory animals even after long periods of drug daily use (Vatansever et al., 2003; Cordell et al., 2009; Zoumalan et al., 2009). Nonetheless, serious ocular adverse effects occur in some patients after sildenafil use. Case reports included cases of central retinal

vein occlusion, cilio-retinal artery occlusion, acute angle closure glaucoma and optic atrophy (Azzouni and Abu samra, 2011).

Electroretinogram (ERG) recordings showed decreases in both a- and b-wave amplitudes in sildenafil-treated patients (Vobig et al., 1999) or inversely, an increase in the scotopic ERG responses, but a decrease in the photopic response (Luu et al., 2001). Other studies reported increase in Naka-Rushton equation Vmax, suggesting higher rod response after 50 or 100 mg sildenafil ingestion (Gabrieli et al., 2001; Gabrieli et al., 2003). More consistently, among all human studies, sildenafil enlarged the latencies of the different responses (Luu et al., 2001; Jagle et al., 2004; Jagle et al., 2005). *Ex vivo* experiments showed also contradictory results. Sildenafil has been shown to increase ERG amplitudes in the rat retina (Barabas et al., 2003), whereas it decreases ERG amplitudes in bovine and human retinas, while increasing the latencies (Luke et al., 2005; Luke et al., 2007).

Although not completely elucidated, the effects of sildenafil on retinal function might result from the inhibition of PDE5, expressed in retinal cells, including human RGCs (Foresta et al., 2008). However, apart from the inhibition of PDE5, other PDEs may be inhibited by sildenafil, namely PDE6, which controls the phototransduction cascade in photoreceptors (Beavo, 1995; Lamb, 2013). For detailed description of phototransduction cascade see section 1.1.2. Sildenafil appears almost equally potent on cone PDE6 as on PDE5, whereas it seems slightly less potent on rod PDE6 (Ballard et al., 1998; Zhang et al., 2005). PDE4 is also expressed in RGCs, bipolar cells, cholinergic amacrine cells and rods (Whitaker and Cooper, 2009), whereas PDE1 and PDE9 were described so far in bipolar cells (Dhingra et al., 2008).

1.4 – Objectives

NPY is widely distributed in central and peripheral nervous system and present neuromodulatory and neuroprotective properties (Xapelli et al., 2006). In the retina, NPY presence has been demonstrated in different species, though NPY receptor localization has been scarcely investigated (Santos-Carvalho et al., 2014). We and others have presented evidence suggesting a neuromodulatory role of NPY in the retina. NPY application regulates neurotransmitter release in rabbit and chicken retinas (Bruun and Ehinger, 1993). Also, NPY attenuates depolarization-induced increase in $[Ca^{2+}]_i$ in primary retinal cell cultures (Alvaro et al., 2009), and decreases depolarization-dependent Ca^{2+} influx into bipolar cells (D'Angelo and Brecha, 2004). Moreover, in retinas with selective ablation of NPY-expressing amacrine cells, it was reported an alteration in the receptive field properties of RGCs, though a direct effect of NPY was not demonstrated (Sinclair et al., 2004). These results suggest that NPY-induced modulation of visual circuitry might result in changes of RGC spiking activity. Therefore, in the first part of the present study, we intended to further investigate the presence of NPY and NPY receptors in the retina at mRNA and protein level, and also, we intended to study the NPY modulatory potential at RGC level using purified RGC cultures and *ex vivo* retinal preparations. In purified RGC cultures, we have evaluated the effect of exogenous application of NPY in $[Ca^{2+}]_i$ changes triggered by glutamate, and in *ex vivo* retinal preparations we have assessed the light- or NMDA-stimulated RGC spiking activity.

Previous work from our laboratory have shown that NPY exerts a neuroprotective action against different toxic insults. In primary rat retinal cell cultures NPY pre-treatment prevented increased cell death induced by both MDMA and glutamate (Alvaro et al., 2008b; Santos-Carvalho et al., 2013b). In an animal model of excitotoxicity-induced retinal injury, intravitreal administration of NPY inhibited both the increase in cell death, and RGC loss induced by glutamate (Santos-Carvalho et al., 2013b). Retinal degenerative diseases affecting RGCs, in particular, glaucoma which is the major cause of irreversible blindness worldwide (Quigley and Broman, 2006), remain with no effective treatment able to halt the progression of RGC death. Therefore, we also evaluated the potential neuroprotective effects of NPY application against RGC death in an *in vitro* model of excitotoxicty and in an animal model of retinal I-R injury.

Sildenafil is a PDE type 5 inhibitor widely used for treatment of erectile dysfunction (Salonia et al., 2003), and also for pulmonary arterial hypertension (Montani et al., 2013). Patients with erectile dysfunction have experienced transient and mild impairments of colour discrimination, which are occurring at the peak of the drug action (Laties and Zrenner, 2002). Moreover, sildenafil was found to decrease visual performance, particularly temporal response, in S-cone isolating conditions (Stockman et al., 2007), and, in rare cases, transient blindness was reported (Montastruc et al., 2006). In order to understand the effects of sildenafil on retinal function different electrophysiological studies have been performed. However, these studies have yielded contradictory results. *In vivo* ERG recordings showed decreases in both a- and b-wave amplitudes in sildenafil-treated patients (Vobig et al., 1999), or inversely, an increase in the scotopic ERG responses, but a decrease in the photopic response (Luu et al., 2001). *Ex vivo* experiments have also shown some contradictory results. Sildenafil has been shown to increase ERG amplitudes in the rat retina (Barabas et al., 2003), whereas it decreases ERG amplitudes in bovine and human retinas, while increasing the latencies (Luke et al., 2005; Luke et al., 2007). To our knowledge, no studies so far have evaluated the effects of sildenafil, directly on RGC spiking activity, which forms the retinal output signal to the brain. Therefore, to further elucidate this issue, in the second part of the present study, we intended to investigate, using a MEA and *ex vivo* retinal preparations, the effect of different concentrations of sildenafil on principal characteristics of light-induced RGC responses (magnitude and latency) and the spontaneous RGC spiking activity.

CHAPTER 2
Materials & Methods

2.1 – Animals

Wistar rats, 8-10 weeks old, were obtained from Charles River, France. Long Evans rats, 8-10 weeks old, were obtained from Charles River for retinal ganglion cell (RGC) purification experiments and from Janvier Labs, Le Genest Saint Isle, France, for multi-electrode array (MEA) experiments. Animals were housed in a temperature- and humidity-controlled environment and were provided with standard rodent diet and water *ad libitum* while kept on a 12 h light/12 h dark cycle. All procedures involving the animals were in agreement with the guidelines on the ethical use of animals from the European Community Council Directive 2010/63/EU, transposed to Portuguese law in "Decreto-Lei nº 113/2013".

2.2 – Drugs and reagents

NPY and NPY receptor agonists and antagonists, as well as glutamate (L-glutamic acid), *N*-methyl-D-aspartic acid (NMDA), glycine, and sildenafil were exogenously applied to retinal cells and are listed in Table 1. NPY and NPY receptor agonist stock solutions (100-1000x) were dissolved in 0.0001% Tween 20 (Merck Millipore, Billerica, MA, USA) to reduce adsorption to plastic. For the remaining reagents, the manufacturer is indicated throughout the text. When not indicated, the reagent was obtained from Sigma-Aldrich, St. Louis, MO, USA.

Table 1. List of drugs used in the various experiments.

Drug	Purpose	Concentration	Catalog number	Manufacturer[a]
NPY	$Y_1/Y_2/Y_4/Y_5$ agonist	1-10 µM	H-6375	Bachem
(Leu^{31}, Pro^{34})-NPY	Y_1/Y_5 agonist	1 µM	H-3306	Bachem
NPY (13-36)	Y_2 agonist	0.3-1 µM	H-3324	Bachem
(Gly^1, …Aib^{32})-PP[b]	Y_5 agonist	1 µM	H-5088	Bachem
BIBP 3226	Y_1 antagonist	1 µM	2707	Tocris
BIBO 3304	Y_1 antagonist	10 µM	2412	Tocris
BIIE 0246	Y_2 antagonist	1-10 µM	1700	Tocris
L-152,804	Y_5 antagonist	1-100 µM	1382	Tocris
NMDA	NMDAR agonist	30-300 µM	M3262	Sigma-Aldrich
L-Glutamic acid	Agonist of all glutamate receptors	1-1000 µM	G1251	Sigma-Aldrich
Glycine	Co-agonist of NMDAR	10 µM	104201	Calbiochem
Sildenafil	PDE5 inhibitor	0.3-30 µM	PZ0003	Sigma-Aldrich

NMDAR, NMDA receptor
[a]Bachem, Bubendorf, Switzerland
Tocris Bioscience, Bristol, UK
Sigma-Aldrich, St. Louis, MO, USA
Calbiochem, Merck Millipore, Billerica, MA, USA
[b](Gly^1, Ser^{3,22}, Gln^{4,34}, Thr^6, Arg^{19}, Tyr^{21}, Ala^{23,31},Aib^{32})-pancreatic polypeptide

2.3 – Retinal ganglion cell purification

Purified RGCs were obtained from the retinas of either 3-4 days old pups or 8-10 weeks old Wistar or Long Evans rats by sequential immunopanning (Fig. 2.1), as previously described (Barres et al., 1988), with some modifications. This procedure is based on the expression of cell surface protein Thy 1 on RGCs, which is used to isolate RGCs in an immunopanning step. Other cell types, non-RGCs, namely macrophages and endothelial cells that also adhere to anti-Thy-1 coated plates (Barres et al., 1988), are removed in a preceding step with anti-macrophage serum. Next, the entire procedure is detailed. Rats were killed by decapitation or

cervical dislocation, the eyes enucleated and the retinas dissected in ice cold sterile Dulbecco's Modified Eagle Medium (DMEM; Gibco, Life Technologies, Grand Island, NY, USA) supplemented with 5% D-glucose and 44 mM NaHCO$_3$. Retinas were incubated for 30 min at 37 °C in Earl's Balanced Salt Solution (EBSS; in mM: 1.8 CaCl$_2$, 0.8 MgSO$_4$, 5.3 KCl, 26 NaHCO$_3$, 117 NaCl, 1 NaH$_2$PO$_4$, 5.6 D-glucose, pH 7.4) containing 16.5 U/ml papain (Worthington Biochemical, Lakewood, NJ, USA), 1.65 mM L-cysteine, and 124 U/ml deoxyribonuclease I (DNase I), to allow tissue digestion. The cell suspension was gently triturated in an enzyme inhibitor solution containing 1.5 mg/ml ovomucoid (Roche, Basel, Switzerland), 1.5 mg/ml bovine albumin serum (BSA) and 124 U/ml DNase I in EBSS. The retinal tissue was allowed to settle for 1-2 min. Then, ovomucoid solution was discarded and retinal tissue further triturated in a solution containing 1.5 mg/ml ovomucoid (Roche), 1.5 mg/ml BSA, 124 U/ml DNase I and 1:125 (v:v) rabbit anti-rat macrophage antiserum (Accurate Chemical, Westbury, NY, USA), to yield a single cell suspension, and incubated for 10 minutes at RT. After centrifugation for 11 min at 190 g at RT, the supernatant was discarded and cells were resuspended in EBSS containing 10 mg/ml ovomucoid (Roche) and 10 mg/ml BSA and then centrifuged for 10 min at 190 g at RT. The supernatant was discarded and cells resuspended in Dulbecco's Phosphate Buffered Saline (DPBS; in mM: 0.9 CaCl$_2$, 0.5 MgCl$_2$, 2.7 KCl, 1.47 KH$_2$PO$_4$, 138 NaCl, 8 Na$_2$HPO$_4$, 0.33 sodium pyruvate (Gibco), 5.6 D-glucose, pH 7.4) containing 0.2 mg/ml BSA and 5 µg/ml insulin. Cell suspension was plated in a 150 mm Petri dish coated with 5.3 µg/ml goat anti-rabbit IgG (H+L) antibody (Rockland Immunochemicals, Gilbertsville, PA, USA). After 30 min at RT, non-adherent cells were removed to a second 150 mm Petri dish coated similarly. After 30 min at RT, non-adherent cells were removed to a 100 mm dish coated with 6.7 µg/ml goat anti-mouse IgM antibody (Rockland Immunochemicals) and mouse anti-rat Thy1.1 hybridoma supernatant of T11D7e cell line (TIB-103, ATCC, Manassas, VA, USA). After 30 min, the non-adherent cells were washed out with Ca^{2+}- and Mg^{2+}-free DPBS (in mM: 138 NaCl, 2.7 KCl, 8 Na$_2$HPO$_4$, 1.47 KH$_2$PO$_4$, pH 7.4), and the adherent RGCs were detached with a 0.125% trypsin solution in Ca^{2+}- and Mg^{2+}-free EBSS (in mM: 116 NaCl, 5.3 KCl, 1 NaH$_2$PO$_4$, 5.6 D-glucose, 26 NaHCO$_3$, pH 7.4). Trypsinization was stopped with 30% FBS (Gibco) in Neurobasal-A (Gibco), and the RGCs were detached. The cell suspension was centrifuged for 10 min at 190 g, at RT, and the supernatant was discarded.

For cell culturing, RGCs were resuspended in Neurobasal-A (Gibco) medium containing 1x B27 supplement (Gibco), 5 µg/ml insulin, 1mM sodium pyruvate (Gibco), 1x Sato/Bottenstein supplement which includes 100 µg/ml transferrin, 100 µg/ml BSA, 16 µg/ml

putrescine, 62 ng/ml progesterone, and 40 ng/ml sodium selenite, 40 ng/ml triiodo-L-thyronine, 2 mM L-glutamine, 5 mg/ml N-acetylcysteine, 100 µM inosine, 20 ng/ml ciliary neurotrophic factor (Peprotech, Rocky Hill, NJ, USA), 25 ng/ml brain-derived neurotrophic factor (Peprotech), 5 µM forskolin, 10 ng/ml basic fibroblast growth factor (Gibco) and 50 µg/ml gentamicin (Gibco), and were plated at a density of 460 cells/mm^2 on 12 mm glass coverslips coated with 10 µg/ml poly-D-lysine and 10 µg/ml laminin. Cells were cultured for 16 to 48 h at 37 °C in a humidified environment of 5% CO_2. For RNA extraction, the cell pellet was lysed in TRIzol^{TM} reagent, as further described below.
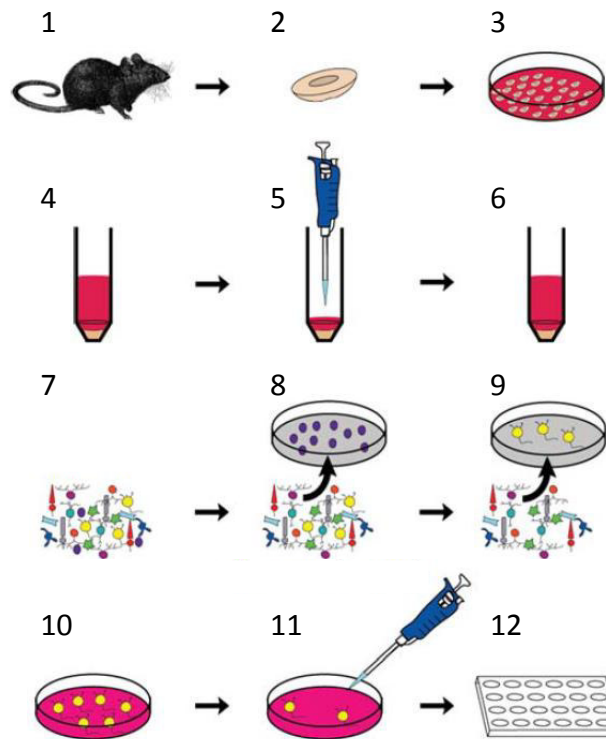
Figure 2.1. RGC purification by sequential immunopanning. Eyes from Wistar or Long Evans rats (1) were enucleated (2) and the retinas dissected (3). Retinas were incubated with papain (4) to allow tissue digestion. Retinas were then gently triturated (5) and the cell suspension incubated with rabbit anti-rat macrophage antiserum (6). After further dissociation and centrifugation to remove papain, the obtained cell suspension (7) was plated in a Petri dish coated with anti-rabbit IgG to remove non-RGCs expressing Thy1 (8; blue cells). Then non-adherent cells were plated in a Petri dish coated with anti-rat Thy1.1 hybridoma supernatant to isolate RGCs (9; yellow cells). Non-adherent cells were discarded and the adherent RGCs were incubated with trypsin (10). RGCs were then detached (11) and cultured up to 48 h (12). Adapted from (Winzeler and Wang, 2013).

2.4 – Culture of retinal explants

Wistar rats (8-10 weeks old) were killed by cervical dislocation. Retinas were dissected in Ca^{2+}- and Mg^{2+}-free Hank's Balanced Salt Solution (HBSS, in mM: 5.4 KCl, 0.44 KH_2PO_4, 137 NaCl, 4.2 $NaHCO_3$, 0.34 Na_2HPO_4, 5.6 D-glucose, 10 HEPES, 1 sodium pyruvate, pH 7.4) and flat-mounted onto 30 mm diameter culture plate inserts with a 0.4 µm pore size (Millicell, Merck Millipore, Billerica, MA, USA), with the GCL facing upward (Fig. 2.2). The retinal explants were cultured in six-well plates in Neurobasal-A (Gibco, Life Technologies, Grand Island, NY, USA) medium containing 1x B27 supplement (Gibco), 2 mM L-glutamine and 50 µg/ml

gentamicin (Gibco), and maintained for 4 days *in vitro* (DIV) in a humidified environment at 37 °C and 5% CO_2.

Figure 2.2. Cultured retinal explant. Example of a retinal explant on a culture insert with the GCL facing upward.

2.5 – Reverse-transcription polymerase chain reaction (RT-PCR)

Total RNA was isolated from RGCs using TRIzol™ reagent (Ambion, Life Technologies, Grand Island, NY, USA). Subsequently, cDNA first strand synthesis was performed from 2 µg DNase-treated RNA using random primers and SuperScript II Reverse Transcriptase (Invitrogen, Life Technologies). The resulting cDNA (0.5 µl) was used for amplification of respective targets with AmpliTaq Gold DNA polymerase (Applied Biosystems, Life Technologies), 200 nM of primer and 2 mM $MgCl_2$, in a Veriti thermal cycler (Applied Biosystems). Reactions were performed as follows: denaturation for 3 min at 95 °C; 40 cycles, each consisting of 95 °C for 30 sec, annealing temperature for 30 sec, and 72 °C for 30 sec; and final extension at 72 °C for 5 min. The primers used are indicated in Table 2. PCR products were separated on a 1.5% agarose gel. β-actin was used as an internal control. The gel images were digitally acquired in a Gel/ChemiDoc (Bio-Rad Laboratories, Hercules, CA, USA) and the level of gene transcription was evaluated and categorized as detected or not detected.

Table 2. Primers used for RT-PCR.

Target	Forward Primer (5'-3') Reverse Primer (5'-3')	Annealing Temperature	Product Size
NPY	AGAGATCCAGCCCTGAGACA TTTCATTTCCCATCACCACA	57 ºC	110 bp
Y_1 receptor	ACGTTCGCTTGAAAAGGAGA CATGACGTTGATTCGTTTGG	57 ºC	89 bp
Y_2 receptor	CAGTTTTGTGCCATTTGGTG AGGAAGCTGATTTGCTTGGA	60 ºC	142 bp
Y_4 receptor	ATCTCATGGCCTCCCTTTCT TCTCAACGCTGTAGGTGGTG	57 ºC	141 bp
Y_5 receptor	ATACAGCTGCTGCTCGGAAT GATTGCCCATAAAGCCAAGA	57 ºC	126 bp
Brn3a	CCCTGAGCACAAGTACCCGTCGCTGC CCGGCTTGAAAGGATGGCTCTTGCCC	60 ºC	184 bp
GFAP	TGGTATCGGTCCAAGTTTGCA TGGCGGCGATAGTCATTAGC	60 ºC	98 bp
CD11b	GATGCTTACTTGGGTTATGCTT CGAGGTGCCCCTAAAACCA	60 ºC	74 bp
β-actin	CTAAGGCCAACCGTGAAAAG ATCACAATGCCGTGGTACG	60 ºC	124 bp

bp, base pairs

2.6 – Immunofluorescence labelling

2.6.1 – Immunocytochemistry in purified retinal ganglion cells

Purified RGCs were fixed with 4% paraformaldehyde (PFA) for 20 min at RT in phosphate buffer saline (PBS; in mM: 137 NaCl, 2.7 KCl, 1.8 KH_2PO_4, 10 Na_2HPO_4, pH 7.4), washed three times in PBS and permeabilized with 1% Triton X-100 in PBS for 5 min at RT. After washing three times in PBS, the unspecific binding was prevented by incubating cells in a 3% BSA and 0.2% Tween 20 (Merck Millipore, Billerica, MA, USA) blocking solution, in PBS for 60 min at RT. Then, cells were incubated with primary antibodies (Table 3) diluted in blocking solution for 90 min at RT as follows: rabbit anti-NPY (1:1000), anti-Y_1 (1:500), anti-Y_2 (1:500), anti-Y_4 (1:25), anti-Y_5 (1:250), or anti-Brn3a (1:25). After washing three times in PBS, cells were incubated with the secondary antibodies diluted in blocking solution for 60 min at RT as follows: Alexa Fluor (AF) 568 anti-mouse (1:200), AF 488 anti-rabbit (1:200), or AF 488 anti-sheep (1:200). After washing three times in PBS, the nuclei were stained with 2.5 μg/ml

DAPI (Molecular Probes, Life Technologies, Grand Island, NY, USA) for 10 min at RT. After washing three times in PBS, the coverslips were mounted on glass slides using Glycergel™ mounting medium (Dako, Agilent Technologies, Santa Clara, CA, USA). Images were acquired in a laser scanning confocal microscope LSM 710 (Zeiss, Oberkochen, Germany).

Table 3. List of antibodies used for immunofluorescence labelling.

Antibody	Dilution	Catalog Number	Manufacturer[a]
Rabbit anti-NPY	1:1000 - 1:10000	N9528	Sigma-Aldrich
Sheep anti-Y_1 receptor	1:200 - 1:500	6732-0150	AbD Serotec
Rabbit anti-Y_2 receptor	1:500 - 1:2000	ANR-022	Alomone Labs
Rabbit anti-Y_4 receptor	1:25 - 1:200	ANR-024	Alomone Labs
Rabbit anti-Y_5 receptor	1:250 - 1:2000	ANR-025	Alomone Labs
Mouse anti-Brn3a	1:25 - 1:500	MAB 1585	Merk Millipore
Mouse anti-Vimentin	1:500	MS129P1	Lab Vision
AF 568 goat anti-rabbit	1:500	A-11011	Molecular Probes
AF 488 goat anti-rabbit	1:200	A-11008	Molecular Probes
AF 568 goat anti-mouse	1:200 - 1:500	A-11004	Molecular Probes
AF 488 goat anti-mouse	1:500	A-11001	Molecular Probes
AF 488 donkey anti-sheep	1:200 - 1:500	A-11015	Molecular Probes

AF, Alexa Fluor
[a]Sigma-Aldrich, St. Louis, MO, USA
AbD Serotec, Bio-Rad Laboratories, Hercules, CA, USA
Alomone Labs, Jerusalem, Israel
Merck Millipore, Billerica, MA, USA
Lab Vision, Thermo Fisher Scientific, Walthman, MA, USA
Molecular Probes, Life Technologies, Grand Island, NY, USA

2.6.2 – Immunohistochemistry in retinal sections

Adult Wistar rats were transcardially perfused with 250 ml PBS followed by 250 ml 4% PFA at RT, under deep anaesthesia with 90 mg/kg (ip) ketamine (Imalgene™, Merial, Porto Salvo, Portugal) and 10 mg/kg (ip) xylazine (Rompun™, Bayer, Leverkusen, Germany). Then, the eyes were enucleated and the lens were removed. The eye cup was further fixed for 60 min in PFA. After washing in PBS, the tissue was transferred sequentially to 15% and 30% (w/v) sucrose in PBS for at least 120 min each. The eye cup was embedded in a mixture 1:1 of 30% sucrose and cryomatrix embedding resin (Thermo Fisher Scientific, Walthman, MA, USA), and stored at -80 °C. Retinal sections, 10 µm thickness, were obtained in a cryostat and collected on SuperFrost Plus glass slides (Menzel-Glaser, Thermo Fisher Scientific) and stored at -20 °C. Retinal sections air dried for at least 45 min at RT and were fixed with acetone for 10 min at -

20 °C. In the case of Y_2, Y_4, and Y_5 receptors, the fixation with acetone was replaced by an antigen retrieval step with 10 mM sodium citrate (Panreac, Barcelona, Spain) and 0.05% Tween 20 (Merck Millipore), pH 6, for 30 min at 95 °C. The sections were then washed two times in PBS and permeabilized in 0.25% Triton X-100 in PBS for 30 min at RT. Sections were blocked in 1% BSA and 10% goat serum (donkey serum in the case of Y_1) in PBS for 30 min at RT. Sections were incubated overnight at 4 °C with primary antibodies (Table 3) diluted in 1% BSA in PBS: anti-NPY (1:10000), anti-Y_1 (1:200), anti-Y_2 (1:2000), anti-Y_4 (1:200), anti-Y_5 (1:2000), anti-Brn3a (1:500), or anti-Vimentin (1:500). After washing three times in PBS for a total of 30 min, sections were incubated for 60 min at RT with the corresponding secondary antibodies diluted in 1% BSA in PBS: AF 488 anti-mouse (1:500), AF 568 anti-mouse (1:500), AF 568 anti-rabbit (1:500), or AF 488 anti-sheep (1:500). After washing three times in PBS for a total of 30 min, the nuclei were stained with DAPI (2.5 µg/ml, Molecular Probes) in PBS for 10 min at RT and the sections were coverslipped using Glycergel^{TM} mounting medium (Dako). Images were acquired in a laser scanning confocal microscope LSM 710 (Zeiss).

2.6.3 – Immunohistochemistry in retinal explants

Retinal explants were washed two times with PBS and fixed in 100% ethanol (Merck Millipore) at -20 °C for 10 min. After washing the explants three times in PBS, unspecific binding was prevented by incubating explants in a 10% goat serum, 1% BSA, and 0.1% Tween 20 (Merck Millipore) in PBS blocking solution for 60 min at RT. Retinal explants were then incubated with anti-Brna3a antibody (Table 3) diluted (1:500) in blocking solution for 3 days at 4 °C. After washing again the explants more than six times in PBS for a total of 24 h, explants were incubated with the secondary antibody AF 568 anti-mouse (1:200). Then, after washing explants more than six times in PBS for a total of 24 h, explants were coverslipped using Glycergel^{TM} mounting medium (Dako). Images were acquired in a laser scanning confocal microscope LSM 710 (Zeiss).

2.7 – TdT-mediated dUTP nick-end labelling (TUNEL) assay

2.7.1 – TUNEL in retinal slices

The TUNEL assay measures the fragmented DNA of apoptotic cells by incorporating fluorescein labelled dUTPs at 3'-OH DNA ends using terminal deoxynucleotidyl transferase (TdT). The TdT enzyme forms a polymeric tail allowing visualization in histological sections (Gavrieli et al., 1992). TUNEL assays was performed following the manufacturer's instructions (Catalog number: G3250; Promega, Madison, WI, USA). After Brn3a labelling procedure as above mentioned, retinal sections were washed three times in PBS for a total of 30 min and then permeabilized with 20 µg/ml proteinase K in PBS for 10 min at RT. After washing in PBS for 5 min, the sections were incubated with equilibration buffer (in mM: 200 potassium cacodylate, 25 Tris, 0.2 dithiothreitol, 2.5 $CoCl_2$, and 0.25 mg/ml BSA, pH 6.6) for 10 min at RT. Next, sections were incubated with 600 U/ml recombinant TdT enzyme and nucleotide mix containing 5 µM fluorescein-12-dUTPs, 10 µM dATP, and 0.1 mM EDTA, diluted in equilibration buffer at 37 °C for 60 min. The reaction was stopped by immersing the slides in saline-citrate buffer (in mM: 300 NaCl, 30 sodium citrate, pH 7.0) for 15 min at RT. After washing three times in PBS, the nuclei were stained with DAPI (2.5 µg/ml, Molecular Probes, Life Technologies, Grand Island, NY, USA) for 10 min at RT. After washing three times in PBS sections were mounted with Glycergel™ mounting medium (Dako, Agilent Technologies, Santa Clara, CA, USA). Images of retinal sections were acquired in a fluorescence microscope (DM IRE2, Leica, Wetzlar, Germany). The Brn3a- and TUNEL-positive cells were counted and results were expressed per mm of GCL length.

2.7.2 – TUNEL in retinal explants

Retinal explants were fixed in 4% PFA in PBS for 15 min at RT and permeabilized with 20 µg/ml proteinase K in PBS for 15 min at RT. After washing in PBS, retinal explants were fixed in 4% PFA in PBS for 5 min, washed in PBS, and incubated in equilibration buffer for 10 min at RT. Then, retinal explants were incubated with 600 U/ml recombinant TdT enzyme and nucleotide mix containing 5 µM fluorescein-12-dUTPs, 10 µM dATP, and 0.1 mM EDTA, diluted in equilibration buffer at 37 °C for 60 min. The reaction was stopped by incubating the retinal explants in saline-citrate buffer for 15 min at RT. After washing in PBS, the nuclei were stained with DAPI (2.5 µg/ml, Molecular Probes) in PBS for 15 min at RT and retinal explants mounted

with Glycergel™ mounting medium (Dako). At least 12 images of GCL per retinal explant (three images per each quadrant) were acquired in a laser scanning confocal microscope LSM 710 (Zeiss, Oberkochen, Germany).

2.8 – Propidium iodide incorporation assay

Propidium iodide (PI) binds nucleic acids by intercalating the bases and can be visualized under fluorescence microscope, with maximum fluorescence emission at 608 nm (red) and maximum excitation at 540 nm (green). PI is only incorporated in dead or dying cells with disrupted cell membranes, thus allowing evaluating cells undergoing necrotic or late apoptotic cell death. For PI incorporation assay, cultured retinal explants were incubated with 2 µM PI for 180 min at DIV2 and at DIV4. Images comprising the four quadrants of retinal explant were acquired in a fluorescence microscope (DM IRE2, Leica, Wetzlar, Germany). PI-positive cells were counted at DIV2 before NMDA treatment and at DIV4. The extent of cell death was expressed as the ratio between PI-positive cells at DIV4 and DIV2.

2.9 – [^{35}S]GTPγS binding in retinal sections

[^{35}S]GTPγS binding assay has been widely used to evaluate the activation of GPCRs taking advantage of a radiolabeled non-hydrolyzable GTP analogue - [^{35}S]GTPγS (Harrison and Traynor, 2003). Upon activation of the GPCR by an agonist, Gα binds [^{35}S]GTPγS allowing the measurement of the amount of radiolabeled GTP bound to the cell membrane (Fig. 2.3). In order to evaluate the presence of functional active NPY receptors in the rat retina, we used 8-10 weeks old Wistar rats. The eyes were enucleated and frozen in dry ice. Retinal slices, 18 µm thickness, were obtained in a cryostat, collected onto SuperFrost Plus glass slides (Menzel-Glaser, Thermo Fisher Scientific, Walthman, MA, USA) and stored at -80 °C until further processing. Sections were air dried for 30 min at RT and then rehydrated in assay buffer A (in mM: 50 Tris-HCl, 3 MgCl$_2$, 0.2 EGTA, 100 NaCl, pH 7.4) for 10 min at RT. Sections were pre-incubated in assay buffer B [assay buffer A + 0.2 mM dithiothreitol, 1 µM 1,3-dipropyl-8-cyclopentylxanthine (DPCPX), 0.5% w/v BSA, and 2 mM GDP] for 15 min at RT to shift all G-

proteins into the inactive state. Subsequently, incubation of retinal slices was performed in assay buffer B + 50 pM [^{35}S]GTPγS (1250 Ci/mmol; PerkinElmer, Waltham, MA, USA) for 60 min at RT with 1-10 µM NPY. In each experiment, basal binding was determined by incubation without NPY receptor ligands but with assay buffer B + 50 pM [^{35}S]GTPγS (1250 Ci/mmol). Specificity was confirmed by adding a combination of the NPY receptor antagonists: 10 µM BIBO 3304 for Y_1; 10 µM BIIE 0246 for Y_2; 100 µM L-152,804 for Y_5. For antagonistic studies, NPY receptor antagonists were also added to the pre-incubation buffer B. Incubation was terminated by two washes of 5 min each in ice cold 50 mM Tris-HCl buffer, pH 7.4, followed by a final wash in deionised water. Sections were air dried at RT and exposed to Kodak BioMax MR autoradiography films (Carestream Health, Rochester, NY, USA) together with ^{14}C-microscales (Amersham, GE Healthcare, Little Chalfont, UK) for 5 days at -20 °C. The films were developed in Kodak GBX developer. Retinal slices in autoradiography films were acquired with a digital camera Axiocam ERc5s (Zeiss, Oberkochen, Germany) coupled to a stereo microscope Discovery.V8 (Zeiss). The optical densities of retinal slices were measured using ImageJ software (http://imagej.nih.gov/ij/) and the values obtained converted to estimated nCi/g tissue using ^{14}C-microscales.
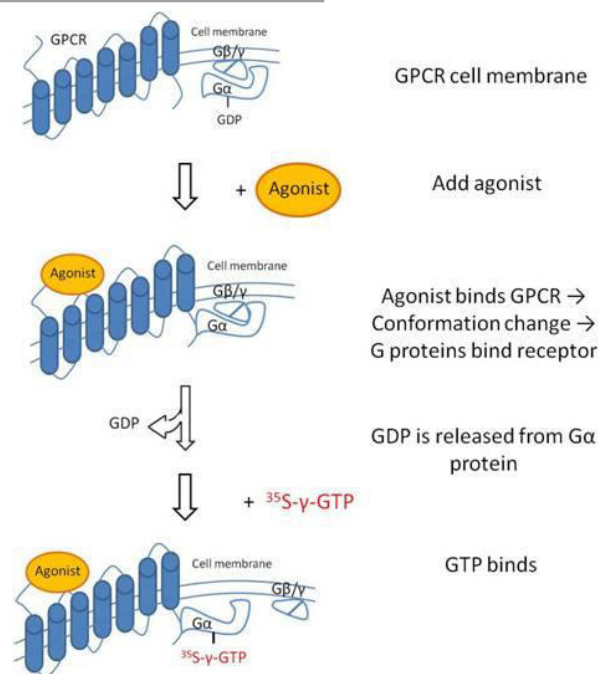
Figure 2.3. [^{35}S]GTPγS binding to GPCR. Upon activation of the GPCR by an agonist, Gα subunit release GDP and binds [^{35}S]GTPγS. From www.perkinelmer.com.

2.10 – Ca^{2+} imaging in purified retinal ganglion cells

Purified RGCs cultured for 1 or 2 DIVs were used to assess the [Ca^{2+}]$_i$ using the Ca^{2+} dye Fura-2-acetoxymethyl ester (Fura-2-AM). Fura-2-AM is a membrane permeable ratiometric calcium indicator which fluorescence excitation spectrum shifts to shorter wavelengths upon binding to Ca^{2+} (Grynkiewicz et al., 1985). This property allows for measurements of [Ca^{2+}]$_i$ based on ratio calculation between fluorescence obtained when excited at 340 and 380 nm. The AM group enable Fura-2 to cross the cell membrane. Once the dye is taken up into cells the AM group is removed by esterases and the dye is trapped inside. Next, the entire procedure is detailed. Purified RGC cultures were washed two times in 0.1% free fatty acid BSA (Calbiochem, Merck Millipore, Billerica, MA, USA) in Mg^{2+}-free HBSS solution (in mM: 138 NaCl, 5.3 KCl, 0.34 Na$_2$HPO$_4$, 0.44 KH$_2$PO$_4$, 2.6 CaCl$_2$, 5.6 D-glucose, 15 HEPES, 4.2 NaHCO$_3$, pH 7.4) at 37 °C. After washing, RGCs were then loaded with 5 µM Fura-2-AM in the presence of 0.02% Pluronic F-127 (both Molecular Probes, Life Technologies, Grand Island, NY, USA) in 0.1% free fatty acid BSA in Mg^{2+}-free HBSS for 45 min at 37 °C. After washing two times in 0.1% free fatty acid BSA in Mg^{2+}-free HBSS at 37 °C, RGCs were incubated in Mg^{2+}-free HBSS for 15 min at 37 °C. Under continuous perfusion (2.9 ± 0.1 ml/min) with Mg^{2+}-free HBSS solution,

RGCs were exposed to glutamate for 30 sec (Fig. 2.4 A, B), and all glutamate stimuli included 10 µM glycine, a co-agonist of NMDA glutamate receptor, as previously described (Hartwick et al., 2004). RGCs were alternately excited at 340 and 380 nm, with a fluorescence microscope Axiovert 200 (Zeiss, Oberkochen, Germany) coupled to a perfusion system. A ratio of fluorescence intensity (340 nm / 380 nm), as indicative of $[Ca^{2+}]_i$, was calculated for each individual cell by Metafluor software (Molecular Devices, Sunnyvale, CA, USA). The increase above basal Fura-2 ratio (340 nm / 380 nm) was quantified for each stimulus as a Delta value (Fig. 2.4 C). Fura-2 ratios (R) were converted to $[Ca^{2+}]_i$ in separate calibration experiments (Fig. 2.4 D) using the formula:

$$[Ca^{2+}]_i = [K_d(F_0/F_S)][(R - R_{min})/(R_{max} - R)],$$

with K_d for Fura-2 of 224 nM, and where F_0/F_S is the ratio of fluorescence intensity at 380 nm excitation in calcium-free solution over the intensity in solution with saturated Ca^{2+} levels. The minimum value for the Fura-2 ratio (R_{min}) was obtained using Ca^{2+}-free HBSS (in mM: 138 NaCl, 5.3 KCl, 0.34 Na_2HPO_4, 0.44 KH_2PO_4, 5.6 D-glucose, 15 HEPES, 4.2 $NaHCO_3$, 5 EGTA, pH 8.0) and 1 µM ionomycin, after which the cells were perfused with Mg^{2+}-free HBSS and 1 µM ionomycin in order to calculate the maximum value for Fura-2 ratio (R_{max}). We obtained basal values for $[Ca^{2+}]_i$ in purified RGC of 54 ± 6 nM, while upon stimulation with 30 µM glutamate and 10 µM glycine $[Ca^{2+}]_i$ values increased to 733 ± 59 nM, which are in agreement with previous studies (Hartwick et al., 2004; Hartwick et al., 2008).

A

B

C

D
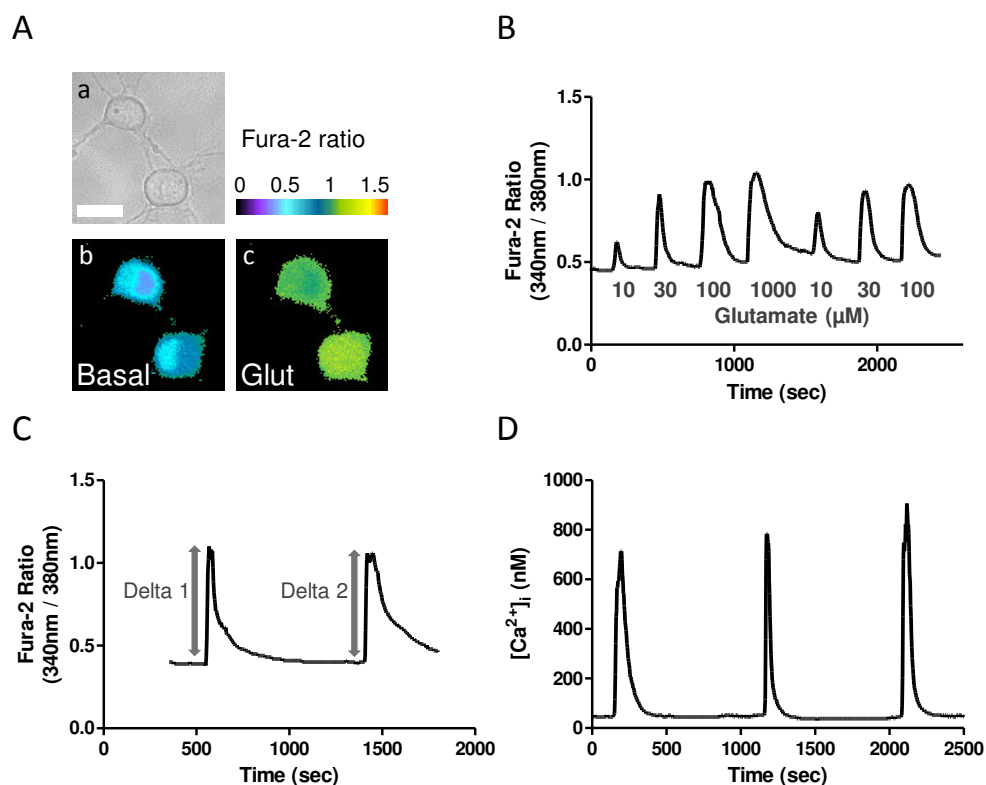
Figure 2.4. Ca²⁺ imaging in purified retinal ganglion cells. (A) Cultured RGCs are shown. Bright field image (a) and pseudocolour representation of Fura-2 ratio on basal condition (b) and after stimulation with 30 µM glutamate (c) are shown. (B) Fura-2 ratio trace from a cultured RGC illustrating the response of RGCs to increasing concentrations of glutamate (10 - 1000 µM). (C) Fura-2 ratio traces showing RGC responses to two consecutive 30 µM glutamate stimuli for 30 sec each. The increase above basal Fura-2 ratio 340 nm / 380 nm was quantified for each stimulus as a Delta value. (D) Representative $[Ca^{2+}]_i$ trace from a cultured RGC upon three consecutive stimuli of 30 µM glutamate, after conversion of Fura-2 ratio to is illustrated $[Ca^{2+}]_i$.

2.11 – *Ex vivo* multi-electrode array recordings

2.11.1 – Stimulation and multi-electrode array recordings

Recording of extracellular action potentials from RGCs is a useful technique to assess the effect of exogenously applied drugs on *ex vivo* retinas (Meister et al., 1994; Rosolen et al., 2008). Long Evans rats (8 weeks old) were killed by CO_2 inhalation and quick cervical dislocation under dim red light. Eyes were enucleated and placed in oxygenated Ames' medium (Sigma-Aldrich) at RT. Square pieces of retina (1-2 mm²) were placed into the recording chamber (Fig. 2.5 A), with the GCL facing the MEA60 biochip electrode array. The electrode array was composed of 60 titanium nitride electrodes (Fig. 2.5 B), 10 µm diameter

each, disposed in an 8×8 layout with 100 μm inter-electrode spacing (Multi Channel Systems, GmbH, Reutlingen, Germany). Retinas were held in the centre of the electrode array using a piece of polycarbonate membrane covered by a U-shaped platinum ring with a nylon mesh. During recording sessions, retinas were continuously perfused with Ames' medium equilibrated with 95% O_2 and 5% CO_2, pH 7.4, at a rate flow of 1.3 ml/min. Retinas were maintained at 34-37 °C through a heating pad of the recording system. In order to obtain stable recordings, each session started 60 min after placing the retina in MEA recording chamber.
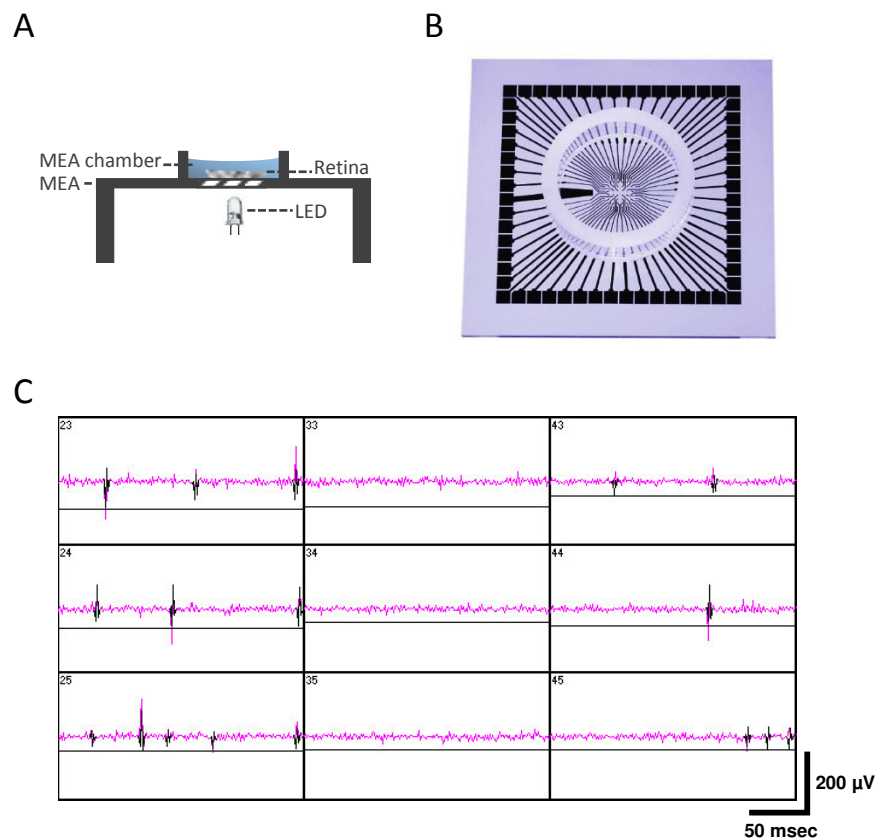
Figure 2.5. MEA recordings from RGCs. (A) Scheme of the MEA recording system illustrating the position of the retina in the centre of MEA chamber and the light-emitting diode (LED) used to elicit light responses. (B) The MEA60 biochip included a MEA chamber where 60 electrodes are positioned in the centre. Note that MEA is built on glass allowing for light stimulation through the bottom. (C) Examples of RGC spiking activity over 9 electrodes during a recording session using MC_Rack software. When the raw waveform (pink) exceeds the manually adjusted threshold (horizontal line) for each electrode it is quantified as en event.

MEA recordings were conducted using MEA60 setup (Multi Channel Systems). The analogue extracellular neuronal signals from 60 channels were AC amplified (×1000-1200), band-pass filtered (200-3000 Hz), sampled at 20-30 kHz, and saved in PC-compatible computer

for subsequent off-line analysis. RGC spiking activity was monitored during recording sessions (Fig. 2.5 C) using MC_Rack software (Multi Channel Systems). Light-induced responses were evaluated under dark conditions (Fig. 2.6 A). To elicit light responses in the RGCs, white light episodes from light-emitting diodes (LEDs) driven by a stimulus generator STG-1008 (Multi Channel Systems) were applied. The LEDs were positioned 5 mm below the transparent MEA chamber and used to generate full-field stimuli in the photopic range (5.0 cd/m^2). Stimulus consisted of 10 consecutive stimulus blocks with 5 sec light followed by 10 sec dark each.

2.11.2 – Spike sorting and data analysis

The recordings were subsequently subjected to off-line spike sorting and analysis using Spike2 (Cambridge Electronic Design, Cambridge, UK). Waveforms were isolated using a combination of template matching algorithm and cluster cutting based on principal components of individual waveforms (Fig. 2.6 B). The spontaneous activity was calculated for each RGC as spiking rate (Hz).
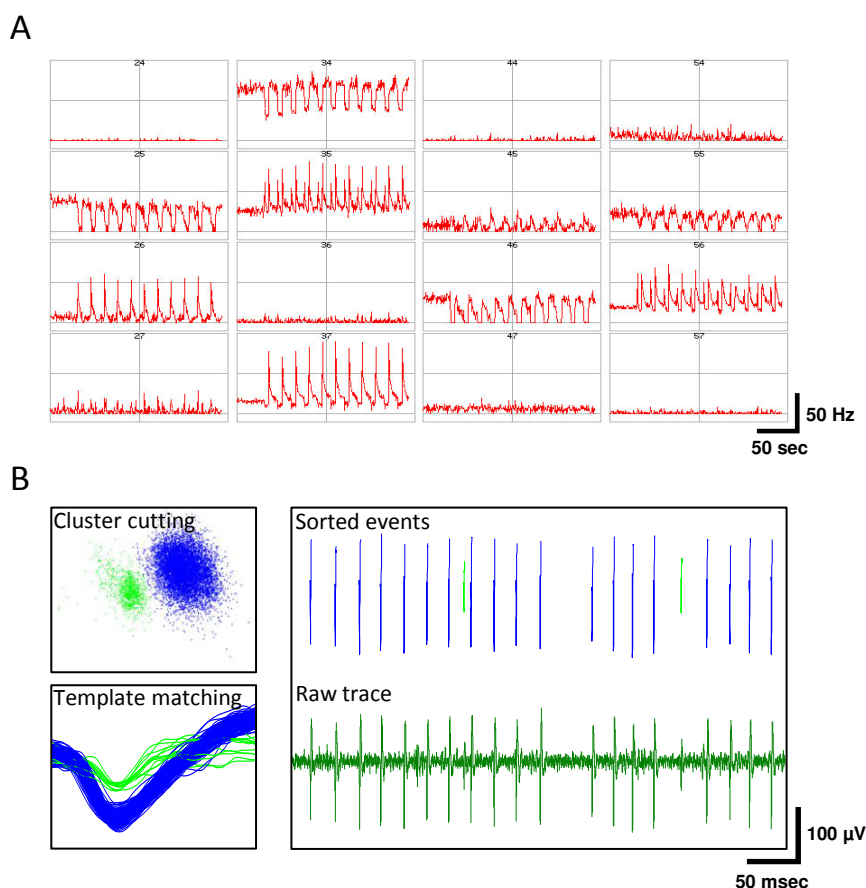
Figure 2.6. MEA recordings from RGCs. (A) Examples of RGC spiking frequency changes over 16 electrodes upon repeated light stimulation using MC_Rack software. Frequency of detected events is shown (red) for each electrode. Note that we only used MC_Rack for live monitoring of spiking activity during recording sessions. (B) The spike activity quantification was performed after off-line spike sorting using Spike2 software. In order to isolate individual RGC spiking activity, a combination of template matching and cluster cutting based on principal components of individual waveforms was used. In this example, blue spikes are taken and green spikes are discarded.

To detect changes in spontaneous activity induced by light, the raster and peri-stimulus time histograms (PSTH) were generated from 10 stimulus blocks using 50 msec bin widths (Fig. 2.7). The onset of ON- and OFF-type RGC responses were defined as an increase in spike

number higher than 2SD than the pre-stimulus frequency over at least three consecutive bins. The initial burst responses to both light onset (ON-type RGCs, Fig. 2.7 A) and dark onset (OFF-type RGCs, Fig. 2.7 B) were quantified over a 50 msec bin. The mean spiking rates over 1 and 5 sec after light onset (ON-type RGCs) or dark onset (OFF-type RGCs) were also quantified. The majority of RGC light responses were classified as transient showing an initial burst response to light or dark onset followed by a rapid decrease in spiking activity. Latency was defined as the time delay between light or dark period onset (ON- or OFF-type RGCs respectively) and the RGC light response as defined above, when aligned in raster plots for consecutive light stimuli. In addition to light stimulation, in some experiments, 30 µM NMDA was applied for 5 min to induce increased RGC spiking activity. Under continuous perfusion different drugs were bath-applied: 1 µM NPY, 1 µM (Leu^{31}, Pro^{34})-NPY, 1µM NPY (13-36), 1 µM (Gly^1, …Aib^{32})-PP, or 0.3 to 30 µM sildenafil citrate. Effects of each drug and concentrations was assessed in, at least, 3 different retinal preparations.
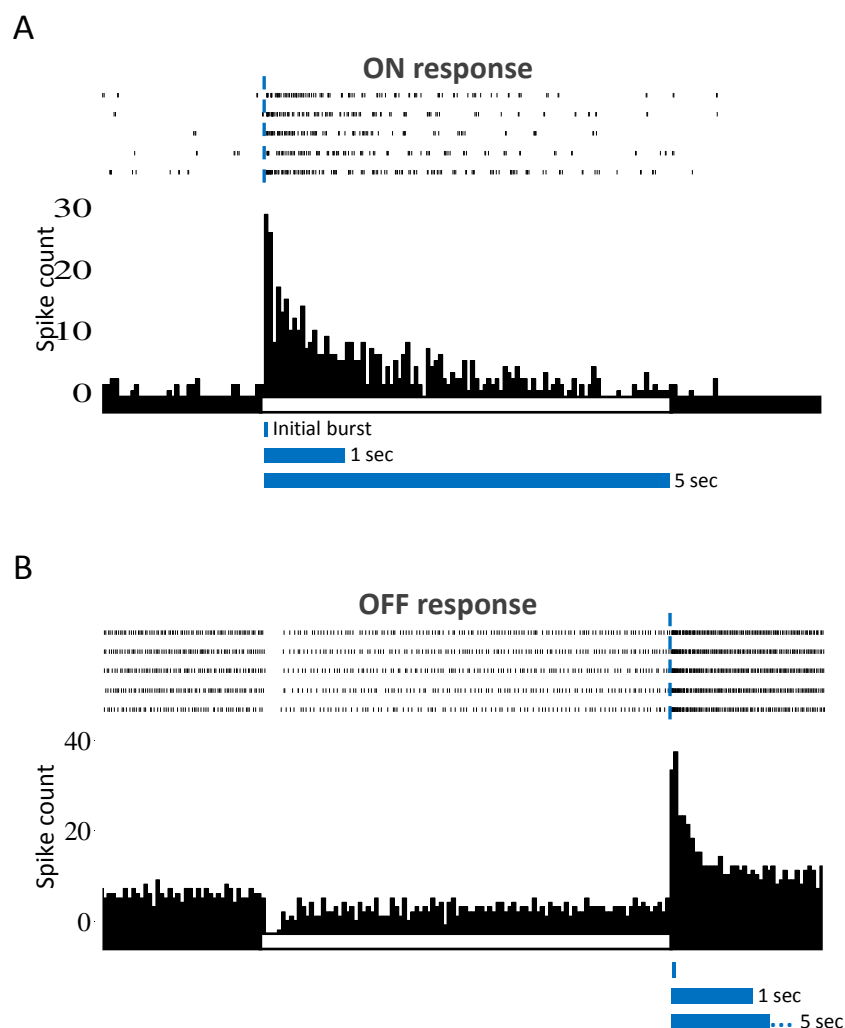
Figure 2.7. RGC light response quantification. Examples of peri-stimulus time histograms (PSTHs) and raster plots for ON- (A) and OFF-type (B) RGC light responses are shown for five consecutive stimulus blocks. White bars indicate duration of light period. Blue horizontal bars indicate the time window used for quantification of light stimulus-induced mean spiking rate for ON-type RGCs (A), namely initial burst (50 msec), 1 sec, and 5 sec. (B) OFF-type RGC light responses were quantified similarly, though the starting point for quantification corresponded to dark onset. Note that the 5 sec bar was shortened to fit in the figure. Vertical dashed lines indicate the position used for latency quantification for ON- (A) and OFF-type (B) RGC light responses, determined in aligned raster plots for consecutive light stimuli.

2.12 – Intravitreal injections and retinal ischemia-reperfusion injury

Wistar rats were anaesthetized by 2.5% isoflurane (Abbott Laboratories, North Chicago, IL, USA) inhalation, using a gas-anaesthetizing system (VetEquip, Pleasanton, CA, USA) and the O_2 flowmeter adjusted to 1 l/min. Then, 4 mg/ml oxybuprocaine (Laboratórios Edol, Linda-a-Velha, Portugal) anaesthetic was applied topically to the eyes and the pupils dilated with 10 mg/ml tropicamide (Laboratórios Edol). Intravitreal injection of 5 μl containing 10 μg NPY or sterile saline solution was performed using a 10 μl Hamilton syringe (Hamilton, Reno, NV, USA) with a 30-gauge needle, in both eyes, 120 min before the induction of retinal ischemia-reperfusion (I-R). Fusidic acid (10 mg/g, Leo Pharmaceutical, Bellerup, Denmark) ointment was applied in the conjunctival sac after the intravitreal injections.

Retinal I-R injury was induced in one eye by elevating the intraocular pressure (IOP) to 80 mmHg for 60 min. IOP was measured with a tonometer (Tonolab, Icare, Vantaa, Finland). The anterior chamber of one eye was cannulated (Fig. 2.8 A) with a 30-gauge needle connected to a reservoir infusing sterile saline solution (Fig. 2.8 B). The contralateral eye was taken as the control eye. The IOP was raised by elevating the reservoir to a height of 1.8 m. Retinal ischemia was confirmed by whitening of the iris and loss of the red reflex. In order to avoid corneal opacity, 2% methocel™ (Dávi II, Barcarena, Portugal) was applied to both eyes. After 60 min of ischemia, the needle was withdrawn and the reperfusion was established. Fusidic acid ointment (10 mg/g) was applied at the end of the experiment. Animals were killed after 24 h of reperfusion.

A

B
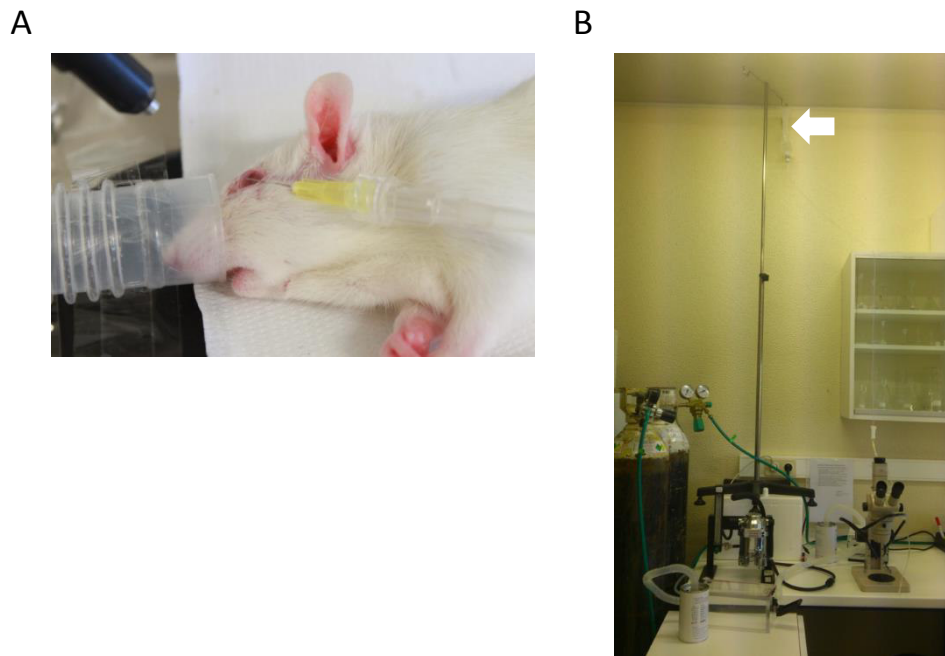
Figure 2.8. I-R injury model. (A) Picture illustrating a cannulated rat eye in the anterior chamber. (B) Scheme showing the reservoir (arrow) containing the saline solution and the gas-anaesthetizing system.

2.13 – Electroretinogram recordings

Electroretinogram (ERG) recordings are an effective and non-invasive method to study *in vivo* retinal light responses (Rosolen et al., 2005). In some animals subjected to I-R injury (three animals per each experimental group), ERGs were recorded before the onset of I-R injury (Baseline) and after 24 h of reperfusion. After dark adaptation for at least 12 h the animals were anaesthetized with 90 mg/kg (ip) ketamine (Imalgene™, Merial, Porto Salvo, Portugal) and 10 mg/kg (ip) xylazine (Rompun™, Bayer, Leverkusen, Germany). Then, 4 mg/ml oxybuprocaine (Laboratórios Edol, Linda-a-Velha, Portugal) anaesthetic was applied topically to the eyes and the pupils dilated with 10 mg/ml tropicamide (Laboratórios Edol) under dim red light illumination. The body temperature was maintained with a heating pad set to 37 °C. Using a Ganzfeld stimulator (Fig. 2.9 A), white light flashes (9.49 cd-s/m²) were applied under scotopic and photopic conditions (in the latter case, after light adaptation to a white background, 25 cd/m²) in order to saturate the rod photoreceptor response. Scotopic ERGs result mainly from rod photoreceptor activity, while photopic ERGs result from cone photoreceptor activity. ERGs were recorded with a corneal gold wire electrode, a reference

electrode at the head, and a ground electrode in the tail of the animal. A band width of 1 - 300 Hz and sampling rate of 3.4 kHz were used for acquisition (Roland Consult GmbH, Brandenburg and der Havel, Germany). The scotopic and photopic ERGs were evaluated (Fig. 2.9 B). The a-wave allows for evaluation of photoreceptor activity and the amplitude was measured from the baseline to the a-wave through (Fig. 2.9 C). The a-wave latency was measured from the light stimulus onset to the a-wave through. The b-wave allows for evaluation of bipolar cell and amacrine cell activity and the amplitude was measured from the a-wave through to the b-wave peak, and the b-wave latency was measured from the light stimulus onset to the b-wave peak (Fig. 2.9 D). Note that in the photopic ERG no clear a-wave is detected due to the low number of cone photoreceptors in rodent retina (Cone, 1964; Bayer et al., 2001). OFF-line high frequency cut-off of 50 Hz digital filter was applied to determine b-wave, with the RETIport software (Roland Consult GmbH).
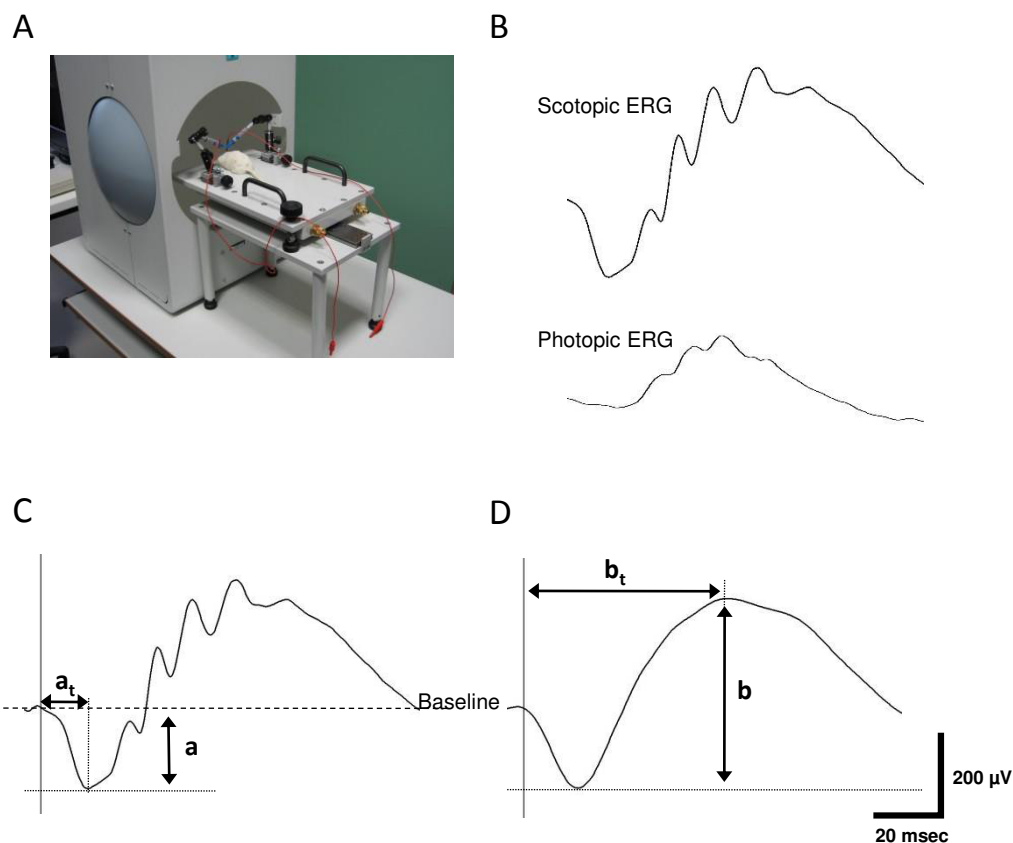
Figure 2.9. ERG recordings. (A) Picture illustrating an ERG recording set up. Note that the animal is placed on a heating pad and the head is positioned inside the Ganzfeld stimulator. (B) Examples of scotopic and photopic ERG waveforms. (C) Example of an ERG waveform, where the a-wave amplitude (a) and latency (a_t) quantification is indicated. (D) Example of an ERG waveform, where the b-wave amplitude (b) and latency (b_t) quantification after high frequency cut-off of 50 Hz is shown. Vertical line indicates the onset of light stimulus.

2.14 – Statistical analysis

Statistical analysis was performed with Prism 5 (GraphPad, La Jolla, CA, USA) using one-way ANOVA followed by Bonferroni's test. When distribution normality was not possible to evaluate, or not achieved, one-way Kruskal-Wallis test was used followed by Dunn's test, as indicated in figure legends. P values less than 0.05 were taken as significant. All values are presented as mean ± SEM.

CHAPTER 3

Neuromodulatory and Neuroprotective Effects

of Neuropeptide Y in the Retina

3.1 – Introduction

NPY is widely distributed in central and peripheral nervous system. This peptide belongs to a family of highly conserved peptides which also includes PP, and PYY, (Michel et al., 1998). During the last three decades NPY has been associated with a multitude of physiological functions such as energy homeostasis (Chambers and Woods, 2012), stress response (Hirsch and Zukowska, 2012), circadian rhythm (Yannielli and Harrington, 2004), bone physiology (Lee and Herzog, 2009), neurogenesis (Malva et al., 2012), and immune system regulation (Dimitrijevic and Stanojevic, 2013). NPY, PYY, and PP, all activate seven transmembrane G protein-coupled receptors named NPY receptors. These receptors all bind to G_i/G_0 proteins which results in inhibition of AC. Other signalling pathways are also regulated such as Ca^{2+} channels and GIRK channels, (Sun and Miller, 1999), phospholipase C (Perney and Miller, 1989), and phosphoinositide 3-kinase (Rosmaninho-Salgado et al., 2012). In humans, only four NPY receptors were cloned and known to be functionally active, Y_1, Y_2, Y_4, and Y_5 (Babilon et al., 2013). These receptors have been regarded as potential therapeutic targets since NPY was shown to present anti-epileptic and neuroprotective properties (Xapelli et al., 2006). Indeed NPY receptor activation has been shown to prevent neuronal cell death induced by excitotoxic insult (Silva et al., 2003; Xapelli et al., 2007).

In the retina, NPY presence has been demonstrated in different species, though NPY receptor localization has been scarcely investigated (Santos-Carvalho et al., 2014). Nevertheless, previous work from our laboratory have shown that NPY exerts a neuroprotective action against different toxic insults. In primary rat retinal cell cultures NPY pre-treatment prevented increased cell death induced by both MDMA and glutamate (Alvaro et al., 2008b; Santos-Carvalho et al., 2013b). In an animal model of excitotoxicity-induced retinal injury, intravitreal administration of NPY inhibited both the increase in cell death, and RGC loss induced by glutamate (Santos-Carvalho et al., 2013b). In addition, we and others presented evidence suggesting a neuromodulatory role of NPY in the retina. NPY application regulates neurotransmitter release in rabbit and chicken retinas (Bruun and Ehinger, 1993). Also, NPY attenuates depolarization-induced increase in $[Ca^{2+}]_i$ in primary retinal cell cultures (Alvaro et al., 2009). Moreover, NPY decreases depolarization-dependent Ca^{2+} influx into bipolar cells via activation of Y_2 receptors (D'Angelo and Brecha, 2004), and in retinas with selective ablation of NPY-expressing amacrine cells, it was reported an alteration in the

receptive field properties of RGCs, though a direct effect of NPY was not demonstrated (Sinclair et al., 2004). These results suggest that NPY-induced modulation of visual circuitry might result in changes of RGC spiking activity. Therefore, in this study, we intended to evaluate NPY modulatory potential at RGC level using a purified RGC culture and an *ex vivo* retinal preparation. In addition, since RGC are lost in retinal degenerative diseases such as glaucoma, we also evaluated the neuroprotective potential of NPY against excitotoxic or I-R injury.

3.2 – Results

3.2.1 – Expression of NPY and NPY receptors in retinal ganglion cells

In order to assess the presence of NPY and NPY receptors (Y_1, Y_2, Y_4, and Y_5) in RGCs we used a method for RGC isolation by immunopanning. After purification of RGC by this method, cells were used for RNA extraction or cultured overnight for immunocytochemistry assays. To assess the presence of mRNA for NPY and NPY receptors (Y_1, Y_2, Y_4, and Y_5) by RT-PCR, we used RGCs isolated from the retinas of P3-4 pups and 8 weeks old adult rats of two different strains: Wistar and Long Evans (Fig. 3.1). We found that mRNA for both NPY and NPY receptors (Y_1, Y_2, Y_4, and Y_5) were detected in purified RGCs from both rat strains and ages. Brn3a (RGC marker) mRNA was clearly detected while glial fibrillary acidic protein GFAP (macroglia cell marker) and Cd11b (microglia cell marker) mRNAs were not detected or barely detected indicating high purity of the isolated RGCs.

We also evaluated the immunoreactivity for NPY and NPY receptors in purified RGCs from P3-4 Wistar rats cultured overnight. We found NPY-ir in RGCs with co-localization with the RGC marker Brn3a (Fig. 3.2 a). A less intense Y_1 receptor-ir was also detected in Brn3a-positve RGCs (Fig. 3.2 b). Similar to NPY-ir, immunoreactivty for Y_2, Y_4, and Y_5 receptors was also detected in RGCs (Fig. 3.2 c-e). In addition, we assessed the localization of NPY and NPY receptors in retinal sections of adult Wistar rats. NPY-ir was detected in ramified dendrites in strata 1, 3, and 5 of IPL, and cell bodies of GCL and INL (Fig. 3.3 a, arrows). These NPY-ir cells were already described as amacrine cells (Oh et al., 2002). A low intensity Y_1 receptor-ir was detected in GCL similar to the immunoreactivity found in cultured RGCs (Fig. 3.3 b, arrow). Y_2 receptor-ir was found in stratum 1 of IPL and in cell bodies in proximal INL (Fig. 3.3 c, arrow). Y_4 receptor-ir was localized in cell bodies of GCL, and proximal and distal INL (Fig. 3.3 d, white arrows). The cell bodies in GCL that were immunoreactive for Y_4 receptor were both RGC (co-localized with Brn3a, Fig. 3.3 d, green arrow) and non-Brn3a-positive cells, likely displaced amacrine cells (Fig. 3.3 d, yellow arrow). Concerning Y_5 receptor, immunoreactivity was detected in Müller cells (Fig. 3.3 e, arrow). Co-localization of Y_5 receptor-ir with vimentin in Müller cells confirmed this result (Fig. 3.4). The lack of clear immunoreactivity for NPY, and for

Y$_2$ and Y$_5$ receptors in RGCs in retinal sections of adult rat (Fig. 3.3), while it could be found in cultured RGCs from P3-4 rats (Fig. 3.2), may indicate decreased expression in adulthood.
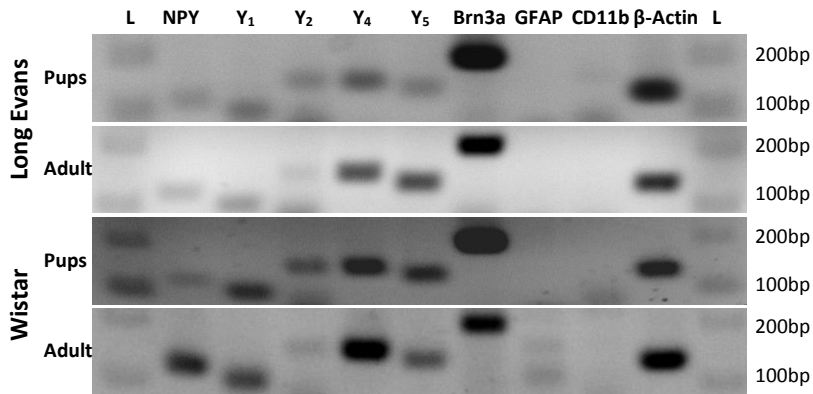
Figure 3.1. Detection of mRNA expression by RT-PCR for NPY and NPY receptors (Y$_1$, Y$_2$, Y$_4$, and Y$_5$) in RGCs purified by immunopanning. NPY and NPY receptors mRNA was detected in RGCs isolated from the retinas either pups or young adults Long Evans and Wistar rats. The clear presence of Brn3a mRNA and the barely detected mRNAs for GFAP (macroglial cell marker) and Cd11b (microglial cell marker) indicate high purity of the isolated RGCs. L, DNA ladder.
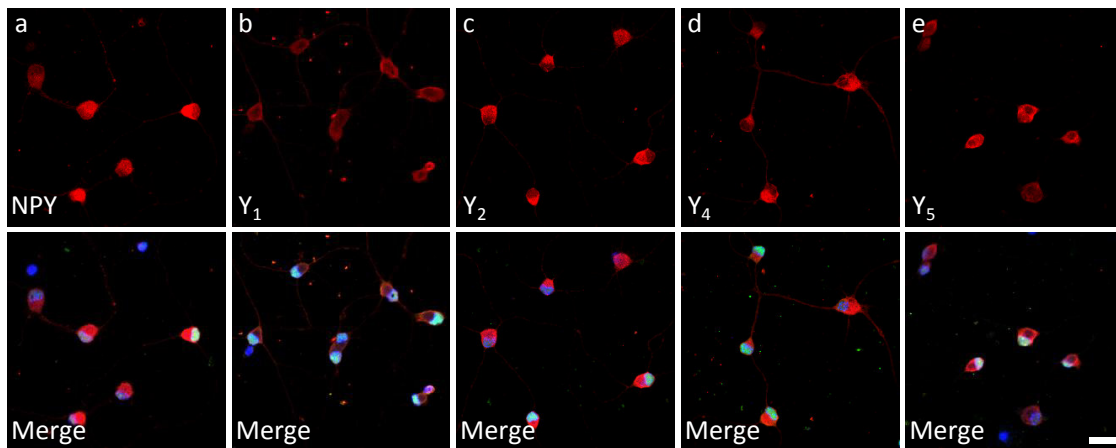
Figure 3.2. NPY and NPY receptor immunoreactivity (ir) in purified RGC cultures. Cell cultures were obtained from Wistar pups, purified by immunopanning and cultured for 16 h. NPY (a, red) and NPY receptor-ir (b-e, red) were detected in Brn3a (RGC marker, green) positive cells. Nuclei are stained with DAPI (blue). Scale bar: 20 μm.
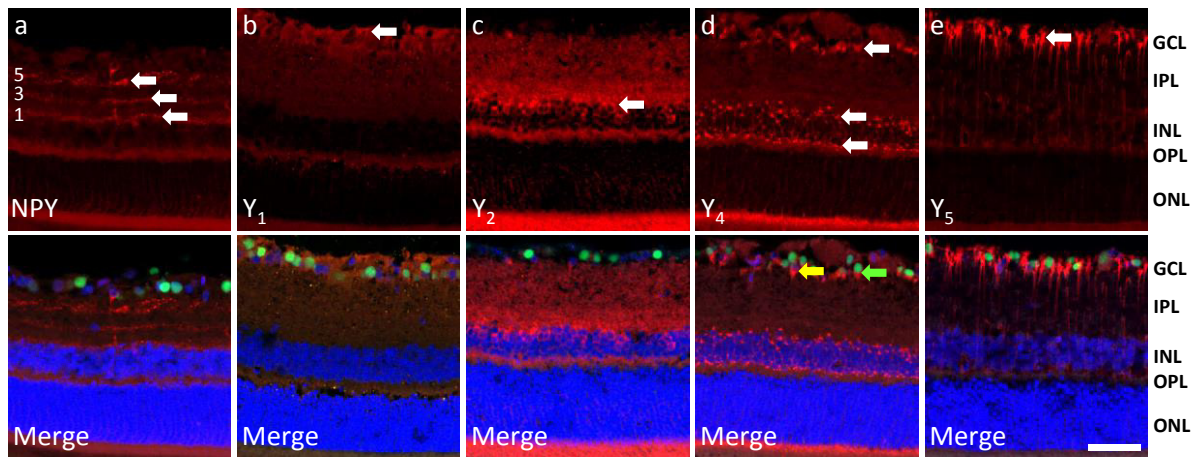
Figure 3.3. NPY-ir and NPY receptor-ir in the rat retina. Retinal slices were obtained from young adult Wistar rats. RGCs were stained with the RGC marker Brn3a (green) and nuclei with DAPI (blue). NPY-ir was detected in strata 1, 3, and 5 of IPL (a, red, arrows). Y_1-ir was detected in GCL (b, red, arrow). Y_2-ir was detected in INL (c, red, arrow). Y4-ir was detected in INL and GCL (d, red, arrows) and Y_5-ir was detected in Müller cells (e, red, arrow). GCL, ganglion cell layer; IPL, inner plexiform layer; INL, inner nuclear layer; OPL, outer plexiform layer; ONL, outer nuclear layer. Scale bar: 50 μm.
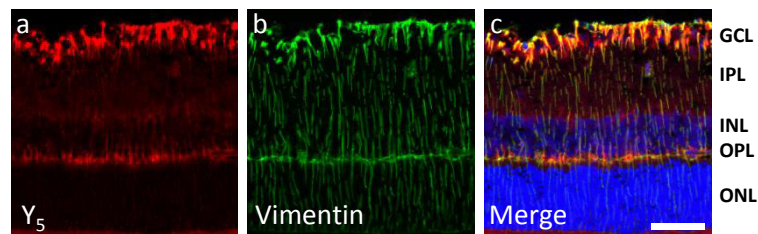
Figure 3.4. Immunoreactivity for Y_5 receptor in Müller cells in the rat retina. Y_5-ir (a, red) is co-localized (c) with vimentin in Müller cells (b, green) in retinal slices. Müller cells were identified by vimentin-ir (green). Nuclei were stained with DAPI (blue). GCL, ganglion cell layer; IPL, inner plexiform layer; INL, inner nuclear layer; OPL, outer plexiform layer; ONL, outer nuclear layer. Scale bar: 50 μm.

3.2.2 – NPY stimulates functional binding in retinal slices

We performed [^{35}S]GTPγS binding assay to assess the functional activity of NPY receptors in retinal slices from adult Wistar rats (Fig. 3.5). [^{35}S]GTPγS binding assay is able to evaluate the activation of G-protein-coupled receptors (GPCRs) by measuring the amount of radiolabeled GTP bound to the cell membrane using an autoradiography film. After incubation with 10 µM NPY for 60 min, we detected an increase in [^{35}S]GTPγS binding in inner retinal layers (134.5 ± 6.4% comparing to basal conditions, non-stimulated retinal slices; Fig. 3.5 A and B). Autoradiography films did not allow obtaining higher magnification/resolution imaging of retinal slices due to the small size of retinal tissue and low [^{35}S]GTPγS binding signal (Fig. 3.5 A). However, when comparing the hematoxylin-eosin staining of native retinal slices with MR autoradiography film pictures of the same retinal slices, we found that the retinal layers presenting increased [^{35}S]GTPγS binding upon NPY stimulation were both GCL and IPL. It is also of note the intense binding signal detected in photoreceptor layer both in basal and NPY-stimulated conditions (Fig. 3.5 Aa and Ab, white arrows) that likely represents the high amount of G proteins in photoreceptor outer segments, mainly transducin (Arshavsky et al., 2002). Moreover, NPY did not induce a statistically significant increase in binding signal in photoreceptor layer. Since 1 µM NPY was not sufficient to increase [^{35}S]GTPγS binding in retinal sections, we speculated that low levels of NPY receptors were functionally active in frozen retinal sections, thus requiring increased concentrations of NPY. A cocktail of NPY receptor antagonists (10 µM BIBO 3304 for Y_1; 10 µM BIIE 0246 for Y_2; 100 µM L-152,804 for Y_5) was used to evaluate the selectivity of NPY-stimulated [^{35}S]GTPγS binding. The blockade of Y_1, Y_2, and Y_5 receptors prevented the increased binding induced by NPY confirming the selectivity of binding signal. To assess the non-specific binding (NSB), a competitive control with non-radioactive GTPγS was used, which exhibit no clear binding signal in MR autoradiography film (Fig. 3.5 Ad).

A

B
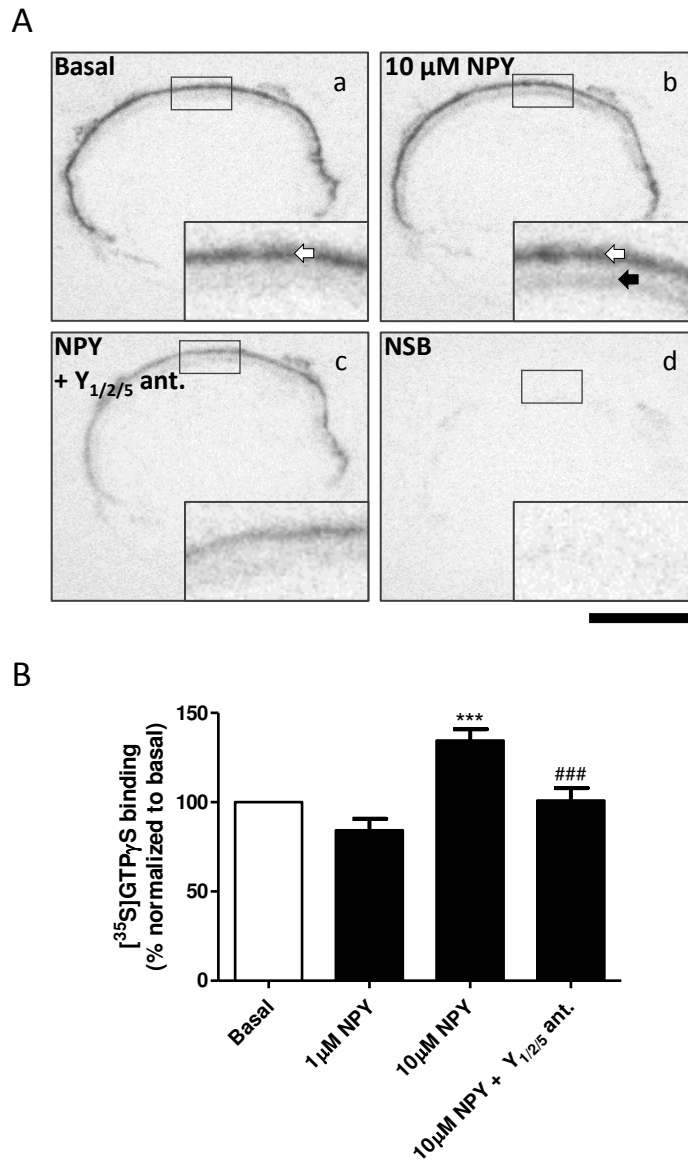
Figure 3.5. NPY increases [^{35}S]GTPγS binding in retinal sections. (A) Examples of retinal sections from MR autoradiography films after [^{35}S]GTPγS binding assay. (B) Quantification of [^{35}S]GTPγS binding in inner retinal layers. Incubation with 10µM NPY increased the [^{35}S]GTPγS binding in inner retinal layers (Ab, black arrow) compared to basal binding (Aa). An intense signal was found in photoreceptor layer (white arrows) both in basal and NPY-stimulated binding conditions that may represent the high amount of G proteins in photoreceptor outer segments, mainly transducin. The blockade of Y_1, Y_2, and Y_5 receptors prevented the increased [^{35}S]GTPγS binding induced by NPY (Ac). NSB refers to non-specific binding, a competitive control with non-radioactive GTPγS (Ad). Antagonists used: Y_1, BIBO 3304 (10 µM); Y_2, BIIE 0246 (10 µM); Y_5, L-152,804 (100 µM). Bar: 2 mm. Data are presented as mean ± SEM of n = 8-10 independent experiments, except 1µM NPY, which was not used for statistical comparisons (n = 2). ***$p<0.001$, compared to basal; ###$p<0.001$, compared to 10 µM NPY. One-way ANOVA followed by Bonferroni's test.

3.2.3 – NPY attenuates glutamate-induced [Ca^{2+}]$_i$ increase in purified retinal ganglion cells

We aimed to evaluate the modulatory effect of NPY directly on RGCs. For this purpose, we cultured purified RGCs and performed intracellular free calcium concentration - [Ca^{2+}]$_i$, measurements using Fura-2 calcium indicator. Following a similar protocol described previously (Hartwick et al., 2004), we stimulated RGCs with different glutamate concentrations (1 to 1000 μM) for 30 sec, including also 10 μM glycine (Methods section). After testing these glutamate concentrations, in the following experiments we used 30 μM glutamate since this concentration was able to induce a non-saturating increase in [Ca^{2+}]$_i$ that was easily reversible. The ratios between emissions of Fura-2 when excited by light at 340 nm and 380 nm wavelengths were quantified in cell bodies of RGCs, as indicative of [Ca^{2+}]$_i$. After the first glutamate stimulus, we applied different drugs for 10 min: NPY (1 μM), the Y$_1$/Y$_5$ agonist (Leu^{31}, Pro^{34})-NPY (1 μM), the Y$_2$ agonist NPY (13-36) (300 nM), and the Y$_5$ agonist (Gly^1, …Aib^{32})-PP (1 μM), or a drug-free solution (control), followed by a second glutamate stimulus (Fig. 3.6 A). The increase above basal Fura-2 ratio was quantified for each stimulus as a Delta value. When evaluating the average [Ca^{2+}]$_i$ responses of the cell population analysed, a small decrease in Delta 2 / Delta 1 ratios was found for NPY (0.83 ± 0.04) and (Leu^{31}, Pro^{34})-NPY (0.81 ± 0.05), compared to control (0.93 ± 0.02) (Fig. 3.6 C). In fact, a small significant change may be hard to detect within the overall population, as can be observed in scatter plots showing individual RGCs from an independent experiment (Fig. 3.6 D). Hence, we quantified the percentage of RGCs where the Delta 2 / Delta 1 ratio value was lower than 0.9 (Fig. 3.6 E). The application of NPY or (Leu^{31}, Pro^{34})-NPY for 10 min significantly increased the percentage of cells with Delta 2 / Delta 1 ratio below 0.9 (77.7 ± 10.3% or 68.5 ± 8.3%, respectively), compared to control (32.7 ± 8.4%). Since the Y$_5$ receptor agonist alone was not able to affect the RGC response to glutamate, it is likely that the effect of NPY or (Leu^{31}, Pro^{34})-NPY might occur via Y$_1$ receptor activation.
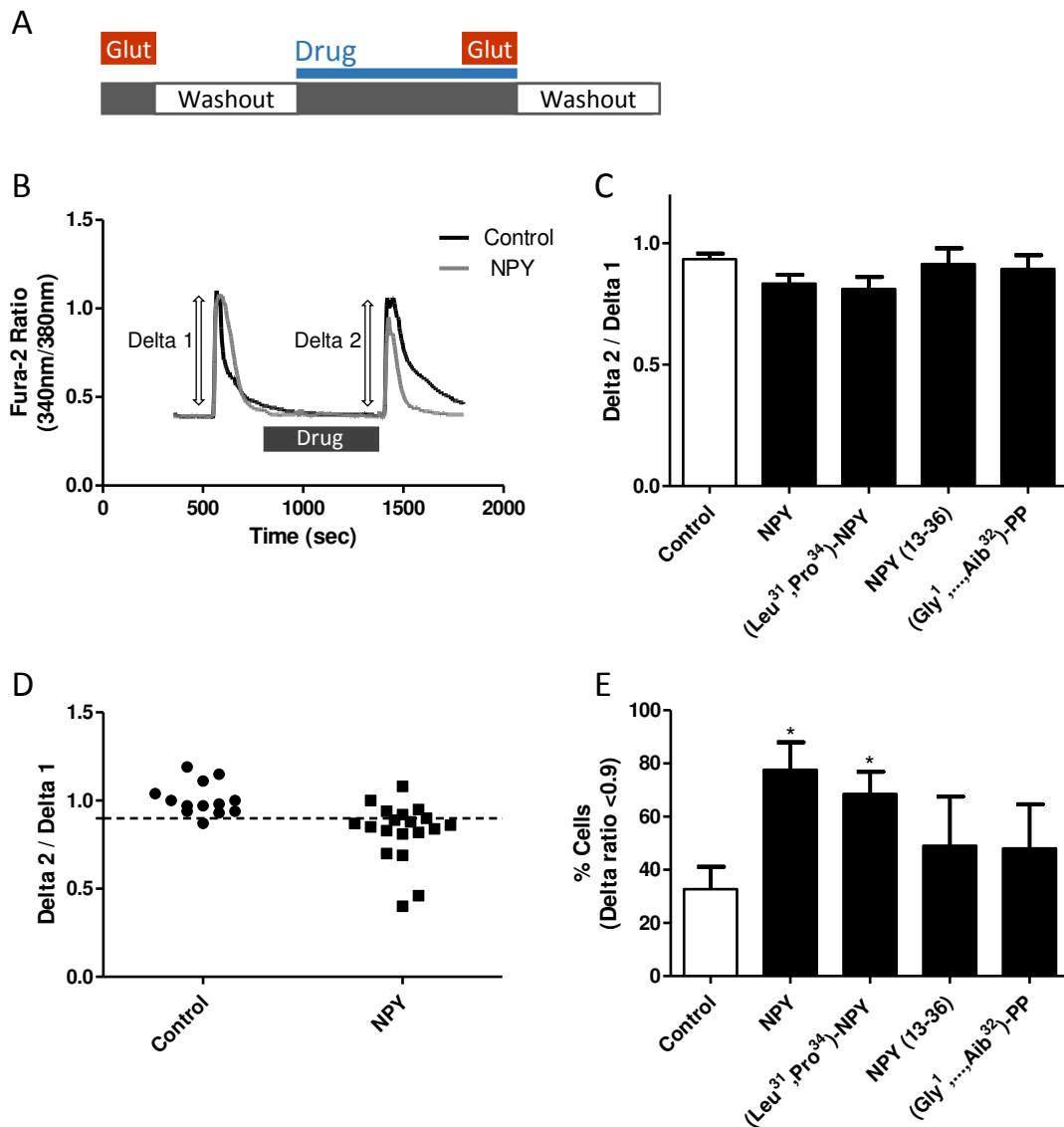
Figure 3.6. NPY attenuates glutamate-induced $[Ca^{2+}]_i$ increase in purified RGCs. (A) Schematic experimental protocol for Ca^{2+} imaging in RGCs. After the first glutamate stimulus (30 µM for 30 sec) and a period of washout for at least 210 sec, 1 µM NPY, 1 µM (Leu[31], Pro[34])-NPY, 300 nM NPY (13-36), 1µM (Gly[1], ...Aib[32])-PP, or a drug-free solution (control), were applied to RGCs during 10 min followed by a second glutamate stimulus and washout. (B) Examples of $[Ca^{2+}]_i$ traces of RGC responses to consecutive glutamate stimuli (30 µM) for 30 sec each stimulus. After the first glutamate stimulus, 1 µM NPY or a drug-free solution (control) were applied to RGCs during 10 min followed by a second glutamate stimulus. (C) The increase above basal Fura-2 ratio 340 nm / 380 nm was quantified for each stimulus as a Delta value. The Delta 2 (2nd stimulus) / Delta 1 (1st stimulus) ratios are presented for different drug applications for 10 min: 1 µM NPY, 1 µM (Leu[31], Pro[34])-NPY, 300 nM NPY (13-36), 1µM (Gly[1], ...Aib[32])-PP, or a drug-free solution (control). A small decrease in Delta 2 / Delta 1 ratios may be found in RGCs exposed to NPY and (Leu[31], Pro[34])-NPY. (D) Scatter plots for two populations of RGCs from the same independent experiment show the dispersion of Delta 2 / Delta 1 ratio values among cells. RGCs were treated with a drug-free solution (control) or NPY. Note that in NPY-treated population a small downward shift may be observed. Dashed line indicate 0.9 ratio value. (E) Percentage of cells presenting Delta 2 / Delta 1 ratio below 0.9 was quantified. The application of NPY or (Leu[31], Pro[34])-NPY for 10 min increased the percentage

79

of cells with Delta 2 / Delta 1 ratio below 0.9. Data are presented as mean ± SEM of n = 5-10 independent experiments. *p<0.05, compared to control. Kruskal-Wallis followed by Dunn's test.

3.2.4 – RGC spiking activity is modulated by Y_1 receptor activation

Since NPY is able to modulate neuronal activity in various brain regions (Silva et al., 2002; Benarroch, 2009), we hypothesized whether direct application of NPY to *ex vivo* retinas could modulate RGC spiking activity. For this purpose, we used a MEA system allowing recording spiking activity from various RGCs within a square of 0.6 mm^2 comprising 60 electrodes arranged in an 8×8 layout. After spike sorting based on template matching, the spiking rate for individual RGCs was quantified. In the first set of experiments, we recorded RGC spontaneous activity before (Baseline) and after the application of NPY (1 µM), the Y_1/Y_5 agonist (Leu^{31}, Pro^{34})-NPY (1 µM), the Y_2 agonist NPY (13-36), (1 µM), or a drug-free solution (control) for 10 min under continuous perfusion (Fig. 3.7 A). In addition, a period of washout up to 60 min was included. We found a small decrease in RGC spiking rate over time reaching 79.5 ± 7.2% of Baseline in control at 60 min of washout (Fig. 3.7 B). However, exposure to NPY or NPY receptor agonists caused no effect since RGCs presented a decrease in spiking rate similar to control.
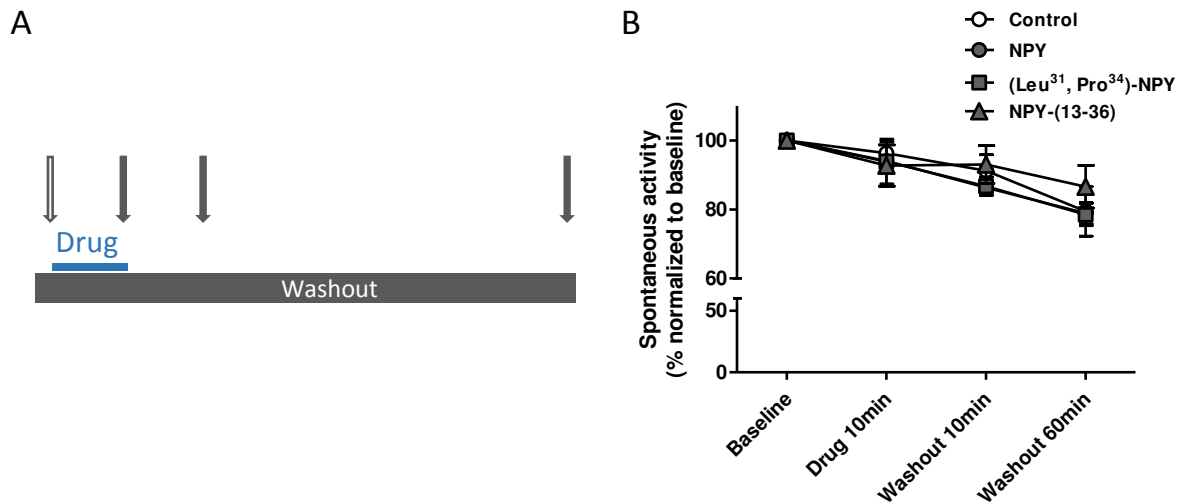
Figure 3.7. NPY or NPY receptor agonists do not changed the spontaneous activity of RGCs. (A) *Ex vivo* retinal preparations were exposed to 1 μM NPY, 1 μM (Leu[31], Pro[34])-NPY, 1μM NPY (13-36), or a drug-free solution (control) for 10 min followed by 60 min of washout. Arrows indicate when MEA recordings were performed. Open arrow indicates Baseline recording. (B) Quantification of RGC spontaneous spiking rate. A decrease in RGC spiking rate was observed over time, though no effects were found for drug treatments.

In order to evaluate the effect of NPY on RGC light responses, *ex vivo* retinas were exposed to light stimuli in the photopic range (5.0 cd/m^2), while RGC spiking activity was recorded in the MEA system. The light stimulation protocol consisted of 10 consecutive stimulation blocks composed of 5 sec light followed by 10 sec dark. RGC light responses were classified as ON- or OFF-type. An ON-type RGC light response was considered if increased spiking activity was detected at light onset and an OFF-type RGC light response was considered when increased spiking activity was detected at dark onset in each stimulation block. The most common RGC light response detected with our stimulation protocol was a transient response, either ON- or OFF-type, characterized by an initial burst response to light or dark onset, respectively, which was followed by a rapid decrease in spiking activity. We also detected a few RGC light responses classified as sustained, which were characterized by a sustained increase in spiking activity during the full light or dark period of a stimulation block and were included in ON- or OFF-type groups, respectively. The peri-stimulus time histograms (PSTHs) were generated from RGC responses to 9 consecutive stimulation blocks and used to calculate the initial burst responses to light or dark onset, as well as the mean spiking rates during the first 1 or 5 sec after light or dark onset, ON- or OFF-type responses, respectively. The latencies

of RGC light responses were also calculated. The first RGC light response to a series of 10 stimulation blocks was always excluded since it was harder to apply the spike sorting procedure due to increased noise in the raw recordings. Thus, in order to evaluate the potential modulatory effect of NPY on RGC light responses, the recordings were performed before (Baseline) and after the application of NPY (1 µM), the Y_1/Y_5 agonist (Leu^{31}, Pro^{34})-NPY (1 µM), the Y_2 agonist NPY (13-36), (1 µM), or a drug-free solution (control) for 10 min under continuous perfusion. Regarding ON-type light response, no effect was found on the initial burst of spiking activity to light onset for the drugs used (Fig. 3.8 A). The same was observed for 1 and 5 sec rate, and also for latency of ON-type RGCs (Fig. 3.8 B, C, D, respectively). However, the application of 1 µM (Leu^{31}, Pro^{34})-NPY for 10 min was able to induce a small, but statistically significant, increase to 112.4 ± 2.8% of baseline on the initial burst of spiking activity triggered by dark onset in OFF-type RGCs (Fig. 3.9 A), when compared to control (100.3 ± 1.1% of baseline). Although a small increase may be observed for 1 (Fig. 3.9 B) and 5 sec rate (Fig. 3.9 C) after the application of (Leu^{31}, Pro^{34})-NPY, no statistically significant differences were found. Also, no statistically significant differences were found after the application of 1 µM NPY or 1 µM NPY (13-36). This result suggests that Y_1 or Y_5 activation may be sufficient to modulate the OFF-type RGC light response directly by changing the receptive field properties or acting upstream of RGCs in the vertical pathway of visual information, namely at the level of bipolar or photoreceptor cells. Concerning latency quantification of OFF-type RGC light responses, no effect was found after the different drug treatments used (Fig. 3.9 D).
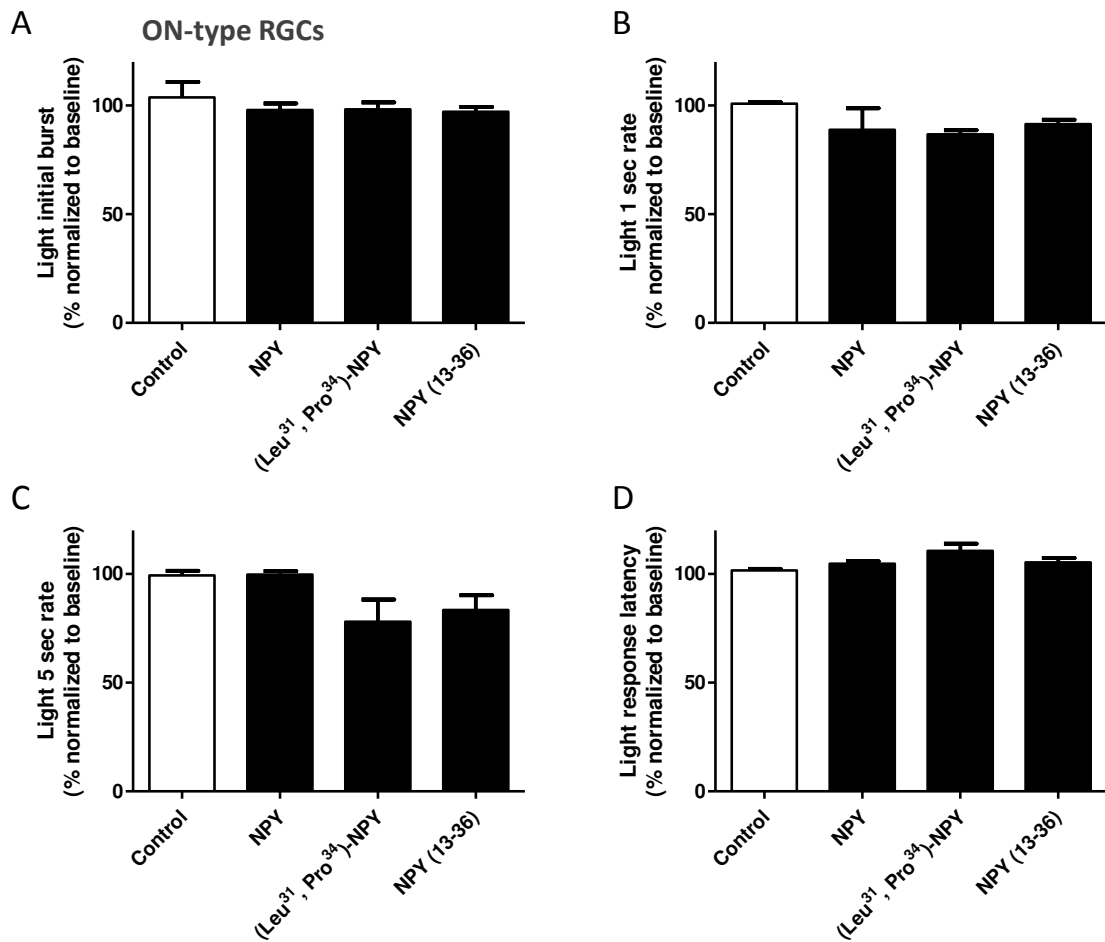
Figure 3.8. NPY or NPY receptor agonists do not change the magnitude and latency of ON-type RGC light responses. (A) Quantification of the Initial burst to light onset of ON-type RGCs after application of the same drug treatments as in Fig 3.7 A. No effect was found for the different drug treatments compared to control. Similarly, no effect of drug treatments was found for 1 (B) and 5 sec rate (C), and also for the latency of ON-type RGCs (D). All data were normalized to the values obtained before drug application (Baseline). Data are presented as mean ± SEM of n = 3-4 independent experiments.
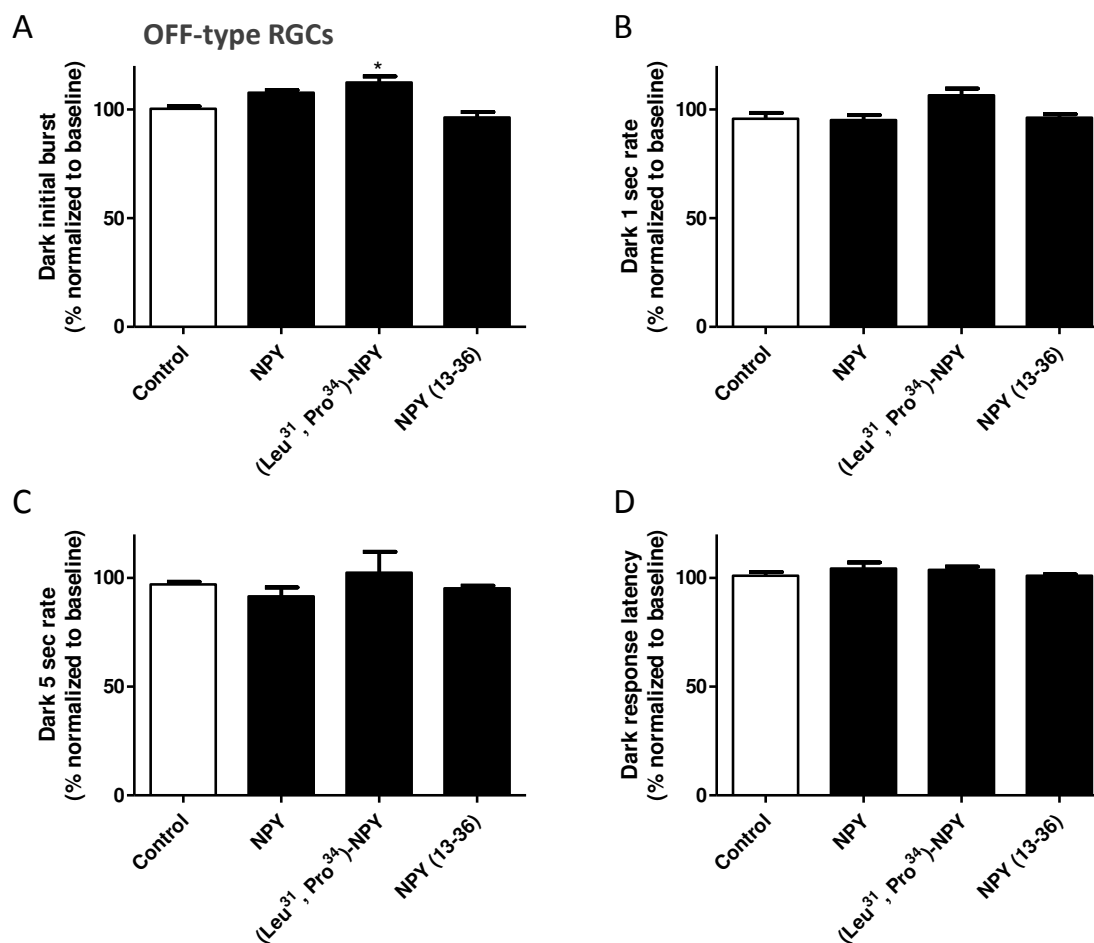
Figure 3.9. (Leu[31], Pro[34])-NPY increases the response of OFF-type RGCs to dark onset. (A) Quantification of the Initial burst to dark onset of OFF-type RGCs after application of the same drug treatments as in Fig. 3.7 A. The application of 1 µM (Leu[31], Pro[34])-NPY for 10 min was able to increase the magnitude of OFF-type response compared to control. Although a small increase may be observed for 1 (B) and 5 sec rate (C) after the application of (Leu[31], Pro[34])-NPY, no statistically significant differences were found. Concerning latency quantification for OFF-type RGCs (D), no effect was detected after the application of different drugs. All data were normalized to the values obtained before drug application (Baseline). Data are presented as mean ± SEM of n = 3-4 independent experiments. *p<0.05, compared to control. Kruskal-Wallis followed by Dunn's test.

In addition to light stimulation experiments, we also evaluated the potential modulatory effect of NPY application on RGC spiking activity upon glutamate receptor activation. Glutamate is easily cleared within the retina by glutamate uptake (Higgs and Lukasiewicz, 1999), and therefore, we applied NMDA directly to *ex vivo* retinas in order to induce synaptic excitation of RGCs (Fig. 3.10 A, B), since NMDA receptors are abundantly expressed in RGCs (Shen et al., 2006). The application of NMDA (30 µM) for 5 min induced an acute increase in RGC spiking activity which was reversible within 10 min of washout (Fig. 3.10 A, B). After washout of the 1st NMDA stimulus different drugs were applied for 10 min under

continuous perfusion: NPY (1 μM), the Y_1/Y_5 agonist (Leu^{31}, Pro^{34})-NPY (1 μM), the Y_2 agonist NPY (13-36) (1μM), the Y_5 agonist (Gly^1, …Aib^{32})-PP (1μM), or a drug-free solution (control). After 10 min of drug treatment a 2nd NMDA stimulus was co-applied, followed by 10 min of washout. The increase above basal spiking rate (Baseline) or above washout was quantified for each NMDA stimulus as a Delta value (Fig. 3.10 B). Subsequently, the Delta 2 (2nd stimulus) / Delta 1 (1st stimulus) ratios were calculated for each individual RGC. We found that application of (Leu^{31}, Pro^{34})-NPY was able to decrease the Delta 2 / Delta 1 ratio to 0.67 ± 0.07, when compared to control, 0.96 ± 0.04 (Fig. 3.11 A), indicating that activation of Y_1 or Y_5 receptor was sufficient to attenuate the NMDA-stimulated RGC spiking activity. For the other drug treatments, no statistically significant alterations were detected compared to control. The effect of (Leu^{31}, Pro^{34})-NPY was confirmed to be mediated by Y_1 receptor activation since the co-application of Y_1 receptor antagonist BIBP 3226 (1 μM) and (Leu^{31}, Pro^{34})-NPY was able to prevent its effect (Fig. 3.11 A). Moreover, the application of the Y_5 receptor agonist alone did not affect the RGC response to NMDA, suggesting that the effect found for (Leu^{31}, Pro^{34})-NPY is not mediated by Y_5 receptor activation.

In order to focus on the RGCs that presented more pronounced differences between responses to 1st and 2nd NMDA stimulus, we calculated the percentage of RGCs presenting Delta 2 / Delta 1 ratio values below 0.9 for each independent experiment (Fig. 3.11 B), thus, overcoming the masking effect associated with overall population mean calculation. As expected, the application of (Leu^{31}, Pro^{34})-NPY increased the percentage of cells (79.0 ± 6.9% of the cells analysed), with Delta 2 / Delta 1 ratio below 0.9, when compared to control (40.8 ± 5.0% of the cells analysed) (Fig. 3.11 B). Also, the Y_1 receptor antagonist BIBP 3226 was able to prevent the effect of (Leu^{31}, Pro^{34})-NPY, confirming the involvement of Y_1 receptor activation. No statistically significant differences were detected for the other drug treatments.

We hypothesize that a possible opposite effect of Y_2 activation might be responsible for counteracting the effect of Y_1 activation by NPY. In this regard, the application of Y_2 agonist NPY (13-36) resulted in a Delta 2 / Delta 1 ratio of 1.2 ± 0.1 (Fig. 3.11 A), and the percentage of cells with Delta 2 / Delta 1 ratio below 0.9 was 24.8 ± 7.2% (Fig. 3.11 B), both values apparently in opposite direction of Y_1 receptor activation, though no statistically significant differences were detected.
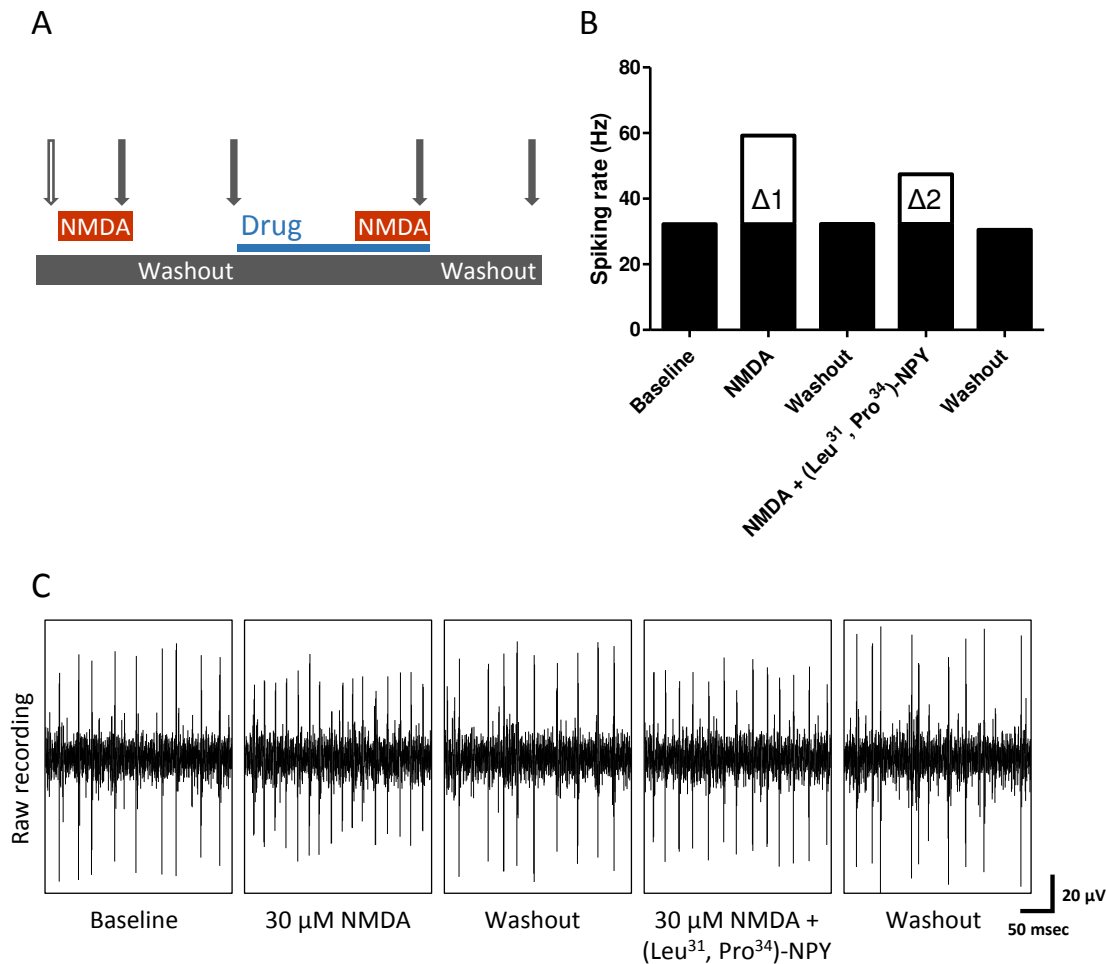
Figure 3.10. Y$_1$ receptor activation decreases NMDA-stimulated RGC spiking activity. (A) NMDA (30 µM) was applied for 5 min followed by a washout period of 10 min. Then, 1 µM NPY, 1 µM (Leu^{31}, Pro^{34})-NPY, 1 µM NPY (13-36), 1 µM (Gly^1, …Aib^{32})-PP, or a drug-free solution (control) were applied under continuous perfusion. A 2nd NMDA stimulus for 5 min was co-applied with drug solutions after 10 min of drug application. Arrows indicate when MEA recordings were performed. Open arrow indicate Baseline recording. (B) The increase above basal spiking rate (Baseline) or above washout was quantified for each NMDA stimulus as a Delta value. (C) Representative recordings of RGC spiking activity recorded in *ex vivo* retina using a MEA. Note the increase in spiking rate upon 30 µM NMDA. After washout of 1st NMDA stimulus, 1 µM (Leu^{31}, Pro^{34})-NPY was applied for 10 min followed by a 2nd NMDA stimulus. Note that the NMDA-induced increase in RGC spiking activity was reduced upon application of (Leu^{31}, Pro^{34})-NPY.
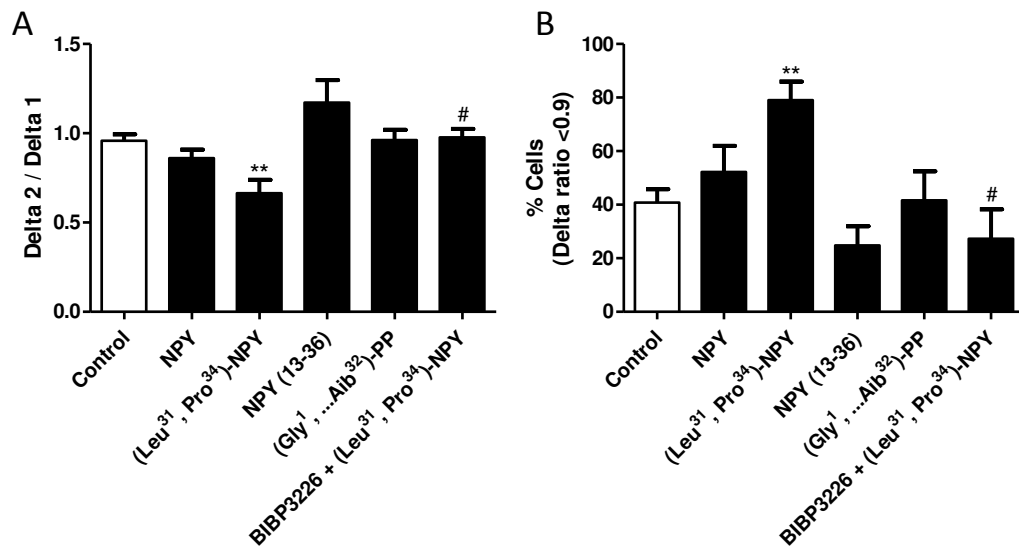
Figure 3.11. Activation of Y_1 receptors decreases NMDA-stimulated RGC spiking activity. (A) The Delta 2 (2nd stimulus) / Delta 1 (1st stimulus) ratios for different drug applications, for 10 min, between NMDA stimuli: 1 µM NPY, 1 µM (Leu^{31}, Pro^{34})-NPY, 1 µM NPY (13-36), 1 µM (Gly^1, …Aib^{32})-PP, or a drug-free solution (control). The application of (Leu^{31}, Pro^{34})-NPY was able to reduce the NMDA-stimulated RGC spiking activity. This effect was blocked by the Y_1 receptor antagonist BIBP 3226 (1 µM). (B) Percentage of RGCs presenting Delta 2 / Delta 1 ratio below 0.9. The application of (Leu^{31}, Pro^{34})-NPY increased the percentage of cells with Delta 2 / Delta 1 ratio below 0.9. BIBP 3226 was able to block the effect of (Leu^{31}, Pro^{34})-NPY confirming the involvement of Y_1 receptor activation. Data are presented as mean ± SEM of n = 3-10 independent experiments. **p<0.01, compared to control; #p<0.05, compared to (Leu^{31}, Pro^{34})-NPY. Kruskal-Wallis followed by Dunn's test.

3.2.5 – NPY prevents NMDA-induced cell death in retinal explants via Y_1 and Y_5 receptor activation

NPY exerts neuroprotective actions in various brain regions, and also in the retina (Alvaro et al., 2008b; Santos-Carvalho et al., 2013b), suggesting that NPY receptors might be possible therapeutic targets for retinal diseases such as glaucoma. Therefore, in addition to the modulatory effect of NPY on RGC activity detected in *ex vivo* retinas, we also evaluated whether NPY could be able to prevent retinal cell death induced by an excitotoxic insult. The excitotoxic insult was induced in retinal explants (cultured for 4 DIV) exposed to 300 µM NMDA for 48 h. Different drug treatments were applied to assess the potential protective effect of NPY receptor activation. Thus, NPY (1 µM), the Y_1/Y_5 agonist (Leu^{31}, Pro^{34})-NPY (1 µM), the Y_2 agonist NPY (13-36), (300 nM), or the Y_5 agonist (Gly^1, …Aib^{32})-PP (1 µM) were applied at DIV1 and DIV2, respectively 24 h and 60 min before NMDA treatment (Fig. 3.12).

Figure 3.12. Schematic representation of the experimental protocol used for NMDA-induced cell death in retinal explants. The scheme shows the drug application protocol in retinal explants, cultured for 4 days, in order to evaluate the potential neuroprotective effect of NPY and NPY receptor agonists. Retinal explants were exposed to 300 μM NMDA for 48 h to induce an excitotoxic insult. Pre-treatment with NPY or NPY receptor agonists was performed 24 h and 60 min before NMDA. NPY receptor antagonists were applied 30 min before NPY or NPY receptor agonists.

Apoptotic retinal cell death was assessed by TUNEL assay (Fig. 3.13) and necrotic or late apoptotic cell death was assessed by PI incorporation assays (Fig. 3.14).

In TUNEL assay experiments, we quantified TUNEL-positive cells localized in GCL, using confocal microscopy, since this layer is highly affected in diseases like glaucoma (Fig. 3.13 A). TUNEL-positive cell counts were then normalized to the value obtained in non-treated retinal explant (control), in each independent experiment (Fig. 3.13 B). In PI assay experiments, since the acquisition of images was performed with live retinal explants using fluorescence microscopy, we quantified PI-positive cells across all retinal layers. PI-positive cells were quantified at DIV2 (before NMDA application) and at DIV4. The ratio between PI-positive cells at DIV4 and DIV2 was calculated to evaluate the effect of NMDA on necrotic or late apoptotic cell death (Fig. 3.14).

Exposure of retinal explants to NMDA for 48 h increased the number of TUNEL-positive cells in the GCL up to 16.3 ± 1.3 times higher than in control (Fig. 3.13 B). There was also an increase in the DIV4 / DIV2 ratio for PI-positive cells compared to control (3.4 ± 0.2 in NMDA-treated explants versus 1.3 ± 0.1 in control) (Fig. 3.14). Pre-treatment with NPY was able to prevent the increase in the number of TUNEL-positive cells induced by NMDA to 4.8 ± 0.5. NPY pre-treatment was also able to prevent the increase in DIV4 / DIV2 ratio for PI-positive cells (1.4 ± 0.2) (Fig. 3.14). The Y_1 antagonist BIBP 3226 (1 μM), or the Y_5 antagonist L-152,804 (1 μM), when applied 30 min before NPY, were able to block its protective effect both on TUNEL and PI assays, indicating the involvement of Y_1 and Y_5 receptor activation on the neuroprotective effects of NPY. The protective effect of Y_1 receptor activation was confirmed by the application of (Leu[31], Pro[34])-NPY which was able to reduce the NMDA-induced increase in TUNEL- and PI-positive cells. Again, the Y_1 antagonist BIBP 3226 blocked this effect. Concerning the Y_5 receptor activation, the use of (Gly[1], …Aib[32])-PP, might have reduced the number of TUNEL-positive cells, comparing to NMDA-treated explants, though no statistically

significant differences were detected. However, it was able to reduce the number of PI-positive cells compared to NMDA condition. This later effect was blocked by L-152,804, thus confirming the protective effect of Y_5 receptor activation. The Y_2 receptor was not involved in the protective action of NPY since the Y_2 antagonist BIIE 0246 (1 µM) did not block the neuroprotective effect of NPY. Also, NPY (13-36) did not prevent the increase in TUNEL- and PI-positive cells induced by NMDA in retinal explants.
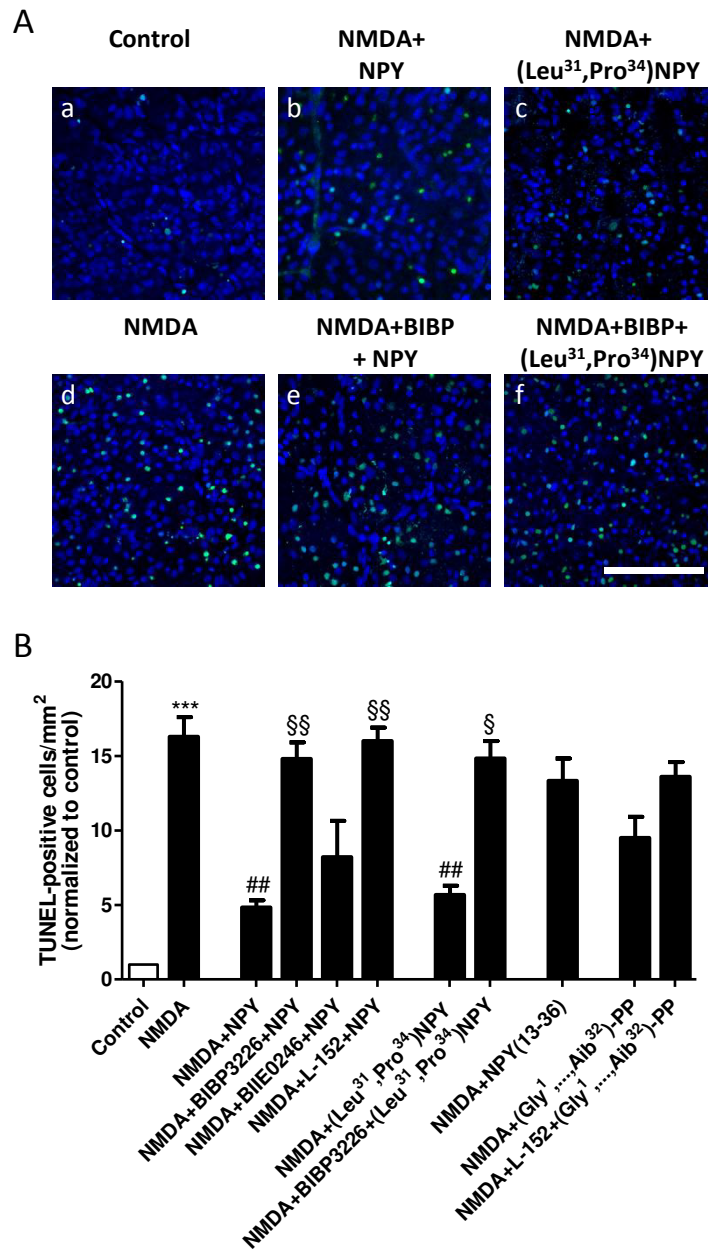
Figure 3.13. NPY prevents NMDA-induced cell death in the GCL in retinal explants via Y_1 and Y_5 receptor activation. (A) Representative images of TUNEL-positive cells (green) in the GCL of control (a) or NMDA-treated (b-f) retinal explants. Nuclei were stained with DAPI (blue). Retinal explants were pre-treated with different drugs 24 h before exposure to NMDA. Scale bar: 100 µm. (B)

Quantification of TUNEL-positive cells. NMDA exposure induced a significant increase in the number of TUNEL-positive cells in the GCL compared to control. Pre-treatment with 1 µM NPY or 1 µM (Leu[31], Pro[34])-NPY (Y_1/Y_5 agonist), 24 h before NMDA, was able to prevent the increase in the number of TUNEL-positive cells induced by NMDA. Pre-treatment with Y_1 or Y_5 receptor antagonist (1 µM BIBP 3226 or 1 µM L-152,804, respectively), when applied 30 min before NPY, blocked its protective effect. The effect of (Leu[31], Pro[34])-NPY was blocked by BIBP 3226. Data are presented as mean ± SEM of n = 5-11 independent experiments. ***p<0.001, compared to control; ##p<0.01, compared to NMDA; §p<0.05, §§p<0.01, compared to NMDA + NPY, or NMDA + (Leu[31], Pro[34])-NPY. Kruskal-Wallis followed by Dunn's test.
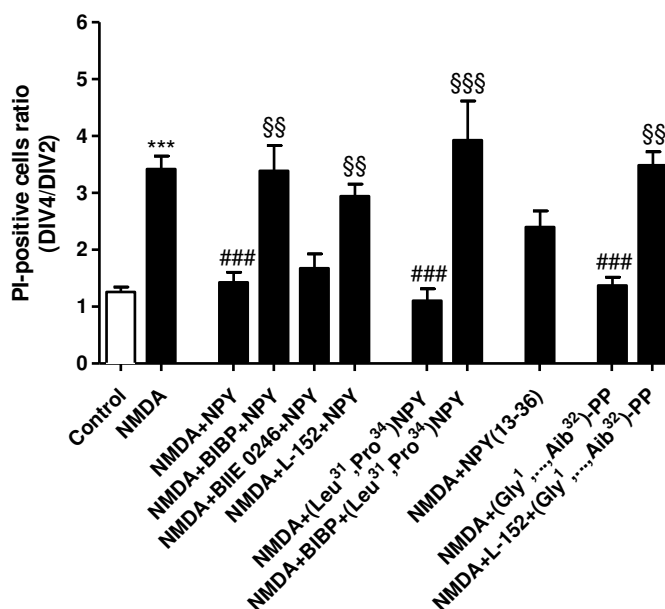
Figure 3.14. NPY prevents NMDA-induced cell death in retinal explants via Y_1 and Y_5 receptor activation. NMDA exposure induced a significant increase in the number of PI-positive cells in retinal explants. Data are presented as the ratio between PI-positive cells at DIV4 and DIV2. NPY or (Leu[31], Pro[34])-NPY (Y_1/Y_5 agonist) was able to prevent the increase in the number of PI-positive cells induced by NMDA. BIBP 3226 or L-152,804 (Y_1 or Y_5 antagonist, respectively) blocked the protective effect of NPY, and BIBP 3226 blocked the protective effect of (Leu[31], Pro[34])-NPY. The application of 1µM (Gly[1], …Aib[32])-PP was able to prevent the increase in PI-positive cells induced by NMDA, and this effect was blocked by L-152,804. This result suggests that NPY is able to protect retinal cells from an excitotoxic insult through the activation of Y_1 and Y_5 receptors. Data are presented as mean ± SEM of n = 5-11 independent experiments. ***p<0.001, compared to control; ###p<0.001, compared to NMDA; §§p<0.01, §§§p<0.001, compared to NMDA + NPY, or NMDA + (Leu[31], Pro[34])-NPY, or NMDA + (Gly[1], …Aib[32])-PP. Kruskal-Wallis followed by Dunn's test.

3.2.6 – NPY does not prevent the reduction in Brn3a-positive RGCs induced by NMDA in retinal explants

Brn3a labelling of RGCs has been used as a valid marker to study the survival of RGCs in injured retinas (Nadal-Nicolas et al., 2009; Nadal-Nicolas et al., 2012). Retinal explants were pre-treated with 1 µM NPY, 24 h and 60 min before exposure to 300 µM NMDA for 48 h (Fig. 3.15 A). NMDA exposure induced a significant decrease in the number of Brn3a-positive RGCs to 274 ± 51 cells/mm^2, compared to control (977 ± 140 cells/mm^2; Fig. 3.15 B). However, pre-treatment with 1µM NPY was not able to prevent this decrease. This result indicates that the neuroprotective effect exerted by NPY pre-treatment found in TUNEL and PI assays might restrict to amacrine cells and does not extend to RGCs.
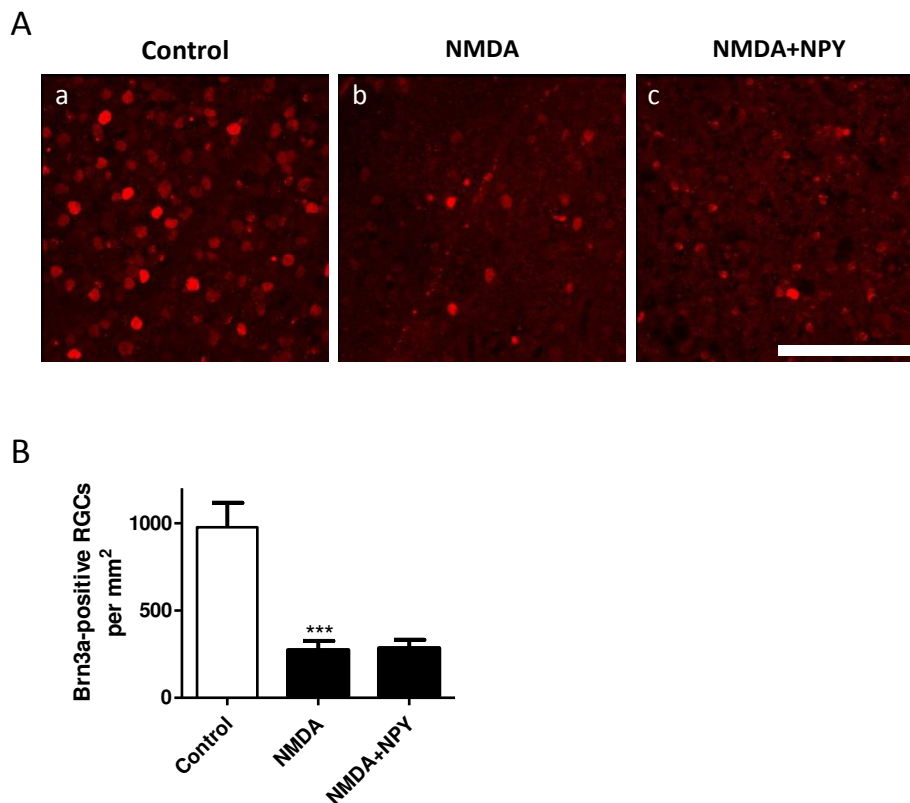
Figure 3.15. NPY does not prevent NMDA-induced reduction in Brn3a-positive RGCs in retinal explants. (A) Representative images of Brn3a-positive RGCs (red) in the GCL of control (a) or NMDA-treated (b, c) retinal explants. Retinal explants were pre-treated with 1 µM NPY, 24 h and 60 min before exposure to 300 µM NMDA for 48 h. Scale bar: 100 µm. (B) NMDA exposure induced a significant decrease in the number of Brn3a-positive RGCs compared to control. Pre-treatment with 1 µM NPY was not able to prevent this decrease. Data are presented as mean ± SEM of n = 9-12 independent experiments. ***p<0.001, compared to control. One-way ANOVA followed by Bonferroni's test.

3.2.7 – Intravitreal administration of NPY does not prevent cell death induced by I-R injury

In addition to cultured retinal explants, we also explored the potential neuroprotective action of NPY in an animal model of retinal damage induced I-R injury (Fig. 3.16 A). Retinal ischemia was induced for 60 min followed by 24 h of reperfusion. Ischemia was induced in one eye, and the contralateral eye was taken as an internal control. Saline or 10 μg (2.34 nmol) NPY were intravitreally injected 2 h before the onset of I-R injury. Retinal cell death was assessed by TUNEL-assay (Fig. 3.16 B). I-R injury induced an increase in the number of TUNEL-positive cells per mm of retinal section length to 31.8 ± 6.6 compared to contralateral eye (0.6 ± 0.3 TUNEL-positive cells across all the retinal nuclear layers) (Fig. 3.16 C). This increase was not prevented by pre-treatment with NPY. RGC survival was evaluated using the RGC marker Brn3a (Nadal-Nicolas et al., 2012). We found that I-R injury decreased the number of Brn3a-positive RGCs per mm of retinal section length to 12.0 ± 2.5 RGCs compared to the contralateral eye (26.0 ± 4.5), and again, this effect was not prevented by NPY administration (Fig. 3.16 D).

We also performed ERGs in order to assess the functional effect of I-R injury on retinal light responses. Scotopic and photopic ERGs were recorded before the onset of I-R injury (Baseline) and after 24 h of reperfusion (Fig. 3.17). The obtained ERG values for amplitudes and latencies were normalized to baseline ERG. We found that the a-wave amplitude was not affected by I-R injury (Fig. 3.18). However, I-R reperfusion injury induced decreased b-wave amplitudes, to 37.7 ± 11.0% of baseline ERG for scotopic ERG (Fig. 3.18 C) and to 10.1± 5.6% of baseline ERG for photopic ERG (Fig. 3.18 E). The amplitudes of scotopic b-wave were reduced in all three animals tested, although no statistically significant differences were detected (Fig. 3.18 C). Also, the latencies for scotopic a-wave and b-wave, and photopic b-wave were not affected by I-R injury (Fig. 3.18 B, D, F, respectively). Similarly to what was found regarding TUNEL and Brn3a results (Fig. 3.16), NPY administration before I-R injury did not prevent the reduction in ERG b-wave amplitudes, both scotopic and photopic (Fig. 3.18 C, E, respectively). Together, these results indicate that, contrarily to the protective action against an excitotoxic injury in retinal explants, NPY pre-treatment was not able to prevent retinal I-R injury within 24 h of reperfusion. Therefore, further studies are needed in order to evaluate whether NPY neuroprotective action translates to *in vivo* models of retinal diseases.
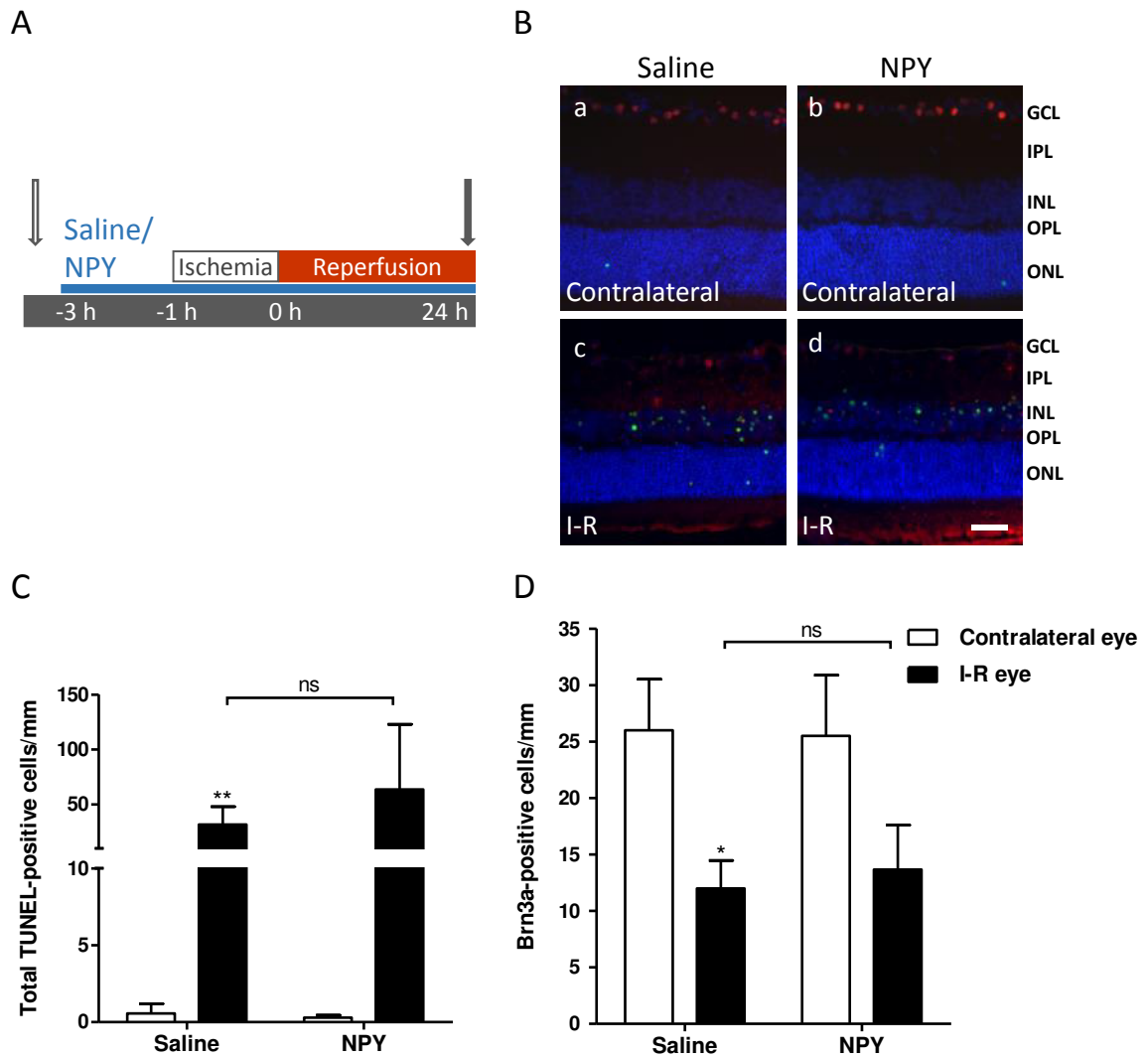
Figure 3.16. Intravitreal administration of NPY is not able to prevent cell death induced by I-R injury at 24 h of reperfusion. (A) Schematic representation of the protocol of retinal I-R injury and intravitreal administration. Retinal ischemia was induced for 60 min followed by 24 h of reperfusion. Saline, or 10 µg NPY, were intravitreally injected 2 h before the onset of I-R injury. Arrows indicate the ERG recordings, performed before (Baseline, open arrow) and 24 h after I-R injury (grey arrow). Ischemia was induced in one eye, and the contralateral eye was taken as an internal control. (B) Representative images of retinal sections showing TUNEL-positive cells (green) and Brn3a-positive RGCs (red). Nuclei were stained with DAPI (blue). Saline (a, c), or 10 µg NPY (b, d) were intravitreally injected 2 h before the onset of I-R injury. GCL, ganglion cell layer; IPL, inner plexiform layer; INL, inner nuclear layer; OPL, outer plexiform layer; ONL, outer nuclear layer. Scale bar: 50 µm. (C) TUNEL-positive cells are expressed per mm of retinal section length. I-R injury induced an increase in the number of TUNEL-positive cells. NPY administration was not able to reduce the number of TUNEL-positive cells. (D) Brn3a-positive RGCs were expressed per mm of retinal section length. NPY administration was not able to prevent the reduction in Brn3a-positive RGC number induced by I-R injury. Data are presented as mean ± SEM of n = 6 independent experiments. *$p < 0.05$, **$p < 0.01$, compared to Contralateral eye. Kruskal-Wallis followed by Dunn's test.
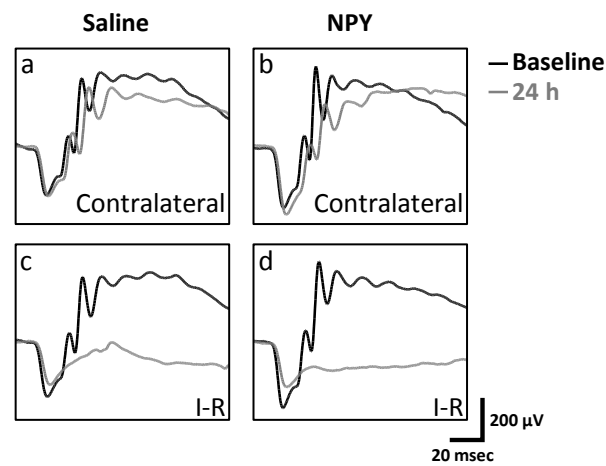
Figure 3.17. Intravitreal administration of NPY is not able to prevent ERG changes induced by I-R injury at 24 h of reperfusion. Ischemia was induced in one eye, and the contralateral eye was taken as an internal control. Examples of scotopic ERG traces for saline (a, c) and NPY-treated eyes (b, d). ERG recordings were performed before (Baseline) and 24 h after I-R injury. Note that in the injured eye the b-wave was abruptly reduced (c). NPY administration did not prevent the reduction in b-wave (d).
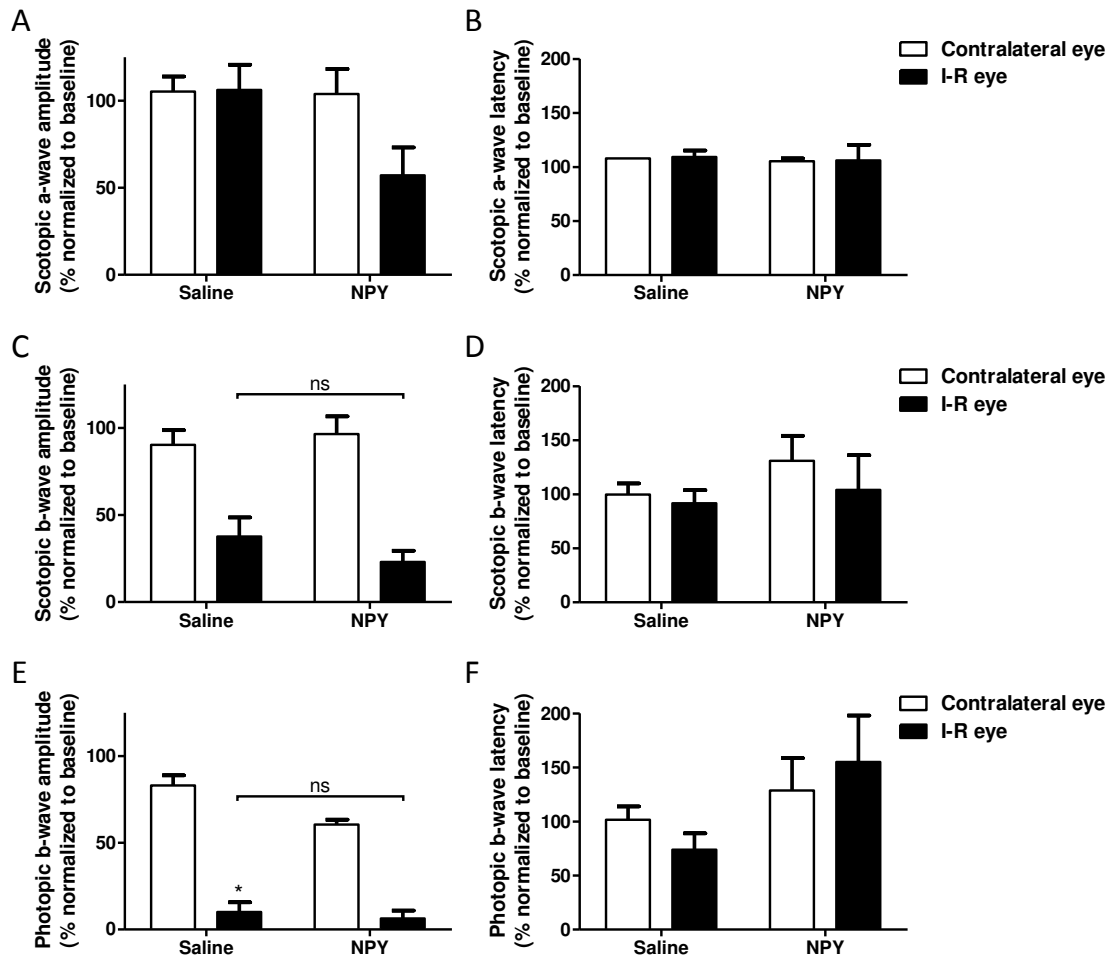
Figure 3.18. Intravitreal administration of NPY was not able to prevent ERG changes induced by I-R injury. Ischemia was induced in one eye, and the contralateral eye was taken as an internal control. Quantification of a-wave amplitude (A) and latency (B), scotopic b-wave amplitude (C) and latency (D), and photopic b-wave amplitude (E) and latency (F). In the injured eye (I-R eye), the a-wave amplitude was not affected (A), but the b-wave amplitude was decreased (C, E). For the a-wave and b-wave latencies, no changes were detected (B, D, E). NPY administration did not prevent the reduction in b-wave amplitudes (C, D). Data are presented as mean ± SEM of n = 3 independent experiments. *p<0.05, compared to Contralateral eye. Kruskal-Wallis followed by Dunn's test.

3.3 – Discussion

In this study, we evaluated the presence and localization of NPY and NPY receptors in the rat retina, particularly at RGC level. The presence of mRNA for both NPY and NPY receptors (Y_1, Y_2, Y_4, and Y_5) in the rat retina have been demonstrated in previous studies (D'Angelo and Brecha, 2004; Alvaro et al., 2007). We now present evidence supporting the presence of NPY and NPY receptors specifically in acutely isolated RGCs from both Wistar and Long Evans rats obtained from P3-4 pups or adult animals (Fig. 3.1). NPY-ir in the retina has been extensively evaluated in different species (Santos-Carvalho et al., 2014). In human retina, NPY-ir was shown to be confined to a subset of amacrine cells and RGCs, which processes extend mainly in the IPL and occasionally in the OPL (Tornqvist and Ehinger, 1988; Straznicky and Hiscock, 1989). In rat retina, NPY-ir was reported to localize in cell bodies of amacrine cells in INL and displaced amacrine cells in GCL and to co-localize mainly with gabaergic neurons. The corresponding cell processes extend and ramify mainly in strata 1, 3, and 5 of IPL, and very occasionally in OPL (Oh et al., 2002). We confirmed these observations in the rat retina using retinal slices of adult rats and showing NPY-ir in cell bodies of GCL and INL and in ramified dendrites in strata 1, 3, and 5 of IPL (Fig. 3.3). In addition, we found NPY-ir in a purified culture of RGCs obtained from P3-4 pups. In a previous study, we have also suggested the presence of NPY-ir in different retinal cell types in a primary culture of retinal cells (Alvaro et al., 2007).

Regarding the localization of NPY receptors in the retina, few studies addressed this issue. In human retina, transcripts for Y_1, Y_2, and Y_5 receptors were detected in RPE (Ammar et al., 1998). Y_1 receptor-ir was detected in glial cells of diseased human retina and in horizontal and amacrine cells of rat retina (Canto Soler et al., 2002; D'Angelo et al., 2002), and we have previously detected immunoreactivity for Y_1 and Y_2 receptors in neurons and glial cells in cultured retinal cells (Santos-Carvalho et al., 2013a). Moreover, we and others have reported functional evidence suggesting the presence of Y_1, Y_2, Y_4, and Y_5 receptors in retinal cells (Bruun et al., 1994; D'Angelo and Brecha, 2004; Milenkovic et al., 2004; Alvaro et al., 2008a; Alvaro et al., 2009; Santos-Carvalho et al., 2013b). Regarding purified RGC cultures, we detected immunoreactivtiy for NPY and Y_1, Y_2, Y_4, and Y_5 receptors in Brn3a-positive RGCs. In retinal sections, Y_1-ir was found in GCL, in agreement with the labelling found in purified RGC cultures. Using an antigen retrieval step, we indeed detected Y_2, Y_4, Y_5 receptor-ir in retinal sections. Y_2 receptor-ir was found in stratum 1 of IPL and in cell bodies in proximal INL. Y_4

receptor-ir was localized in cell bodies of GCL, and proximal and distal INL. The cell bodies in GCL that were immunoreactive for Y_4 receptor were both RGC (co-localized with Brn3a) and non-Brn3a-positive cells, likely displaced amacrine cells. Concerning Y_5 receptor, immunoreactivity was detected in Müller cells confirmed by co-localization with vimentin (Fig. 3.4). The lack of clear immunoreactivity for NPY, and for Y_2 and Y_5 receptors in RGCs in retinal sections of adult rat, while it could be found in cultured RGCs from P3-4 rats, may be explained by decreased expression in adulthood or related with the cell culture conditions, which might favour the expression of NPY or NPY receptors. In addition to immunofluorescence data, we present further evidence showing the presence of functional active NPY receptors in the inner retina using [^{35}S]GTPγS binding assay (Fig. 3.5). Binding signal detected in the photoreceptor layer might represent the high amount of G proteins in photoreceptor outer segments, mainly transducin (Arshavsky et al., 2002).

NPY has been associated with inhibitory actions after electrical or chemical stimulation of excitatory synaptic transmission (El Bahh et al., 2002; Tu et al., 2006; Kovac et al., 2011). In fact, in different neuronal cell types NPY was reported to decrease depolarization-evoked increase in [Ca^{2+}]$_i$ by inhibiting voltage-dependent Ca^{2+} channels. This effect was reported in a variety of neuronal cell types such as dorsal root ganglion neurons (Bleakman et al., 1991), hippocampal neurons (Bleakman et al., 1992), submandibular ganglion neurons (Endoh et al., 2012), and hypothalamic arcuate nucleus neurons (Sun and Miller, 1999). In rat thalamic neurons, NPY was shown to activate GIRK channels via Y_1 and inhibit N and P/Q-type Ca^{2+} channels via Y_2 receptor activation (Sun et al., 2001), whereas in arcuate nucleus neurons, NPY analogues that activated all of the known NPY receptors (Y_1, Y_2, Y_4, and Y_5) were able to both inhibit Ca^{2+} currents and activate inwardly rectifying K^+ currents (Sun and Miller, 1999). Moreover, the activation of Y_1 receptor has been associated with inhibition of neurotransmitter release (Bitran et al., 1999; Hastings et al., 2004; Wang, 2005), though the opposite can be found depending on the neurotransmitter or cell type (Hastings et al., 2001). In the retina, Y_2 receptor activation attenuated depolarization-evoked Ca^{2+} influx in rod bipolar cell terminals (D'Angelo and Brecha, 2004). In addition, previous work in our laboratory has shown that NPY application to retinal cell cultures was able to reduce depolarization-evoked [Ca^{2+}]$_i$ increase via activation of Y_1 and Y_5 receptors (Alvaro et al., 2009). Thus, we now aimed to evaluate the effect of direct application of NPY or NPY receptor agonists on Ca^{2+} influx into RGCs, using a purified RGC culture. Glutamate is the major excitatory neurotransmitter in the retina mediating the communication between bipolar cells and RGCs. In this experiment, 30

µM glutamate plus 10 µM glycine, and a Mg^{2+}-free extracellular solution, was used to stimulate Ca^{2+} influx into cultured RGCs by activating both NMDA and non-NMDA glutamate receptors and indirectly VDCCs, as previously described (Hartwick et al., 2004), though in these conditions Ca^{2+} influx was found to be primarily mediated by NMDA glutamate receptors (Hartwick et al., 2008). We now present evidence showing an inhibitory effect of NPY on glutamate-evoked increase in $[Ca^{2+}]_i$ on purified RGCs likely through Y_1 receptor activation (Fig. 3.6). This result suggests that NPY, released from amacrine cells (Oh et al., 2002), may activate post-synaptic Y_1 receptors on RGCs inhibiting glutamate receptors or VDCC, thus modulating the effect of glutamate released from bipolar cells.

We further explored the modulatory potential of NPY on RGC spiking activity using a MEA (Meister et al., 1994). Although application of NPY or NPY receptor agonists did not affect the spontaneous spiking activity, a small increase was found at the initial burst response of OFF-type RGCs upon Y_1/Y_5 receptor activation (Fig. 3.9). We hypothesized that modulatory effects of NPY receptor activation may be exerted within the circuitry generating centre-surround organization within the receptive field of OFF-type RGCs at the level of amacrine cell-RGCs (Sinclair et al., 2004). A decreased contribution of ON bipolar cell signal to this circuitry could be responsible for this effect although that may not be the case since Y_2 receptor activation, but not Y_1 or Y_5, was reported to inhibit rod bipolar cells (D'Angelo and Brecha, 2004). Another possibility is that the modulatory effect may reside at the level of horizontal cell circuitry at the OPL, since it contributes to centre-surround organization (Wassle and Boycott, 1991), and Y_1 receptor was shown to localize in rat horizontal cells (D'Angelo et al., 2002).

In another experiment paradigm, *ex vivo* retinal preparations were exposed to NMDA to induce an excitatory stimulus to RGCs. We chose NMDA instead of glutamate since in intact retina even high concentrations of glutamate have no effect on RGC Ca^{2+} levels (Hartwick et al., 2004) due to the presence of glutamate uptake systems (Thoreson and Witkovsky, 1999). We confirmed that Y_1 receptor activation is able to modulate directly RGC responses by attenuating the NMDA-induced increase in RGC spiking activity (Fig. 3.11). These results suggest that the activation of Y_1 receptors present in RGC dendrites is responsible for the modulatory effect observed. Nevertheless, the contribution of Y_1 receptor expressing amacrine cell inputs onto RGC dendrites may be also important (D'Angelo et al., 2002). Additional studies are needed to clarify the cellular contribution (RGC versus amacrine cells) and localization of Y_1 receptor activation to the alterations in RGC spiking activity, and whether

Y_1 receptor activation is associated to a particular RGC type or modulates a specific visual task (Gollisch and Meister, 2010).

NPY has been shown to prevent neuronal cell death, also in the retina, induced by excitotoxic insults (Silva et al., 2003; Xapelli et al., 2007; Santos-Carvalho et al., 2013b). To further address this issue in the retina, we used an *in vitro* model, cultured retinal explants exposed to NMDA, as well as an *in vivo* model of retinal I-R injury. Both cultured retinal explants and the I-R model have been used to evaluate potential neuroprotective strategies targeting retinal neurons, specially RGCs (Lagreze et al., 1998; Goodyear and Levin, 2008; Peng et al., 2011; Zhang et al., 2012). We found that NPY pre-treatment was able to prevent NMDA-induced cell death in retinal explants, through the activation of Y_1 and Y_5 receptors (Fig. 3.13). This result confirm previous studies showing neuroprotective effects upon Y_1 or Y_5 receptor activation (Silva et al., 2003; Xapelli et al., 2007; Smialowska et al., 2009), including in retinal neurons (Santos-Carvalho et al., 2013b). However, pre-treatment with NPY was not able to prevent the decrease in Brn3a-positive RGCs induced by NMDA exposure (Fig. 3.15). This result indicates that the neuroprotective effect exerted by NPY pre-treatment found in TUNEL and PI assays might be mainly restricted to amacrine cells and does not extend to RGCs. This selective effect may be explained by the localization of NPY and NPY receptors in the rat retina. In fact, in the GCL, NPY was shown to be localized in displaced amacrine cells but not in RGCs (Oh et al., 2002), and Y_1 receptor was found to be expressed in amacrine cell dendrites in IPL (D'Angelo et al., 2002). Therefore, we hypothesized that the activation of NPY receptors in amacrine cells may be responsible for the protective effect observed in this cell type and not in RGCs. Moreover, in retinal I-R injury model, pre-treatment with NPY was not able to prevent cell death or rescue RGCs (Fig. 3.16). This observation contrasts with the protective effect of NPY when injected intravitreally before the intravitreal injection of glutamate, in a model of glutamate-induced injury in the retina (Santos-Carvalho et al., 2013b). In fact, retinal I-R injury involves a complex cascade of destructive events including excessive glutamatergic stimulation and calcium influx, oxidative stress due to energy failure, and inflammatory processes, making difficult to determine the treatment strategy (Osborne et al., 2004). Therefore, further studies are needed in order to evaluate whether NPY neuroprotective effects detected in cultured retinal explants can be translated to animal models of retinal degenerative diseases.

CHAPTER 4

Sildenafil Acutely Decreases Light Responses

in Retinal Ganglion Cells

4.1 – Introduction

Sildenafil is a PDE type 5 inhibitor widely used for treatment of erectile dysfunction (Salonia et al., 2003), and also for pulmonary arterial hypertension (Montani et al., 2013). Patients with erectile dysfunction have experienced transient and mild impairments of colour discrimination, which are occurring at the peak of the drug action (Laties and Zrenner, 2002). Moreover, sildenafil was found to decrease visual performance, particularly temporal response, in S-cone isolating conditions (Stockman et al., 2007), and, in rare cases, transient blindness was reported (Montastruc et al., 2006). It has also been suggested as a possible, but not yet certain, cause of anterior ischaemic optic neuropathy (Carter, 2007). However, other studies reported no visual toxic effects in both human patients and laboratory animals even after long periods of drug daily use (Vatansever et al., 2003; Cordell et al., 2009; Zoumalan et al., 2009).

Different electrophysiological studies have investigated the effect of the drug on the retinal function. *In vivo* ERG recordings showed decreases in both a- and b-wave amplitudes in sildenafil-treated patients (Vobig et al., 1999), or inversely, an increase in the scotopic ERG responses, but a decrease in the photopic response (Luu et al., 2001). Other studies reported an increase in Naka-Rushton equation Vmax, suggesting higher rod response after sildenafil ingestion (Gabrieli et al., 2001; Gabrieli et al., 2003). More consistently, among all human studies, sildenafil enlarged the latencies of the different responses (Luu et al., 2001; Jagle et al., 2004; Jagle et al., 2005). *Ex vivo* experiments have also shown some contradictory results. Sildenafil has been shown to increase ERG amplitudes in the rat retina (Barabas et al., 2003), whereas it decreases ERG amplitudes in bovine and human retinas, while increasing the latencies (Luke et al., 2005; Luke et al., 2007).

These effects of sildenafil on retinal function could be related to the inhibition of PDE5, which is expressed in retinal cells, including human RGCs (Foresta et al., 2008). However, apart from its effect on PDE5, sildenafil can also inhibit other PDEs including PDE6, which controls the phototransduction cascade in photoreceptors (Beavo, 1995; Lamb, 2013). Sildenafil appears almost equally potent on cone PDE6 as on PDE5, whereas it seems slightly less potent on rod PDE6 (Ballard et al., 1998; Zhang et al., 2005). The functional relevance of blocking photoreceptor PDE6s was demonstrated following rat retinal explant incubation with zaprinast, another mixed PDE5/6 blocker (Zhang et al., 2005). This blocker induced an

elevation of cGMP and the consequent photoreceptor death attributed to an excessive activation of the cGMP-gated channels generating the dark current in photoreceptors (Vallazza-Deschamps et al., 2005). PDE4s are also expressed in RGCs, bipolar cells, cholinergic amacrine cells and rods (Whitaker and Cooper, 2009), whereas PDE1 and PDE9 were described so far in bipolar cells (Dhingra et al., 2008).

Together, the previous studies have reported conflicting results on the effect of sildenafil on retinal function. To further understand the effect of different concentrations of sildenafil on principal characteristics of light-induced RGC responses (magnitude and latency) and the spontaneous firing rate, we have analysed, for the first time, the retinal output signal at the RGC level in the presence of sildenafil.

4.2 – Results

4.2.1 – Sildenafil at high concentration acutely increases RGC spiking activity and abolishes light responses

ON- or OFF-type RGC light responses were recorded on a MEA upon a series of 10 consecutive stimulus blocks consisting of 5 sec light followed by 10 sec dark (Fig. 4.1). After a 10 min application of a high concentration of sildenafil (30 μM), we found a rapid, partial or complete, abolishment of RGC light responses in both ON- and OFF-types (Fig. 4.2 and 4.3, respectively). This result confirms that sildenafil can affect retinal function acutely inhibiting the retinal output. However, we noticed that among the 10 consecutive stimulus blocks, the responses of ON-type RGCs to the first block appeared enlarged in both light and dark period (Fig. 4.2 B). This atypical ON-response, which was only observed at 30 μM sildenafil (Fig. 4.4), was not observed in the following ON responses, which were heavily suppressed (Fig. 4.2 D). When considering the spontaneous activity in dark, sildenafil application (0.3 to 30 μM) for 10 min did not induce statistically significant differences on either ON- or OFF-type RGCs, though some cells exhibited a slight increase in spontaneous activity but only at the highest (30 μM) concentration (Fig. 4.5).
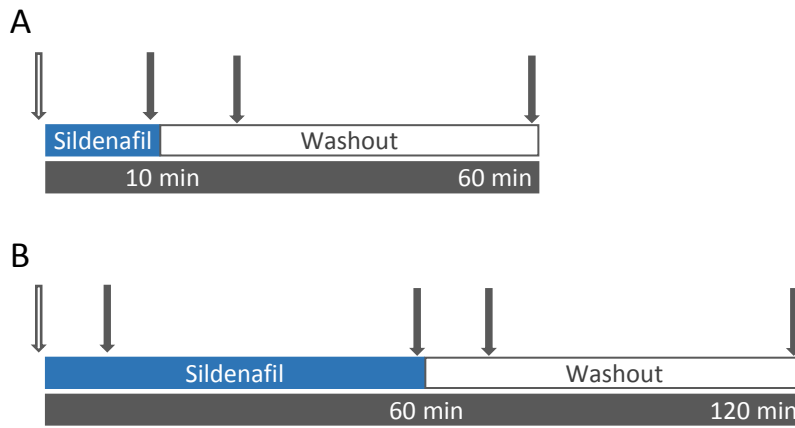
Figure 4.1. Schematic representation of sildenafil application to *ex vivo* retinas. Sildenafil (0.3 to 30 µM) was applied for 10 (A) or 60 min (B) under continuous perfusion. After sildenafil application, a period of 60 min of washout was performed. Arrows indicate MEA recordings, before sildenafil application (Baseline, open arrow), upon sildenafil, or during washout period.
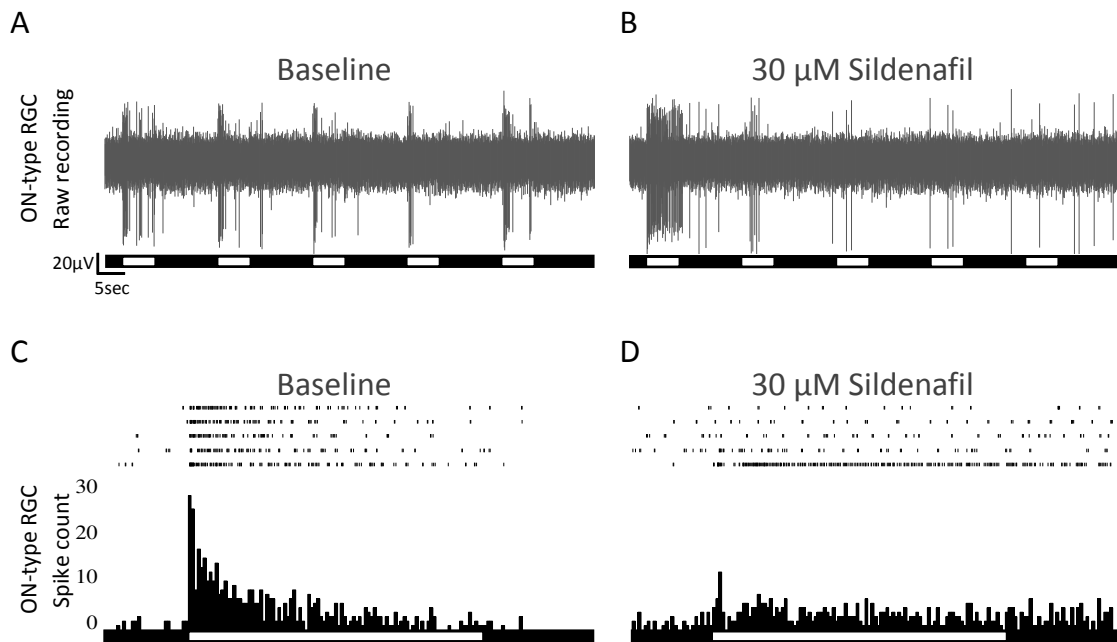
Figure 4.2. Effects of high concentration of sildenafil on ON-type RGC light responses. Examples of RGC light responses before (baseline) and after exposure to 30 µM sildenafil for 10 min. Series of 10 consecutive stimulus blocks, each consisting of 5 sec of light period followed by 10 sec dark, were delivered to *ex vivo* retinas. Raw recordings for 5 consecutive stimulus blocks are shown for an ON-transient RGC, before (A) and after 30 µM sildenafil application for 10 min (B). Note the enlarged response to the first stimulus block. Peri-stimulus time histograms (PSTHs) and raster plots for ON-transient RGC responses are shown for five consecutive stimulus blocks before (C) and after 30 µM sildenafil application for 10 min (D). After 30 µM sildenafil application RGC responses are acutely reduced or abolished. Note that raster plots representing spiking events become not aligned with light period of stimulus blocks (B). White rectangles indicate duration of light period.
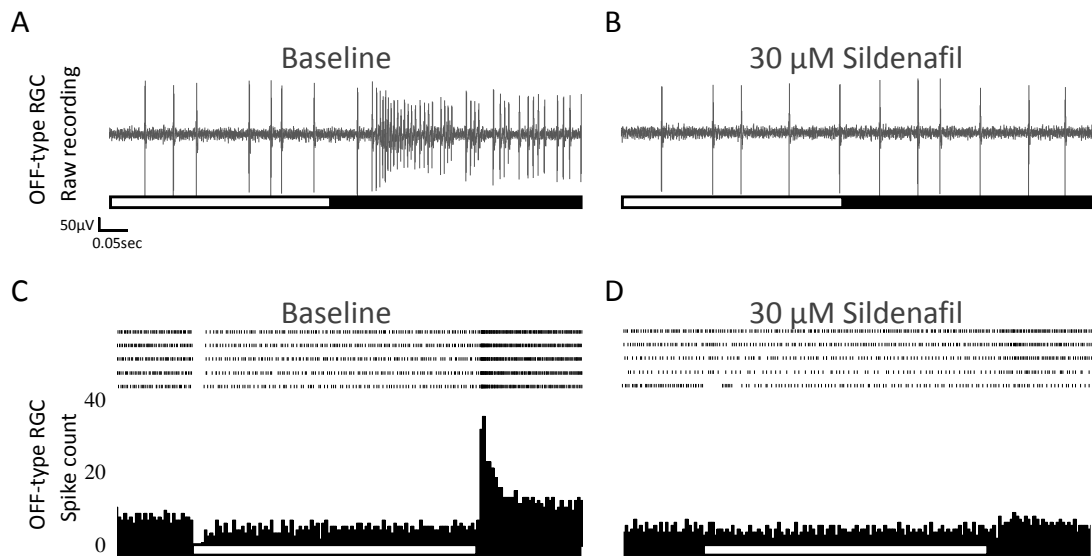
Figure 4.3. Effects of high concentration of sildenafil on OFF-type RGC light responses. Series of 10 consecutive stimulus blocks, each consisting of 5 sec of light period followed by 10 sec dark, were delivered to *ex vivo* retinas. Example of raw recording of an OFF-transient RGC before (A) and after application of 30 μM sildenafil for 10 min (B) is shown. Peri-stimulus time histograms (PSTHs) and raster plots of OFF-transient RGC responses are shown for five consecutive stimulus blocks before (C) and after application of 30 μM sildenafil for 10 min (D). Note that RGCs responses are acutely reduced or abolished after sildenafil application. White rectangles indicate duration of light period.
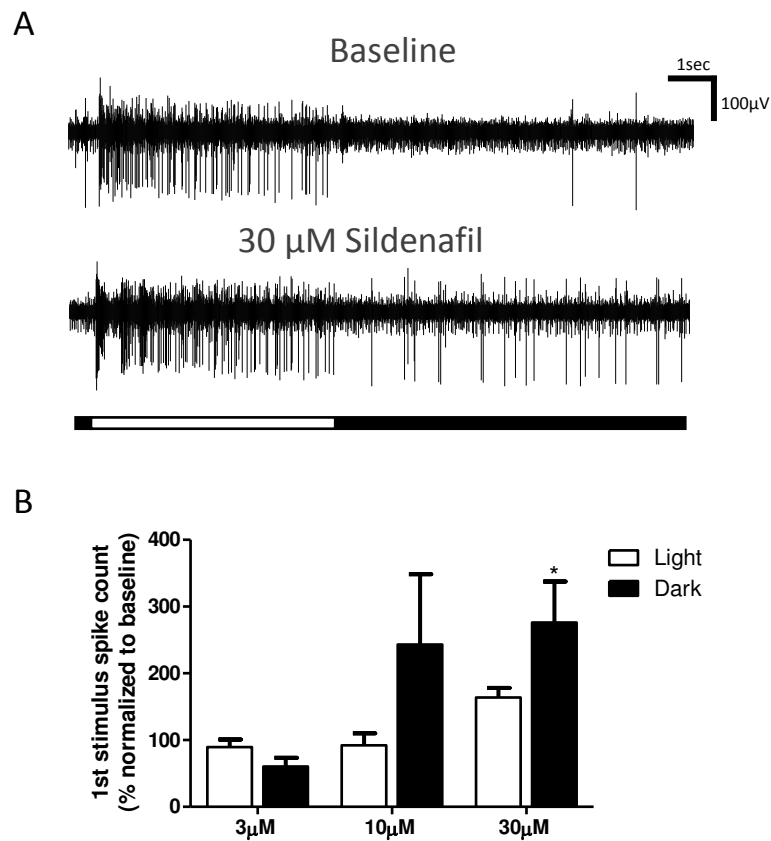
Figure 4.4. Quantification of spiking activity for the first stimulus block of ON-type RGC responses following application of high concentrations of sildenafil. (A) Raw recordings for the first stimulus block for an ON-transient RGC before (baseline) and after exposure to 30 μM sildenafil for 10 min. The white rectangle indicates the duration of light period. (B) Quantification of spiking events for ON-transient RGCs after sildenafil application (3 to 30 μM), for 10 min. The graph indicates the number of spikes during the light period (white bars) and during the dark period (grey bars) of the first stimulus block. The spike count values were normalized to the measurements obtained during the baseline recordings. Sildenafil application induced an increase in spiking activity especially during the dark period of stimulus block. * $p < 0.05$, compared to baseline. Kruskal-Wallis followed by Dunn's test.
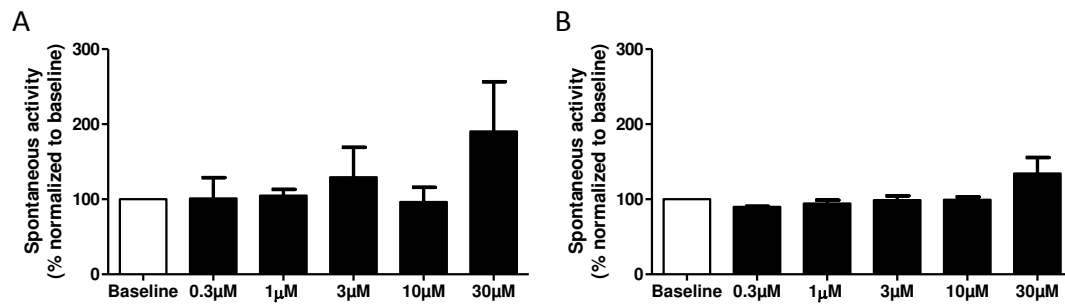
Figure 4.5. Maintenance of the RGC spontaneous firing rate after sildenafil application. Effects of sildenafil application (0.3 to 30 µM, for 10 min) on the RGC spontaneous spiking activity were evaluated. RGCs were divided in ON- (A) and OFF-type (B). Spontaneous spiking rates were normalized to the baseline values obtained before exposure to drug. RGCs exhibited a spontaneous baseline spiking rate of 4.6 ± 4.1 Hz for ON-type RGCs and 19.3 ± 8.6 Hz for OFF-type RGCs. Only at the highest sildenafil concentration (30 µM) some RGCs showed increased spontaneous spiking rate after sildenafil application, although no statistically significant difference was found.

4.2.2 – Sildenafil affects the RGC light responses in a concentration-dependent manner

To further elucidate the sildenafil effects on light responses, we applied escalating sildenafil concentrations from 1 to 30 µM in order to evaluate its concentration-dependent effects. Since the response to the first stimulus block included the response of a non-adapted retina where activity from neighbouring RGCs introduced extra noise in individual recording electrodes, we always excluded the first stimulus block from the measurements for quantification. In ON-type RGCs the application (10 min) of sildenafil induced a concentration-dependent decrease in light response magnitude (Fig. 4.6). Such effect was observed for both initial burst response to light onset (Fig. 4.6 A), and for 1 sec and 5 sec rate (Fig. 4.6 B and C, respectively). The highest sildenafil concentration (30 µM) completely suppressed the ON- and OFF-type light responses in 50% of RGCs. When light responses were detected for 30 µM, they were strongly reduced (Fig. 4.6 A-C).

After sildenafil application, we perfused retinas with a drug-free Ames' medium for up to 60 min to assess the reversibility of sildenafil effects on ON- and OFF-type responses. We also recorded the response to 10 consecutive stimulus blocks every 10 min in order to monitor the RGC light response during the entire protocol. After 60 min of washout, although partial recovery (to 89.8 ± 18.7% for 10 µM and to 60.8 ± 9.4% of initial response for 30 µM) of the magnitude may be seen for the initial burst (Fig. 4.6 A), it was hardly found especially for 5 sec rate (Fig. 4.6 C), which may indicate residual alterations of retinal response for long periods

after cessation of drug exposure. We also quantified the latency of ON-response and found that this principal parameter of light responses was greatly increased in a similar concentration-dependent fashion as response magnitudes (Fig. 4.6 D). For 10 and 30 µM sildenafil concentrations, the increase in latency of ON-responses reached 272.9 ± 55.4 and 387.4 ± 106.0% of initial response, respectively. However, contrarily to ON-response magnitudes, their latencies were clearly recovered, though not completely, after 60 min of washout. For 10 µM sildenafil concentration the ON-response latency recover to 143.0 ± 7.4% and for 30 µM concentration the recovery reached 197.5 ± 21.6% of initial response (Fig. 4.6 D).
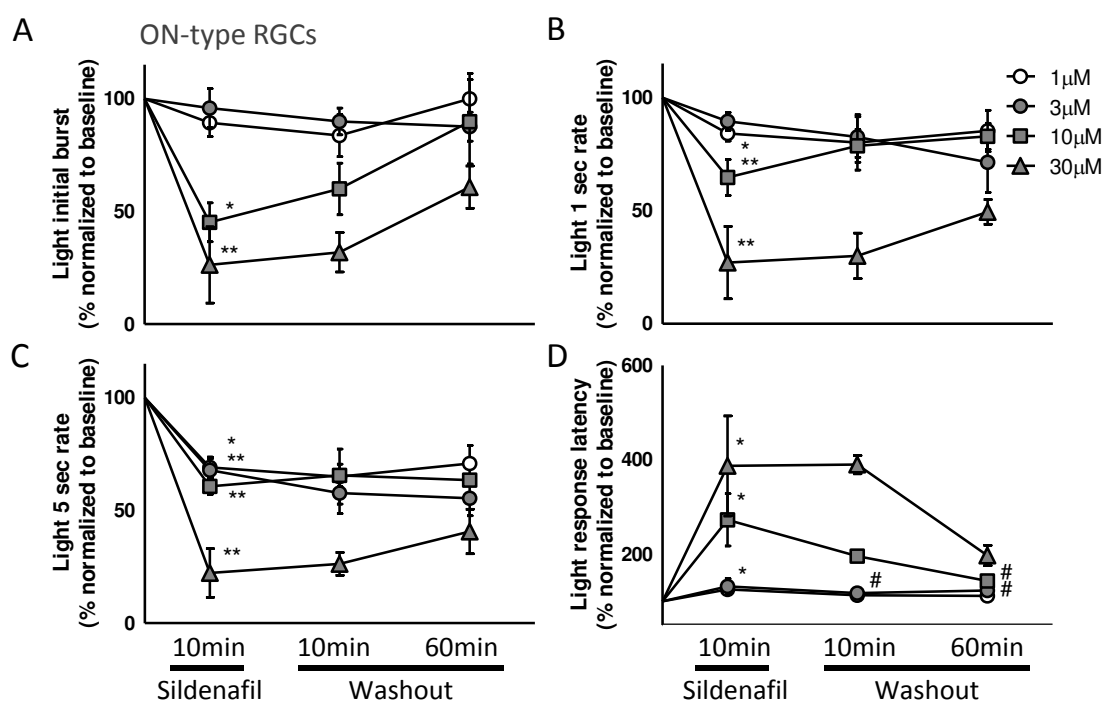
Figure 4.6. Concentration-dependent and reversible effects of sildenafil on ON-type RGC light responses. Sildenafil application (1 to 30 µM) for 10 min concentration-dependently reduces the magnitude of ON-type RGC response to light onset. This reduction was found at both initial burst (A), and 1 sec (B) and 5 sec rate (C). The response latencies were increased in a similar concentration-dependent fashion (D). After 60 min of washout the recovery of response magnitudes were hardly seen especially for 5 sec rate (C). On the contrary, for the response latencies, a clear washout of sildenafil effect was found (D). All results were normalized to the baseline values obtained before drug exposure. *p<0.05, **p<0.01, compared to baseline; #p<0.05, compared to sildenafil (10 min). Kruskal-Wallis followed by Dunn's test.
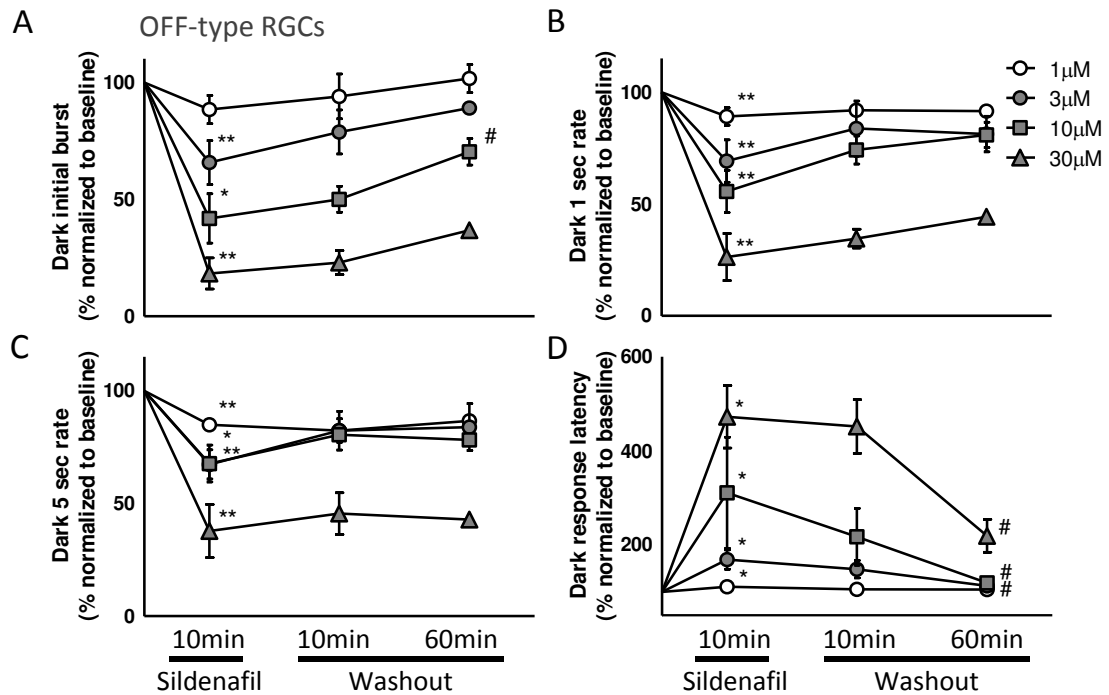
Figure 4.7. Concentration-dependent and reversible effects of sildenafil on OFF-type RGC light responses. Sildenafil application (1 to 30 μM) for 10 min concentration-dependently reduces the magnitude of OFF-type RGC response to dark onset. This reduction was found at both initial burst (A), and at 1 sec (B) and 5 sec rate (C). The response latencies were also increased in a concentration-dependent manner (D). After 60 min of washout, although some partial recovery of response magnitude was seen (A), no recovery was found with increasing sildenafil concentrations (A-C). Similarly to ON-type RGCs, the response latencies showed a clear washout of sildenafil effect (D). All results were normalized to the baseline values obtained before drug exposure. *$p<0.05$, **$p<0.01$, compared to baseline; #$p<0.05$, compared to sildenafil 10 min. Kruskal-Wallis followed by Dunn's test.

Concerning OFF-type RGCs, a similar pattern of concentration-dependent decrease of OFF-response magnitudes was found (Fig. 4.7 A-C). This decrease reached 41.8 ± 10.5% and 18.3 ± 6.7% of the initial response for 10 and 30 μM, respectively, for the initial burst (Fig. 4.7 A). Also, the 1 sec and 5 sec rate were reduced (Fig. 4.7 B and C). After 60 min of washout, although some partial recovery to 70.4 ± 5.7% of response magnitude was seen for RGCs exposed to 10 μM sildenafil (Fig. 4.7 A), no recovery was found with higher (30 μM) concentration (Fig. 4.7 A-C). The response latencies were also greatly increased in a concentration-dependent fashion. This increase reached 311.0 ± 118.5% and 472.9 ± 66.5% of initial response for 10 and 30 μM, respectively. Similarly to ON-type RGCs, a partial recovery was evident upon 60 min washout (Fig. 4.7 D). Although not complete, the latencies returned to 119.3 ± 7.7% and 219.5 ± 35.1% of initial response for 10 and 30 μM, respectively. Together,

these results suggest that although light responses in ON- and OFF-type RGCs recover after removal of sildenafil, some characteristics of responses, as magnitudes and latencies, may be slightly altered for longer periods.

4.2.3 – Potentiation of sildenafil effects with extended exposure

Since it cannot be discarded the possibility of cases of sildenafil abuse such as the combination with illicit drugs (Lowe and Costabile, 2011), resulting in unpredictable pharmacokinetics even with therapeutic doses, we attempted to evaluate how longer exposures to lower concentrations would further potentiate the sildenafil-elicited modifications on RGC light responses. Therefore, the duration of drug application was extended to 60 min for concentrations ranging from 0.3 to 3 µM sildenafil, followed by washout. The response to 10 consecutive stimulus blocks was recorded every 10 min. In ON-type RGCs, even concentrations as low as 0.3 and 1 µM generated higher reduction in response magnitude, to 83.8 ± 12.3% and 69.6 ± 9.9% of initial response, respectively, for initial burst to light onset (Fig. 4.8 A). The sildenafil effect was enhanced with extended exposure for both 1 sec and 5 sec rate (Fig. 4.8 B and C). Note that 60 min of sildenafil washout was not sufficient to recover the initial response magnitude (Fig. 4.8 A-C), suggesting thereby a massive impregnation of the tissue thus requiring longer recovery periods. For response latencies of ON-type RGCs, the same pattern as response magnitudes was found, increased effect of sildenafil in latencies with extended exposure and more difficult recovery upon washout (Fig. 4.8 D).
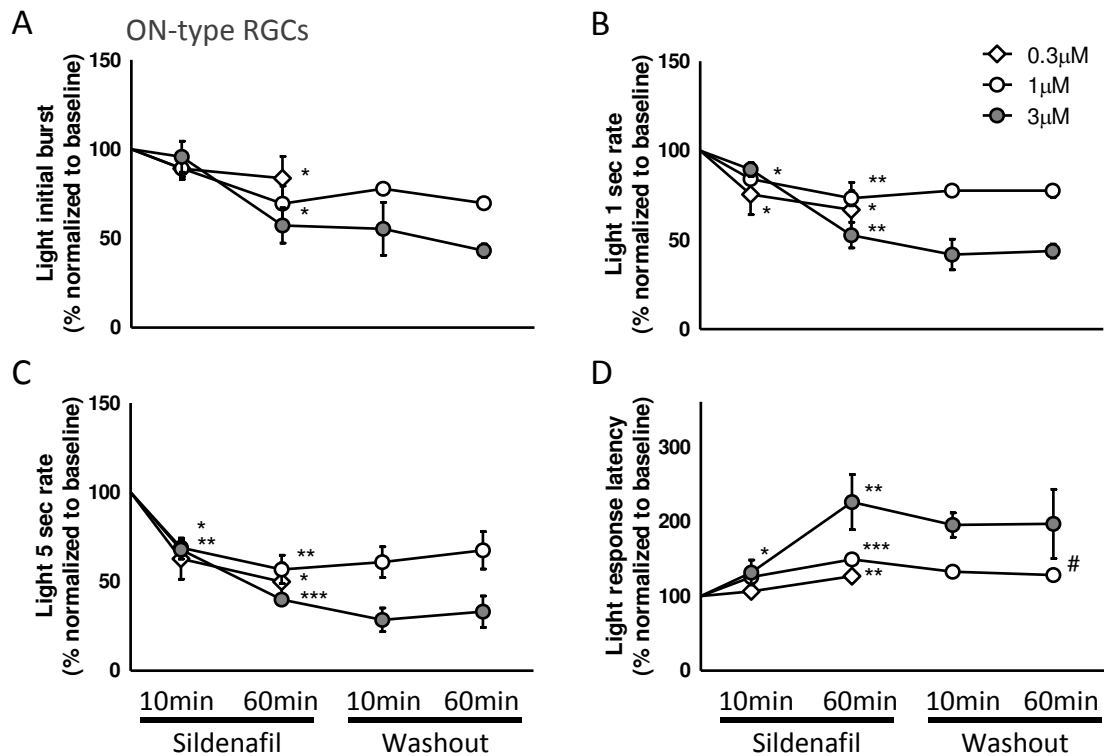
Figure 4.8. Effects of extended exposures to low concentrations of sildenafil on ON-type RGC light responses. Sildenafil application (0.3 and 3 μM) for 60 min induced a reduction of RGC responses to light onset more prominent than 10 min application (A). For initial burst (A), 1 sec (B) and 5 sec rate (C), the reduction of RGC responses were higher compared to sildenafil for 10 min. Also, the reversibility of sildenafil effect upon 60 min of washout was more difficult following 60 min of drug exposure (A-C). For the lowest concentration (0.3 μM), washout periods were not recorded. The response latencies concentration-dependently exhibited increased values after 60 min of sildenafil application (D), and although for 1 μM sildenafil there was a small but statistically significant recovery within 60 min of washout, the same was not observed for 3 μM sildenafil. All results were normalized to the baseline values before drug exposure. *p<0.05, **p<0.01, ***p<0.001, compared to baseline; #p<0.05, compared to sildenafil 60 min. Kruskal-Wallis followed by Dunn's test.

Concerning OFF-type RGCs, extended exposure (60 min) to sildenafil also potentiated the effects on response magnitudes (Fig. 4.9 A-C). For the lowest (0.3 μM) concentration used, the initial burst response was not affected even after 60 min of drug application, suggesting higher resilience of OFF-type RGCs compared to ON-type RGCs for this lowest concentration. Nevertheless, 5 sec rate (Fig. 4.9 C), but not 1 sec rate (Fig. 4.9 B), was reduced to 68.2 ± 10.7% of initial response after 60 min of 0.3 μM sildenafil application. This may be explained by natural decreased spiking activity observed during recording sessions. Nevertheless, we highlight that the initial burst to dark onset was preserved and more reliably indicates whether an OFF response is present. For concentrations of 1 and 3 μM sildenafil, for 60 min, we found a reduction to 59.6 ± 2.7% and 33.4 ± 1.7% for the initial burst, respectively (Fig. 4.9 A), and 1

113

sec and 5 sec rate (Fig. 4.9 B, C) presented similar behaviour. Although for 1 µM sildenafil concentration a small but statistically significant recovery could be found for initial burst within 60 min of washout (Fig. 4.9 A), the same was not clear for 3 µM sildenafil concentration. In addition, no recovery was observed at 1 sec and 5 sec rate for both 1 and 3 µM. In the case of response latencies of OFF-type RGCs, we found increased values after extended sildenafil exposure to 60 min. This increase reached 157.0 ± 5.1% and 312.7 ± 12.8% for 1 and 3 µM, respectively, after 60 min of sildenafil exposure (Fig. 4.9 A). A clear recovery of latencies was observed within 60 min of washout. For 1 and 3 µM sildenafil, latencies returned to 120.8 ± 5.4% and 143.2 ± 5.9% of initial response (Fig. 4.9 D). It must be noted that in ON-type RGCs the recovery from sildenafil effect was not so evident, especially after 60 min of 3 µM sildenafil application (Fig. 4.8 D).
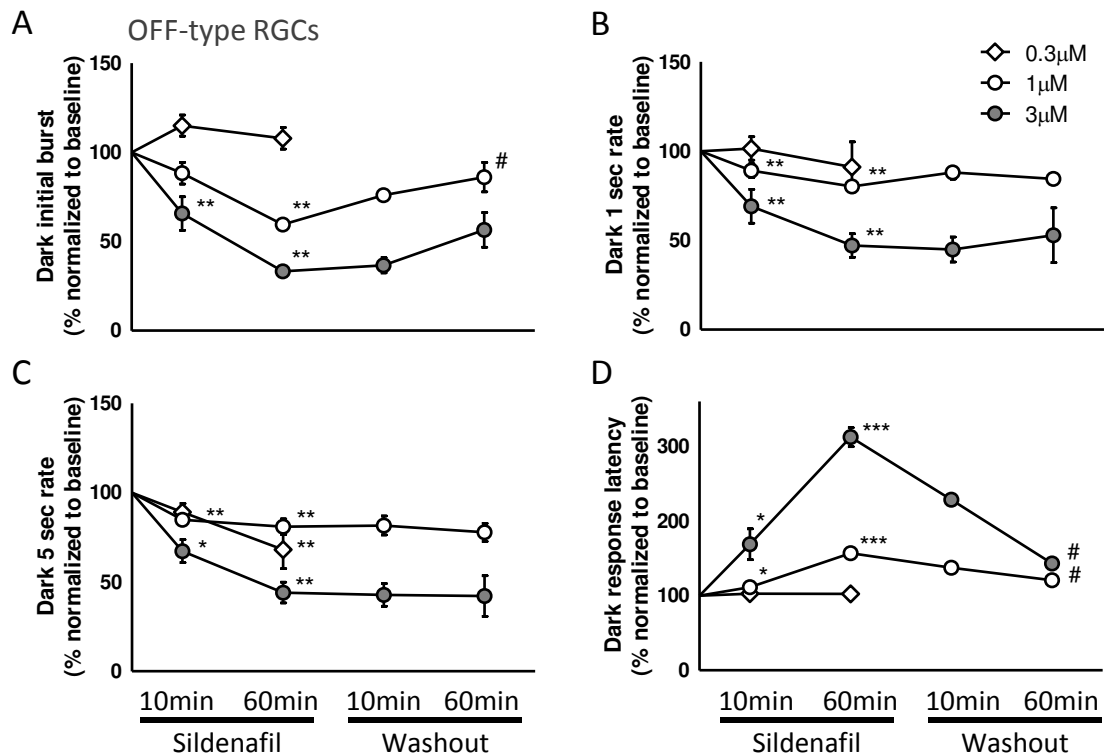
Figure 4.9. Effects of extended exposures to low concentrations of sildenafil on OFF-type RGC light responses. Sildenafil application (0.3 and 3 µM) for 60 min induced a reduction of RGC responses to dark onset more prominent comparing to 10 min application, at the level of initial burst (A), and at 1 sec (B) and 5 sec rate (C). Recovery from sildenafil effect upon 60 min of washout was seen for the initial burst (A), but no recovery was found for 1 sec (B) and 5 sec rate (C). For the lowest concentration (0.3 µM), washout periods were not recorded. The response latencies concentration dependently exhibited increased values after 60 min of sildenafil (D). However, a clear recovery of response latencies was found upon 60 min washout. All results were normalized to the baseline values before drug exposure. *$p<0.05$, **$p<0.01$, ***$p<0.001$, compared to baseline; #$p<0.05$, compared to sildenafil 60 min. Kruskal-Wallis followed by Dunn's test.

Finally, we also evaluated the effect of extended sildenafil (1 and 3 µM) exposure on RGC spontaneous activity. Although we could not assess a genuine dark adapted spontaneous activity since retinal preparations were stimulated each every 10 min to monitor RGC light responses, we quantified spontaneous spiking rates so a mixed effect of sildenafil and light stimulation could be evaluated. For both ON- and OFF-type, RGCs exhibited a small decrease upon 60 min of exposure to 1 µM sildenafil, though no dose-dependent effect was observed (Fig. 4.10 A and B). However, spontaneous activity of both ON- and OFF-type RGCs seems to be decreased after 60 min of washout although statistically significant difference was found

only for OFF-type RGCs (Fig. 4.10 B). This result may reflect a prolonged effect of sildenafil potentiated by light stimulation.
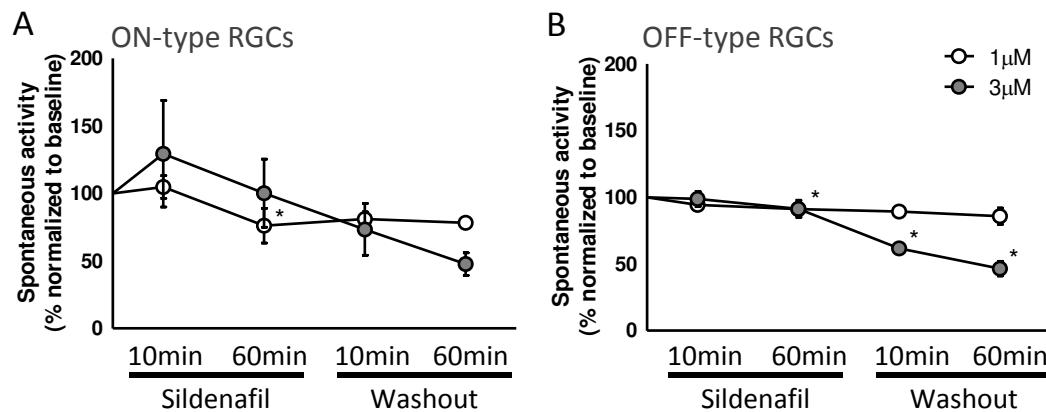
Figure 4.10. Effects of extended exposures to low concentrations of sildenafil on RGC spontaneous activity. Effect of sildenafil application (1 and 3 µM, 10 to 60 min) on the RGC spontaneous spiking activity was evaluated. RGCs were divided in ON- (A) and OFF-type (B). Spontaneous spiking rates, when detected, were normalized to the baseline values obtained before drug exposure. For both ON- and OFF-type, RGCs exhibited a small decrease for 1 µM after 60 min of sildenafil exposure, though no dose-dependent effect was observed. However, spontaneous activity of both ON- and OFF-type RGCs seems to be decreased after 60 min of washout, although statistically significant difference was found only for OFF-type RGCs (B). All results were normalized to the baseline values before drug exposure. *p<0.05, compared to baseline. Kruskal-Wallis followed by Dunn's test.

4.3 – Discussion

Our results demonstrate that sildenafil has a significant and dose-dependent effect on the retina, and in particular, on the RGCs, illustrating the critical changes occurring in RGC light response principal characteristics. These changes include a concentration-dependent decrease in magnitude and increased latency of light responses, which were partly restored during 60 min of washout. Even with low concentrations, which can be measured in human plasma (e.g. 1 μM) after sildenafil administration (Kanjanawart et al., 2011), RGC light responses showed statistically significant decreases in response magnitudes and increased latencies, in particular after prolonged drug exposure (60 min) and repetitive light stimulations. The recovery of light responses was incomplete, especially for ON RGCs even after prolonged (60 min) washout, which, for other chemicals traditionally applied to the retina, takes up to 15 min (Kolomiets et al., 2010).

Since the introduction of sildenafil as treatment for erectile dysfunction, reports of sildenafil-induced visual alterations have emerged (Laties and Zrenner, 2002). Non-arthritic ischemic optic neuropathy has been also reported in patients after sildenafil use, though a direct cause-effect has been difficult to demonstrate (Carter, 2007; Azzouni and Abu samra, 2011). Possible drug-induced modifications of retinal ganglion cell activity could contribute to an optic neuropathy. Thus, the reported transient episode of blindness could result from the complete disappearance of some ON- and OFF-type RGC light responses as observed after high (30 μM) sildenafil concentration (Fig. 4.2 and 4.3). Moderate impairments as in colour discrimination have also been reported in human volunteers after sildenafil administration. These latter transient alterations appeared to correlate with the peak of sildenafil plasma concentration and were fully reversible (Laties and Zrenner, 2002). In a trial assessing ocular safety of sildenafil use for pulmonary arterial hypertension, transient adverse events, such as chromatopsia, photophobia, and visual brightness were reported with the highest dose of 80 mg sildenafil three times daily for twelve weeks, though no permanent detrimental effect on visual function was found after such a chronic dosage of sildenafil (Wirostko et al., 2012). The above mentioned transient visual symptoms could result from the decreased or delayed RGC light responses, as we found in this study. Particularly, the RGC response latencies are known to be a key component in the transmission of spatial structure of images to visual brain centres (Gollisch and Meister, 2008).

Regarding acute sildenafil effects, studies in human and laboratory animals have yield contradictory results. Both increased and decreased light responses have been reported after sildenafil administration, especially in ERG measurements. Such apparently inconsistent results could be attributed to the atypical increase in light response magnitude followed by a decrease. For example, Barabas and colleagues found increased ERG amplitude with 1 µM sildenafil in rat retina (Barabas et al., 2003), while other authors, using bovine retinas, reported decreased a-wave and b-wave amplitudes with sildenafil concentrations as low as 0.3 µM and 0.1 µM, respectively (Luke et al., 2005). Moreover, acute ERG changes, in scotopic range, have been recorded as increased b-wave amplitudes and higher rod light sensitivity after 50 mg sildenafil ingestion in human volunteers (Gabrieli et al., 2003). Other studies found decreased visual sensitivity after 100 mg sildenafil (Stockman et al., 2007). Some of these studies have focused only on one sildenafil dose, but different doses and light stimulation paradigms were applied across these different studies such that results are difficult to compare. In the present study, we intended to evaluate the effects of sildenafil application, particularly onto RGC light responses, which was never addressed before, using various drug concentrations including low concentrations found in human plasma after sildenafil administration (1 µM) (Kanjanawart et al., 2011). In our experiments, the light responses were modified even at the lowest concentrations used (0.3 and 1 µM), whereas the RGC spontaneous activity did not display a statistically significant difference even upon application of the highest drug concentration (Fig. 4.5).

The attenuation of RGC light responses and extended time to peak/latency found in the present study (Fig. 4.6-4.9) are in accordance with previous reports showing decreased ERG amplitudes and increased implicit time in bovine and human retinas (Luke et al., 2005; Luke et al., 2007). Interestingly, we showed that extended exposure at lower concentrations together with the repetitive light stimulation potentiated the effectiveness of sildenafil-induced attenuation of light response (Fig. 4.8 and 4.9). In particular, the ON-type responses did not recover even after extended periods of washout (Fig. 4.9). The concentration of 1 µM is easily found in human plasma after sildenafil use (Kanjanawart et al., 2011). Moreover, it is possible that some patients take doses above the recommended therapeutic dose, reaching peak plasma concentration above 1 µM, particularly patients suffering from liver disease or renal dysfunction. At concentrations of 1 µM and 3 µM, although we did not find strong effects on RGC light-responses after 10 min sildenafil exposure, extending the drug exposure to 60

min, we found a suppression of the light response magnitude and delayed latencies as seen for shorter sildenafil exposure (10 min) with higher concentrations.

When measuring RGC light responses upon the 30 µM sildenafil application, there was an atypical increase in response magnitude in the first stimulus block (Fig. 4.2). However, following responses to subsequent stimuli were greatly decreased. This transient sildenafil potentiation of the light response could result from the reported increase in photoreceptor sensitivity after sildenafil (Barabas et al., 2003; Gabrieli et al., 2003). The partial sildenafil inhibition of PDE6 could have increased the photoreceptor cGMP intracellular concentration thus enlarging the photoreceptor functional dynamics. However, the maintained PDE6 inhibition would lead to a progressive increase in photoreceptor cGMP and a consequent constant photoreceptor depolarization (Zhang et al., 2005; Simon et al., 2006). Such an excessive activation of cGMP-gated channels may generate risks for the cell viability as we previously reported on retinal explants (Vallazza-Deschamps et al., 2005). This transient potentiation of the RGC light responses would be consistent with enhanced PDE6 inhibition by sildenafil upon light stimulation.

In summary, we found that sildenafil concentration-dependently attenuates RGC light responses in terms of magnitude and latencies. Moreover, these effects are potentiated by extended drug exposure and repeated light stimulation. To our knowledge, this is the first time the effects of sildenafil directly on RGC spiking activity are evaluated. The present study highlights the acute effects of sildenafil on RGC light responses, which are transmitted towards brain visual centres. These results on transient losses of light responses or, at least, magnitude decreases warn against sildenafil abuses, which could lead to more severe and irreversible long-term visual losses (Lowe and Costabile, 2011). Since sildenafil and its first metabolite UK-103,320 were identified in human post-mortem vitreous humour, suggesting that the drug can reach the retina directly (Lewis et al., 2006), understanding the acute visual alterations is needed, especially under repeated administration.

CHAPTER 5

General Discussion & Conclusions

In this study, we present evidence supporting the localization of NPY and NPY receptors in the inner retina and indicating a role for NPY system in modulation of retinal circuitry. The presence of mRNA for both NPY and NPY receptors (Y_1, Y_2, Y_4, and Y_5) detected in purified RGCs extends the findings of previous works (D'Angelo and Brecha, 2004; Alvaro et al., 2007). Regarding the immunoreactivity of NPY and NPY receptors in the rat retina, we confirmed that NPY is localized in cell bodies of amacrine cells in INL and displaced amacrine cells in GCL, which the processed extend and ramify in IPL (Oh et al., 2002). We extended the study of Y_1 and Y_2 receptor localization (Canto Soler et al., 2002; D'Angelo et al., 2002; Santos-Carvalho et al., 2013a), showing that Y_1-ir is localized to GCL and Y_2-ir is found in stratum 1 of IPL and in cell bodies of proximal INL. We also present novel evidence indicating the localization of Y_4 receptor in cell bodies of GCL, and proximal and distal INL. Concerning Y_5 receptor, immunoreactivity was detected for the first time in Müller cells. In addition to immunofluorescence data, we present further evidence showing the presence of functional active NPY receptors in the inner retina using [^{35}S]GTPγS binding assay.

We presented evidence showing an inhibitory effect of NPY on glutamate-evoked increase in [Ca^{2+}]$_i$ on purified RGCs likely through Y_1 receptor activation suggesting that NPY, released from amacrine cells (Oh et al., 2002), may activate post-synaptic Y_1 receptors on RGCs. In addition, we found that Y_1/Y_5 receptor activation induces a small increase in the initial burst response of OFF-type RGCs. This result indicates that NPY might exert modulatory effects within the circuitry generating centre-surround organization in the receptive field of RGCs, which extends previous findings in this issue by Sinclair and colleagues (Sinclair et al., 2004). Indeed, we found that Y_1 receptor activation is able to modulate directly RGC responses by attenuating the NMDA-induced increase in RGC spiking activity. Clearly, more studies are needed to clarify whether the activation of Y_1 receptors is associated to a particular RGC type or modulates a specific visual task (Gollisch and Meister, 2010).

We presented evidence supporting that NPY exerts neuroprotective effects, upon Y_1 or Y_5 receptor activation, in cultured retinal explants, confirming previous studies (Silva et al., 2003; Xapelli et al., 2007; Smialowska et al., 2009; Santos-Carvalho et al., 2013b). However, pre-treatment with NPY was not able to prevent the decrease in Brn3a-positive RGCs induced by NMDA exposure to cultured retinal explants or induced by retinal I-R injury. Therefore, further studies are needed in order to evaluate whether NPY neuroprotective effects detected in cultured retinal explants can be translated to animal models of retinal degenerative diseases.

In the second part of this work, we took advantage of MEA technique in *ex vivo* retinal preparations as an easy method to evaluate the acute effects of exogenously applied drugs on RGC activity. We found that sildenafil concentration-dependently attenuates RGC light responses. Even with low concentrations, which can be measured in human plasma (e.g. 1 µM) after sildenafil administration (Kanjanawart et al., 2011), RGC light responses showed decreased response magnitudes and increased latencies, in particular after prolonged drug exposure (60 min) and repetitive light stimulations. These results extend previous findings showing decreased ERG amplitudes and increased implicit time in bovine and human retinas (Luke et al., 2005; Luke et al., 2007). In addition, high sildenafil concentration (30 µM) induced an atypical increase in response magnitude in the first stimulus block, but not in subsequent stimuli which were greatly decreased. This transient sildenafil potentiation of the light response might result from the reported increase in photoreceptor sensitivity after sildenafil (Barabas et al., 2003; Gabrieli et al., 2003) which may be explained by increased photoreceptor cGMP intracellular concentration due to partial inhibition of PDE6 by sildenafil. Altogether, these findings contributes to the understanding of the acute visual alterations reported in patients using sildenafil.

Thus, we show that MEA recordings in *ex vivo* retinas might be a valuable method to understand how RGC circuitry, as the output signal from the retina to the brain, is affected by different drug treatments. This understanding is an important step towards the development of neuroprotective strategies aimed to halt RGC death, and needed for retinal degenerative diseases such as glaucoma.

CHAPTER 6

References

Abe M, Herzog ED, Yamazaki S, Straume M, Tei H, Sakaki Y, Menaker M, Block GD (2002) Circadian rhythms in isolated brain regions. J Neurosci 22:350-356.

Abid K, Rochat B, Lassahn PG, Stocklin R, Michalet S, Brakch N, Aubert JF, Vatansever B, Tella P, De Meester I, Grouzmann E (2009) Kinetic study of neuropeptide Y (NPY) proteolysis in blood and identification of NPY3-35: a new peptide generated by plasma kallikrein. J Biol Chem 284:24715-24724.

Acuna-Goycolea C, Tamamaki N, Yanagawa Y, Obata K, van den Pol AN (2005) Mechanisms of neuropeptide Y, peptide YY, and pancreatic polypeptide inhibition of identified green fluorescent protein-expressing GABA neurons in the hypothalamic neuroendocrine arcuate nucleus. J Neurosci 25:7406-7419.

Agasse F, Bernardino L, Kristiansen H, Christiansen SH, Ferreira R, Silva B, Grade S, Woldbye DP, Malva JO (2008) Neuropeptide Y promotes neurogenesis in murine subventricular zone. Stem Cells 26:1636-1645.

Ahmad I, Del Debbio CB, Das AV, Parameswaran S (2011) Muller glia: a promising target for therapeutic regeneration. Invest Ophthalmol Vis Sci 52:5758-5764.

Alvaro AR, Rosmaninho-Salgado J, Ambrosio AF, Cavadas C (2009) Neuropeptide Y inhibits [Ca2+]i changes in rat retinal neurons through NPY Y1, Y4, and Y5 receptors. J Neurochem 109:1508-1515.

Alvaro AR, Martins J, Araujo IM, Rosmaninho-Salgado J, Ambrosio AF, Cavadas C (2008a) Neuropeptide Y stimulates retinal neural cell proliferation--involvement of nitric oxide. J Neurochem 105:2501-2510.

Alvaro AR, Martins J, Costa AC, Fernandes E, Carvalho F, Ambrosio AF, Cavadas C (2008b) Neuropeptide Y protects retinal neural cells against cell death induced by ecstasy. Neuroscience 152:97-105.

Alvaro AR, Rosmaninho-Salgado J, Santiago AR, Martins J, Aveleira C, Santos PF, Pereira T, Gouveia D, Carvalho AL, Grouzmann E, Ambrosio AF, Cavadas C (2007) NPY in rat retina is present in neurons, in endothelial cells and also in microglial and Muller cells. Neurochem Int 50:757-763.

Ammar DA, Hughes BA, Thompson DA (1998) Neuropeptide Y and the retinal pigment epithelium: receptor subtypes, signaling, and bioelectrical responses. Invest Ophthalmol Vis Sci 39:1870-1878.

Ammar DA, Eadie DM, Wong DJ, Ma YY, Kolakowski LF, Jr., Yang-Feng TL, Thompson DA (1996) Characterization of the human type 2 neuropeptide Y receptor gene (NPY2R) and

localization to the chromosome 4q region containing the type 1 neuropeptide Y receptor gene. Genomics 38:392-398.

Arshavsky VY, Lamb TD, Pugh EN, Jr. (2002) G proteins and phototransduction. Annu Rev Physiol 64:153-187.

Azzouni F, Abu samra K (2011) Are phosphodiesterase type 5 inhibitors associated with vision-threatening adverse events? A critical analysis and review of the literature. J Sex Med 8:2894-2903.

Babilon S, Morl K, Beck-Sickinger AG (2013) Towards improved receptor targeting: anterograde transport, internalization and postendocytic trafficking of neuropeptide Y receptors. Biol Chem 394:921-936.

Bader R, Bettio A, Beck-Sickinger AG, Zerbe O (2001) Structure and dynamics of micelle-bound neuropeptide Y: comparison with unligated NPY and implications for receptor selection. J Mol Biol 305:307-329.

Balasubramanian V, Sterling P (2009) Receptive fields and functional architecture in the retina. J Physiol 587:2753-2767.

Ballard SA, Gingell CJ, Tang K, Turner LA, Price ME, Naylor AM (1998) Effects of sildenafil on the relaxation of human corpus cavernosum tissue in vitro and on the activities of cyclic nucleotide phosphodiesterase isozymes. J Urol 159:2164-2171.

Baltmr A, Duggan J, Nizari S, Salt TE, Cordeiro MF (2010) Neuroprotection in glaucoma - Is there a future role? Exp Eye Res 91:554-566.

Barabas P, Riedl Z, Kardos J (2003) Sildenafil, N-desmethyl-sildenafil and Zaprinast enhance photoreceptor response in the isolated rat retina. Neurochem Int 43:591-595.

Barkana Y, Belkin M (2004) Neuroprotection in ophthalmology: a review. Brain Res Bull 62:447-453.

Barres BA, Silverstein BE, Corey DP, Chun LL (1988) Immunological, morphological, and electrophysiological variation among retinal ganglion cells purified by panning. Neuron 1:791-803.

Bayer AU, Cook P, Brodie SE, Maag KP, Mittag T (2001) Evaluation of different recording parameters to establish a standard for flash electroretinography in rodents. Vision Res 41:2173-2185.

Beal MF, Mazurek MF, Chattha GK, Svendsen CN, Bird ED, Martin JB (1986) Neuropeptide Y immunoreactivity is reduced in cerebral cortex in Alzheimer's disease. Ann Neurol 20:282-288.

Beavo JA (1995) Cyclic nucleotide phosphodiesterases: functional implications of multiple isoforms. Physiol Rev 75:725-748.

Bedoui S, von Horsten S, Gebhardt T (2007) A role for neuropeptide Y (NPY) in phagocytosis: implications for innate and adaptive immunity. Peptides 28:373-376.

Benarroch EE (2009) Neuropeptide Y: its multiple effects in the CNS and potential clinical significance. Neurology 72:1016-1020.

Bernet F, Maubert E, Bernard J, Montel V, Dupouy JP (1994) In vitro steroidogenic effects of neuropeptide Y (NPY1-36), Y1 and Y2 receptor agonists (Leu31-Pro34 NPY, NPY18-36) and peptide YY (PYY) on rat adrenal capsule/zona glomerulosa. Regul Pept 52:187-193.

Berson DM, Dunn FA, Takao M (2002) Phototransduction by retinal ganglion cells that set the circadian clock. Science 295:1070-1073.

Bettio A, Dinger MC, Beck-Sickinger AG (2002) The neuropeptide Y monomer in solution is not folded in the pancreatic-polypeptide fold. Protein Sci 11:1834-1844.

Bitran M, Tapia W, Eugenin E, Orio P, Boric MP (1999) Neuropeptide Y induced inhibition of noradrenaline release in rat hypothalamus: role of receptor subtype and nitric oxide. Brain Res 851:87-93.

Bleakman D, Colmers WF, Fournier A, Miller RJ (1991) Neuropeptide Y inhibits Ca2+ influx into cultured dorsal root ganglion neurones of the rat via a Y2 receptor. Br J Pharmacol 103:1781-1789.

Bleakman D, Harrison NL, Colmers WF, Miller RJ (1992) Investigations into neuropeptide Y-mediated presynaptic inhibition in cultured hippocampal neurones of the rat. Br J Pharmacol 107:334-340.

Blundell TL, Pitts JE, Tickle IJ, Wood SP, Wu CW (1981) X-ray analysis (1. 4-A resolution) of avian pancreatic polypeptide: Small globular protein hormone. Proc Natl Acad Sci U S A 78:4175-4179.

Bohme I, Stichel J, Walther C, Morl K, Beck-Sickinger AG (2008) Agonist induced receptor internalization of neuropeptide Y receptor subtypes depends on third intracellular loop and C-terminus. Cell Signal 20:1740-1749.

Boolell M, Allen MJ, Ballard SA, Gepi-Attee S, Muirhead GJ, Naylor AM, Osterloh IH, Gingell C (1996) Sildenafil: an orally active type 5 cyclic GMP-specific phosphodiesterase inhibitor for the treatment of penile erectile dysfunction. Int J Impot Res 8:47-52.

Borowsky B, Walker MW, Bard J, Weinshank RL, Laz TM, Vaysse P, Branchek TA, Gerald C (1998) Molecular biology and pharmacology of multiple NPY Y5 receptor species homologs. Regul Pept 75-76:45-53.

Bruun A, Ehinger B (1993) NPY-induced neurotransmitter release from the rabbit and chicken retina. Acta Ophthalmol (Copenh) 71:590-596.

Bruun A, Tornqvist K, Ehinger B (1986) Neuropeptide Y (NPY) immunoreactive neurons in the retina of different species. Histochemistry 86:135-140.

Bruun A, Ehinger B, Ekman R (1991) Characterization of neuropeptide Y-like immunoreactivity in vertebrate retina. Exp Eye Res 53:539-543.

Bruun A, Edvinsson L, Ehinger B (1994) Neuropeptide Y inhibits adenylyl cyclase activity in rabbit retina. Acta Ophthalmol (Copenh) 72:326-331.

Bruun A, Ehinger B, Sundler F, Tornqvist K, Uddman R (1984) Neuropeptide Y immunoreactive neurons in the guinea-pig uvea and retina. Invest Ophthalmol Vis Sci 25:1113-1123.

Cannizzaro C, Tel BC, Rose S, Zeng BY, Jenner P (2003) Increased neuropeptide Y mRNA expression in striatum in Parkinson's disease. Brain Res Mol Brain Res 110:169-176.

Canto Soler MV, Gallo JE, Dodds RA, Hokfelt T, Villar MJ, Suburo AM (2002) Y1 receptor of neuropeptide Y as a glial marker in proliferative vitreoretinopathy and diseased human retina. Glia 39:320-324.

Carter JE (2007) Anterior ischemic optic neuropathy and stroke with use of PDE-5 inhibitors for erectile dysfunction: cause or coincidence? J Neurol Sci 262:89-97.

Cerda-Reverter JM, Larhammar D (2000) Neuropeptide Y family of peptides: structure, anatomical expression, function, and molecular evolution. Biochem Cell Biol 78:371-392.

Chambers AP, Woods SC (2012) The role of neuropeptide Y in energy homeostasis. Handb Exp Pharmacol:23-45.

Chen CK (2005) The vertebrate phototransduction cascade: amplification and termination mechanisms. Rev Physiol Biochem Pharmacol 154:101-121.

Chen ST, Shen CL, Wang JP, Chou LS (1999) A comparative study of neuropeptide Y-immunoreactivity in the retina of dolphin and several other mammalian species. Zoological Studies 38:416-422.

Cheung W, Guo L, Cordeiro MF (2008) Neuroprotection in glaucoma: drug-based approaches. Optom Vis Sci 85:406-416.

Chidlow G, Wood JP, Casson RJ (2007) Pharmacological neuroprotection for glaucoma. Drugs 67:725-759.

Chidlow G, Schmidt KG, Wood JP, Melena J, Osborne NN (2002) Alpha-lipoic acid protects the retina against ischemia-reperfusion. Neuropharmacology 43:1015-1025.

Colmers WF (1990) Modulation of synaptic transmission in hippocampus by neuropeptide Y: presynaptic actions. Ann N Y Acad Sci 611:206-218.

Cone RA (1964) The Rat Electroretinogram. I. Contrasting Effects of Adaptation on the Amplitude and Latency of the B-Wave. J Gen Physiol 47:1089-1105.

Conlon JM, Larhammar D (2005) The evolution of neuroendocrine peptides. Gen Comp Endocrinol 142:53-59.

Cordell WH, Maturi RK, Costigan TM, Marmor MF, Weleber RG, Coupland SG, Danis RP, McGettigan JW, Jr., Antoszyk AN, Klise S, Sides GD (2009) Retinal effects of 6 months of daily use of tadalafil or sildenafil. Arch Ophthalmol 127:367-373.

Croce N, Dinallo V, Ricci V, Federici G, Caltagirone C, Bernardini S, Angelucci F (2011) Neuroprotective effect of neuropeptide Y against beta-amyloid 25-35 toxicity in SH-SY5Y neuroblastoma cells is associated with increased neurotrophin production. Neurodegener Dis 8:300-309.

Croce N, Ciotti MT, Gelfo F, Cortelli S, Federici G, Caltagirone C, Bernardini S, Angelucci F (2012) Neuropeptide Y protects rat cortical neurons against beta-amyloid toxicity and re-establishes synthesis and release of nerve growth factor. ACS Chem Neurosci 3:312-318.

D'Angelo I, Brecha NC (2004) Y2 receptor expression and inhibition of voltage-dependent Ca2+ influx into rod bipolar cell terminals. Neuroscience 125:1039-1049.

D'Angelo I, Oh SJ, Chun MH, Brecha NC (2002) Localization of neuropeptide Y1 receptor immunoreactivity in the rat retina and the synaptic connectivity of Y1 immunoreactive cells. J Comp Neurol 454:373-382.

Dacey DM (1999) Primate retina: cell types, circuits and color opponency. Prog Retin Eye Res 18:737-763.

Damiola F, Le Minh N, Preitner N, Kornmann B, Fleury-Olela F, Schibler U (2000) Restricted feeding uncouples circadian oscillators in peripheral tissues from the central pacemaker in the suprachiasmatic nucleus. Genes Dev 14:2950-2961.

Darby K, Eyre HJ, Lapsys N, Copeland NG, Gilbert DJ, Couzens M, Antonova O, Sutherland GR, Jenkins NA, Herzog H (1997) Assignment of the Y4 receptor gene (PPYR1) to human chromosome 10q11.2 and mouse chromosome 14. Genomics 46:513-515.

Decressac M, Barker RA (2012) Neuropeptide Y and its role in CNS disease and repair. Exp Neurol 238:265-272.

Decressac M, Pain S, Chabeauti PY, Frangeul L, Thiriet N, Herzog H, Vergote J, Chalon S, Jaber M, Gaillard A (2012) Neuroprotection by neuropeptide Y in cell and animal models of Parkinson's disease. Neurobiol Aging 33:2125-2137.

DeVries SH, Baylor DA (1995) An alternative pathway for signal flow from rod photoreceptors to ganglion cells in mammalian retina. Proc Natl Acad Sci U S A 92:10658-10662.

Dhingra A, Sulaiman P, Xu Y, Fina ME, Veh RW, Vardi N (2008) Probing neurochemical structure and function of retinal ON bipolar cells with a transgenic mouse. J Comp Neurol 510:484-496.

Dimitrijevic M, Stanojevic S (2013) The intriguing mission of neuropeptide Y in the immune system. Amino Acids 45:41-53.

Domin H, Kajta M, Smialowska M (2006) Neuroprotective effects of MTEP, a selective mGluR5 antagonists and neuropeptide Y on the kainate-induced toxicity in primary neuronal cultures. Pharmacol Rep 58:846-858.

Dores RM, Rubin DA, Quinn TW (1996) Is it possible to construct phylogenetic trees using polypeptide hormone sequences? Gen Comp Endocrinol 103:1-12.

Dumont Y, Fournier A, Quirion R (1998) Expression and characterization of the neuropeptide Y Y5 receptor subtype in the rat brain. J Neurosci 18:5565-5574.

Dun Y, Thangaraju M, Prasad P, Ganapathy V, Smith SB (2007) Prevention of excitotoxicity in primary retinal ganglion cells by (+)-pentazocine, a sigma receptor-1 specific ligand. Invest Ophthalmol Vis Sci 48:4785-4794.

El Bahh B, Cao JQ, Beck-Sickinger AG, Colmers WF (2002) Blockade of neuropeptide Y(2) receptors and suppression of NPY's anti-epileptic actions in the rat hippocampal slice by BIIE0246. Br J Pharmacol 136:502-509.

Endoh T, Nobushima H, Tazaki M (2012) Neuropeptide Y modulates calcium channels in hamster submandibular ganglion neurons. Neurosci Res 73:275-281.

Eva C, Keinanen K, Monyer H, Seeburg P, Sprengel R (1990) Molecular cloning of a novel G protein-coupled receptor that may belong to the neuropeptide receptor family. FEBS Lett 271:81-84.

Ewald DA, Sternweis PC, Miller RJ (1988) Guanine nucleotide-binding protein Go-induced coupling of neuropeptide Y receptors to Ca2+ channels in sensory neurons. Proc Natl Acad Sci U S A 85:3633-3637.

Ferreira R, Xapelli S, Santos T, Silva AP, Cristovao A, Cortes L, Malva JO (2010) Neuropeptide Y modulation of interleukin-1{beta} (IL-1{beta})-induced nitric oxide production in microglia. J Biol Chem 285:41921-41934.

Ferreira R, Santos T, Viegas M, Cortes L, Bernardino L, Vieira OV, Malva JO (2011) Neuropeptide Y inhibits interleukin-1beta-induced phagocytosis by microglial cells. J Neuroinflammation 8:169.

Ferriero DM, Sagar SM (1989) Development of neuropeptide Y-immunoreactive neurons in the rat retina. Brain Res Dev Brain Res 48:19-26.

Foresta C, Caretta N, Zuccarello D, Poletti A, Biagioli A, Caretti L, Galan A (2008) Expression of the PDE5 enzyme on human retinal tissue: new aspects of PDE5 inhibitors ocular side effects. Eye (Lond) 22:144-149.

Fredriksson R, Larson ET, Yan YL, Postlethwait JH, Larhammar D (2004) Novel neuropeptide Y Y2-like receptor subtype in zebrafish and frogs supports early vertebrate chromosome duplications. J Mol Evol 58:106-114.

Funkelstein L, Toneff T, Hwang SR, Reinheckel T, Peters C, Hook V (2008) Cathepsin L participates in the production of neuropeptide Y in secretory vesicles, demonstrated by protease gene knockout and expression. J Neurochem 106:384-391.

Funkelstein L, Lu WD, Koch B, Mosier C, Toneff T, Taupenot L, O'Connor DT, Reinheckel T, Peters C, Hook V (2012) Human cathepsin V protease participates in production of enkephalin and NPY neuropeptide neurotransmitters. J Biol Chem 287:15232-15241.

Gabrieli C, Regine F, Vingolo EM, Rispoli E, Isidori A (2003) Acute electroretinographic changes during sildenafil (Viagra) treatment for erectile dysfunction. Doc Ophthalmol 107:111-114.

Gabrieli CB, Regine F, Vingolo EM, Rispoli E, Fabbri A, Isidori A (2001) Subjective visual halos after sildenafil (Viagra) administration: Electroretinographic evaluation. Ophthalmology 108:877-881.

Gavrieli Y, Sherman Y, Ben-Sasson SA (1992) Identification of programmed cell death in situ via specific labeling of nuclear DNA fragmentation. J Cell Biol 119:493-501.

Gerald C, Walker MW, Criscione L, Gustafson EL, Batzl-Hartmann C, Smith KE, Vaysse P, Durkin MM, Laz TM, Linemeyer DL, Schaffhauser AO, Whitebread S, Hofbauer KG, Taber RI,

Branchek TA, Weinshank RL (1996) A receptor subtype involved in neuropeptide-Y-induced food intake. Nature 382:168-171.

Geringer CC, Imami NR (2008) Medical management of glaucoma. Int Ophthalmol Clin 48:115-141.

Ghofrani HA, Osterloh IH, Grimminger F (2006) Sildenafil: from angina to erectile dysfunction to pulmonary hypertension and beyond. Nat Rev Drug Discov 5:689-702.

Gollisch T, Meister M (2008) Rapid neural coding in the retina with relative spike latencies. Science 319:1108-1111.

Gollisch T, Meister M (2010) Eye smarter than scientists believed: neural computations in circuits of the retina. Neuron 65:150-164.

Goodyear E, Levin LA (2008) Model systems for experimental studies: retinal ganglion cells in culture. Prog Brain Res 173:279-284.

Gregor P, Feng Y, DeCarr LB, Cornfield LJ, McCaleb ML (1996) Molecular characterization of a second mouse pancreatic polypeptide receptor and its inactivated human homologue. J Biol Chem 271:27776-27781.

Grundemar L, Wahlestedt C, Reis DJ (1991) Neuropeptide Y acts at an atypical receptor to evoke cardiovascular depression and to inhibit glutamate responsiveness in the brainstem. J Pharmacol Exp Ther 258:633-638.

Grynkiewicz G, Poenie M, Tsien RY (1985) A new generation of Ca2+ indicators with greatly improved fluorescence properties. J Biol Chem 260:3440-3450.

Haack M, Beck-Sickinger AG (2009) Towards understanding the free and receptor bound conformation of neuropeptide Y by fluorescence resonance energy transfer studies. Chem Biol Drug Des 73:573-583.

Hack I, Peichl L, Brandstatter JH (1999) An alternative pathway for rod signals in the rodent retina: rod photoreceptors, cone bipolar cells, and the localization of glutamate receptors. Proc Natl Acad Sci U S A 96:14130-14135.

Hansel DE, Eipper BA, Ronnett GV (2001) Neuropeptide Y functions as a neuroproliferative factor. Nature 410:940-944.

Harrison C, Traynor JR (2003) The [35S]GTPgammaS binding assay: approaches and applications in pharmacology. Life Sci 74:489-508.

Hartwick AT, Hamilton CM, Baldridge WH (2008) Glutamatergic calcium dynamics and deregulation of rat retinal ganglion cells. J Physiol 586:3425-3446.

Hartwick AT, Lalonde MR, Barnes S, Baldridge WH (2004) Adenosine A1-receptor modulation of glutamate-induced calcium influx in rat retinal ganglion cells. Invest Ophthalmol Vis Sci 45:3740-3748.

Hastings JA, McClure-Sharp JM, Morris MJ (2001) NPY Y1 receptors exert opposite effects on corticotropin releasing factor and noradrenaline overflow from the rat hypothalamus in vitro. Brain Res 890:32-37.

Hastings JA, Morris MJ, Lambert G, Lambert E, Esler M (2004) NPY and NPY Y1 receptor effects on noradrenaline overflow from the rat brain in vitro. Regul Pept 120:107-112.

Hattar S, Liao HW, Takao M, Berson DM, Yau KW (2002) Melanopsin-containing retinal ganglion cells: architecture, projections, and intrinsic photosensitivity. Science 295:1065-1070.

Haverkamp S, Wassle H (2000) Immunocytochemical analysis of the mouse retina. J Comp Neurol 424:1-23.

Heilig M (2004) The NPY system in stress, anxiety and depression. Neuropeptides 38:213-224.

Hernandez M, Urcola JH, Vecino E (2008) Retinal ganglion cell neuroprotection in a rat model of glaucoma following brimonidine, latanoprost or combined treatments. Exp Eye Res 86:798-806.

Herzog H, Baumgartner M, Vivero C, Selbie LA, Auer B, Shine J (1993) Genomic organization, localization, and allelic differences in the gene for the human neuropeptide Y Y1 receptor. J Biol Chem 268:6703-6707.

Higgs MH, Lukasiewicz PD (1999) Glutamate uptake limits synaptic excitation of retinal ganglion cells. J Neurosci 19:3691-3700.

Hirabayashi A, Nishiwaki K, Shimada Y, Ishikawa N (1996) Role of neuropeptide Y and its receptor subtypes in neurogenic pulmonary edema. Eur J Pharmacol 296:297-305.

Hirsch D, Zukowska Z (2012) NPY and stress 30 years later: the peripheral view. Cell Mol Neurobiol 32:645-659.

Hiscock J, Straznicky C (1989) Neuropeptide Y-like immunoreactive amacrine cells in the retina of Bufo marinus. Brain Res 494:55-64.

Hiscock J, Straznicky C (1990) Neuropeptide Y- and substance P-like immunoreactive amacrine cells in the retina of the developing Xenopus laevis. Brain Res Dev Brain Res 54:105-113.

Hook VY, Schiller MR, Azaryan AV (1996) The processing proteases prohormone thiol protease, PC1/3 and PC2, and 70-kDa aspartic proteinase show preferences among

proenkephalin, proneuropeptide Y, and proopiomelanocortin substrates. Arch Biochem Biophys 328:107-114.

Hoon M, Okawa H, Della Santina L, Wong RO (2014) Functional architecture of the retina: Development and disease. Prog Retin Eye Res.

Hu Y, Cho S, Goldberg JL (2010) Neurotrophic effect of a novel TrkB agonist on retinal ganglion cells. Invest Ophthalmol Vis Sci 51:1747-1754.

Hu Y, Bloomquist BT, Cornfield LJ, DeCarr LB, Flores-Riveros JR, Friedman L, Jiang P, Lewis-Higgins L, Sadlowski Y, Schaefer J, Velazquez N, McCaleb ML (1996) Identification of a novel hypothalamic neuropeptide Y receptor associated with feeding behavior. J Biol Chem 271:26315-26319.

Hutsler JJ, Chalupa LM (1994) Neuropeptide Y immunoreactivity identifies a regularly arrayed group of amacrine cells within the cat retina. J Comp Neurol 346:481-489.

Hutsler JJ, Chalupa LM (1995) Development of neuropeptide Y immunoreactive amacrine and ganglion cells in the pre- and postnatal cat retina. J Comp Neurol 361:152-164.

Hutsler JJ, White CA, Chalupa LM (1993) Neuropeptide Y immunoreactivity identifies a group of gamma-type retinal ganglion cells in the cat. J Comp Neurol 336:468-480.

Ishikawa M, Yoshitomi T, Zorumski CF, Izumi Y (2010) Effects of acutely elevated hydrostatic pressure in a rat ex vivo retinal preparation. Invest Ophthalmol Vis Sci 51:6414-6423.

Jagle H, Jagle C, Serey L, Sharpe LT (2005) Dose-dependency and time-course of electrophysiologic short-term effects of VIAGRA: a case study. Doc Ophthalmol 110:247-254.

Jagle H, Jagle C, Serey L, Yu A, Rilk A, Sadowski B, Besch D, Zrenner E, Sharpe LT (2004) Visual short-term effects of Viagra: double-blind study in healthy young subjects. Am J Ophthalmol 137:842-849.

Jen PY, Li WW, Yew DT (1994) Immunohistochemical localization of neuropeptide Y and somatostatin in human fetal retina. Neuroscience 60:727-735.

Johnson JE, Barde YA, Schwab M, Thoenen H (1986) Brain-derived neurotrophic factor supports the survival of cultured rat retinal ganglion cells. J Neurosci 6:3031-3038.

Jotwani G, Itoh K, Wadhwa S (1994) Immunohistochemical localization of tyrosine hydroxylase, substance P, neuropeptide-Y and leucine-enkephalin in developing human retinal amacrine cells. Brain Res Dev Brain Res 77:285-289.

Kang WS, Lim MY, Lee EJ, Kim IB, Oh SJ, Brecha NC, Park CB, Chun MH (2001) Light- and electron-microscopic analysis of neuropeptide Y-immunoreactive amacrine cells in the guinea pig retina. Cell Tissue Res 306:363-371.

Kanjanawart S, Gaysonsiri D, Tangsucharit P, Vannaprasaht S, Phunikhom K, Kaewkamson T, Wattanachai N, Tassaneeyakul W (2011) Comparative bioavailability of two sildenafil tablet formulations after single-dose administration in healthy Thai male volunteers. Int J Clin Pharmacol Ther 49:525-530.

Kapin MA, Doshi R, Scatton B, DeSantis LM, Chandler ML (1999) Neuroprotective effects of eliprodil in retinal excitotoxicity and ischemia. Invest Ophthalmol Vis Sci 40:1177-1182.

Keffel S, Schmidt M, Bischoff A, Michel MC (1999) Neuropeptide-Y stimulation of extracellular signal-regulated kinases in human erythroleukemia cells. J Pharmacol Exp Ther 291:1172-1178.

Kerkerian-Le Goff L, Forni C, Samuel D, Bloc A, Dusticier N, Nieoullon A (1992) Intracerebroventricular administration of neuropeptide Y affects parameters of dopamine, glutamate and GABA activities in the rat striatum. Brain Res Bull 28:187-193.

Khor EC, Baldock P (2012) The NPY system and its neural and neuroendocrine regulation of bone. Curr Osteoporos Rep 10:160-168.

Kikuchi M, Tenneti L, Lipton SA (2000) Role of p38 mitogen-activated protein kinase in axotomy-induced apoptosis of rat retinal ganglion cells. J Neurosci 20:5037-5044.

Kolb H (1995) Neurotransmitters in the Retina. In: Webvision: The Organization of the Retina and Visual System (Kolb H, Fernandez E, Nelson R, eds). Salt Lake City (UT).

Kolomiets B, Dubus E, Simonutti M, Rosolen S, Sahel JA, Picaud S (2010) Late histological and functional changes in the P23H rat retina after photoreceptor loss. Neurobiol Dis 38:47-58.

Koob GF (2008) A role for brain stress systems in addiction. Neuron 59:11-34.

Kovac S, Megalogeni M, Walker M (2011) In vitro effects of neuropeptide Y in rat neocortical and hippocampal tissue. Neurosci Lett 492:43-46.

Lagreze WA, Knorle R, Bach M, Feuerstein TJ (1998) Memantine is neuroprotective in a rat model of pressure-induced retinal ischemia. Invest Ophthalmol Vis Sci 39:1063-1066.

Lamb TD (2013) Evolution of phototransduction, vertebrate photoreceptors and retina. Prog Retin Eye Res 36:52-119.

Larhammar D, Salaneck E (2004) Molecular evolution of NPY receptor subtypes. Neuropeptides 38:141-151.

Larhammar D, Bergqvist CA (2013) Ancient Grandeur of the Vertebrate Neuropeptide Y System Shown by the Coelacanth Latimeria chalumnae. Front Neurosci 7:27.

Larhammar D, Sundstrom G, Dreborg S, Daza DO, Larsson TA (2009) Major genomic events and their consequences for vertebrate evolution and endocrinology. Ann N Y Acad Sci 1163:201-208.

Larsson TA, Olsson F, Sundstrom G, Lundin LG, Brenner S, Venkatesh B, Larhammar D (2008) Early vertebrate chromosome duplications and the evolution of the neuropeptide Y receptor gene regions. BMC Evol Biol 8:184.

Laties A, Zrenner E (2002) Viagra (sildenafil citrate) and ophthalmology. Prog Retin Eye Res 21:485-506.

Le Rouëdec D, Rayner K, Rex M, Wigmore PM, Scotting PJ (2002) The transcription factor cSox2 and Neuropeptide Y define a novel subgroup of amacrine cells in the retina. J Anat 200:51-56.

Lee NJ, Herzog H (2009) NPY regulation of bone remodelling. Neuropeptides 43:457-463.

Lerch M, Mayrhofer M, Zerbe O (2004) Structural similarities of micelle-bound peptide YY (PYY) and neuropeptide Y (NPY) are related to their affinity profiles at the Y receptors. J Mol Biol 339:1153-1168.

Lerch M, Gafner V, Bader R, Christen B, Folkers G, Zerbe O (2002) Bovine pancreatic polypeptide (bPP) undergoes significant changes in conformation and dynamics upon binding to DPC micelles. J Mol Biol 322:1117-1133.

Lewis RJ, Johnson RD, Blank CL (2006) Quantitative determination of sildenafil (Viagra) and its metabolite (UK-103,320) in fluid and tissue specimens obtained from six aviation fatalities. J Anal Toxicol 30:14-20.

Linnertz R, Wurm A, Pannicke T, Krugel K, Hollborn M, Hartig W, Iandiev I, Wiedemann P, Reichenbach A, Bringmann A (2011) Activation of voltage-gated Na(+) and Ca(2)(+) channels is required for glutamate release from retinal glial cells implicated in cell volume regulation. Neuroscience 188:23-34.

Lowe G, Costabile R (2011) Phosphodiesterase type 5 inhibitor abuse: a critical review. Curr Drug Abuse Rev 4:87-94.

Lu C, Everhart L, Tilan J, Kuo L, Sun CC, Munivenkatappa RB, Jonsson-Rylander AC, Sun J, Kuan-Celarier A, Li L, Abe K, Zukowska Z, Toretsky JA, Kitlinska J (2010) Neuropeptide Y and its Y2 receptor: potential targets in neuroblastoma therapy. Oncogene 29:5630-5642.

Luke M, Szurman P, Schneider T, Luke C (2007) The effects of the phosphodiesterase type V inhibitor sildenafil on human and bovine retinal function in vitro. Graefes Arch Clin Exp Ophthalmol 245:1211-1215.

Luke M, Luke C, Hescheler J, Schneider T, Sickel W (2005) Effects of phosphodiesterase type 5 inhibitor sildenafil on retinal function in isolated superfused retina. J Ocul Pharmacol Ther 21:305-314.

Lundell I, Berglund MM, Starback P, Salaneck E, Gehlert DR, Larhammar D (1997) Cloning and characterization of a novel neuropeptide Y receptor subtype in the zebrafish. DNA Cell Biol 16:1357-1363.

Lundell I, Blomqvist AG, Berglund MM, Schober DA, Johnson D, Statnick MA, Gadski RA, Gehlert DR, Larhammar D (1995) Cloning of a human receptor of the NPY receptor family with high affinity for pancreatic polypeptide and peptide YY. J Biol Chem 270:29123-29128.

Luu JK, Chappelow AV, McCulley TJ, Marmor MF (2001) Acute effects of sildenafil on the electroretinogram and multifocal electroretinogram. Am J Ophthalmol 132:388-394.

Lynch DR, Walker MW, Miller RJ, Snyder SH (1989) Neuropeptide Y receptor binding sites in rat brain: differential autoradiographic localizations with 125I-peptide YY and 125I-neuropeptide Y imply receptor heterogeneity. J Neurosci 9:2607-2619.

Main CM, Wilhelm M, Gabriel R (1993) Colocalization of GABA-immunoreactivity in neuropeptide- and monoamine-containing amacrine cells in the retina of Bufo marinus. Arch Histol Cytol 56:161-166.

Malva JO, Xapelli S, Baptista S, Valero J, Agasse F, Ferreira R, Silva AP (2012) Multifaces of neuropeptide Y in the brain--neuroprotection, neurogenesis and neuroinflammation. Neuropeptides 46:299-308.

Masland RH (2001) Neuronal diversity in the retina. Curr Opin Neurobiol 11:431-436.

Mathieu M, Tagliafierro G, Bruzzone F, Vallarino M (2002) Neuropeptide tyrosine-like immunoreactive system in the brain, olfactory organ and retina of the zebrafish, Danio rerio, during development. Brain Res Dev Brain Res 139:255-265.

Matsumoto M, Nomura T, Momose K, Ikeda Y, Kondou Y, Akiho H, Togami J, Kimura Y, Okada M, Yamaguchi T (1996) Inactivation of a novel neuropeptide Y/peptide YY receptor gene in primate species. J Biol Chem 271:27217-27220.

Medeiros MdS, Turner AJ (1996) Metabolism and functions of neuropeptide Y. Neurochem Res 21:1125-1132.

Meister M, Pine J, Baylor DA (1994) Multi-neuronal signals from the retina: acquisition and analysis. J Neurosci Methods 51:95-106.

Michel MC, Rascher W (1995) Neuropeptide Y: a possible role in hypertension? J Hypertens 13:385-395.

Michel MC, Beck-Sickinger A, Cox H, Doods HN, Herzog H, Larhammar D, Quirion R, Schwartz T, Westfall T (1998) XVI. International Union of Pharmacology recommendations for the nomenclature of neuropeptide Y, peptide YY, and pancreatic polypeptide receptors. Pharmacol Rev 50:143-150.

Milenkovic I, Weick M, Wiedemann P, Reichenbach A, Bringmann A (2004) Neuropeptide Y-evoked proliferation of retinal glial (Muller) cells. Graefes Arch Clin Exp Ophthalmol 242:944-950.

Millar BC, Weis T, Piper HM, Weber M, Borchard U, McDermott BJ, Balasubramaniam A (1991) Positive and negative contractile effects of neuropeptide Y on ventricular cardiomyocytes. Am J Physiol 261:H1727-1733.

Minth CD, Bloom SR, Polak JM, Dixon JE (1984) Cloning, characterization, and DNA sequence of a human cDNA encoding neuropeptide tyrosine. Proc Natl Acad Sci U S A 81:4577-4581.

Minthon L, Edvinsson L, Ekman R, Gustafson L (1990) Neuropeptide levels in Alzheimer's disease and dementia with frontotemporal degeneration. J Neural Transm Suppl 30:57-67.

Montani D, Gunther S, Dorfmuller P, Perros F, Girerd B, Garcia G, Jais X, Savale L, Artaud-Macari E, Price LC, Humbert M, Simonneau G, Sitbon O (2013) Pulmonary arterial hypertension. Orphanet J Rare Dis 8:97.

Montastruc JL, Bagheri H, Gardette V, Durrieu G, Olivier P (2006) Actualites 2006 de Pharmacovigilance. Service de Pharmacologie Clinique, Centre Midi-Pyrénées de PharmacoVigilance, de Pharmacoépidémiologie et d'Informations sur le Médicament, Faculty of Medicine of Toulouse.

Moore RY, Card JP (1990) Neuropeptide Y in the circadian timing system. Ann N Y Acad Sci 611:247-257.

Morin LP, Allen CN (2006) The circadian visual system, 2005. Brain Res Rev 51:1-60.

Morris JL (1999) Cotransmission from sympathetic vasoconstrictor neurons to small cutaneous arteries in vivo. Am J Physiol 277:H58-64.

Morrison JC, Moore CG, Deppmeier LM, Gold BG, Meshul CK, Johnson EC (1997) A rat model of chronic pressure-induced optic nerve damage. Exp Eye Res 64:85-96.

Motulsky HJ, Michel MC (1988) Neuropeptide Y mobilizes Ca2+ and inhibits adenylate cyclase in human erythroleukemia cells. Am J Physiol 255:E880-885.

Muske LE, Dockray GJ, Chohan KS, Stell WK (1987) Segregation of FMRF amide-immunoreactive efferent fibers from NPY-immunoreactive amacrine cells in goldfish retina. Cell Tissue Res 247:299-307.

Nadal-Nicolas FM, Jimenez-Lopez M, Salinas-Navarro M, Sobrado-Calvo P, Alburquerque-Bejar JJ, Vidal-Sanz M, Agudo-Barriuso M (2012) Whole number, distribution and co-expression of brn3 transcription factors in retinal ganglion cells of adult albino and pigmented rats. PLoS One 7:e49830.

Nadal-Nicolas FM, Jimenez-Lopez M, Sobrado-Calvo P, Nieto-Lopez L, Canovas-Martinez I, Salinas-Navarro M, Vidal-Sanz M, Agudo M (2009) Brn3a as a marker of retinal ganglion cells: qualitative and quantitative time course studies in naive and optic nerve-injured retinas. Invest Ophthalmol Vis Sci 50:3860-3868.

Nadler JV, Tu B, Timofeeva O, Jiao Y, Herzog H (2007) Neuropeptide Y in the recurrent mossy fiber pathway. Peptides 28:357-364.

Nakajima Y, Iwakabe H, Akazawa C, Nawa H, Shigemoto R, Mizuno N, Nakanishi S (1993) Molecular characterization of a novel retinal metabotropic glutamate receptor mGluR6 with a high agonist selectivity for L-2-amino-4-phosphonobutyrate. J Biol Chem 268:11868-11873.

Nash MS, Wood JP, Melena J, Osborne NN (2000) Flupirtine ameliorates ischaemic-like death of rat retinal ganglion cells by preventing calcium influx. Brain Res 856:236-239.

Nie M, Selbie LA (1998) Neuropeptide Y Y1 and Y2 receptor-mediated stimulation of mitogen-activated protein kinase activity. Regul Pept 75-76:207-213.

Oh SJ, D'Angelo I, Lee EJ, Chun MH, Brecha NC (2002) Distribution and synaptic connectivity of neuropeptide Y-immunoreactive amacrine cells in the rat retina. J Comp Neurol 446:219-234.

Osborne NN (2009) Recent clinical findings with memantine should not mean that the idea of neuroprotection in glaucoma is abandoned. Acta Ophthalmol 87:450-454.

Osborne NN, Patel S, Terenghi G, Allen JM, Polak JM, Bloom SR (1985) Neuropeptide Y (NPY)-like immunoreactive amacrine cells in retinas of frog and goldfish. Cell Tissue Res 241:651-656.

Osborne NN, Casson RJ, Wood JP, Chidlow G, Graham M, Melena J (2004) Retinal ischemia: mechanisms of damage and potential therapeutic strategies. Prog Retin Eye Res 23:91-147.

Pang IH, Wexler EM, Nawy S, DeSantis L, Kapin MA (1999) Protection by eliprodil against excitotoxicity in cultured rat retinal ganglion cells. Invest Ophthalmol Vis Sci 40:1170-1176.

Paredes MF, Greenwood J, Baraban SC (2003) Neuropeptide Y modulates a G protein-coupled inwardly rectifying potassium current in the mouse hippocampus. Neurosci Lett 340:9-12.

Parker RM, Herzog H (1999) Regional distribution of Y-receptor subtype mRNAs in rat brain. Eur J Neurosci 11:1431-1448.

Peng PH, Chao HM, Juan SH, Chen CF, Liu JH, Ko ML (2011) Pharmacological preconditioning by low dose cobalt protoporphyrin induces heme oxygenase-1 overexpression and alleviates retinal ischemia-reperfusion injury in rats. Curr Eye Res 36:238-246.

Perney TM, Miller RJ (1989) Two different G-proteins mediate neuropeptide Y and bradykinin-stimulated phospholipid breakdown in cultured rat sensory neurons. J Biol Chem 264:7317-7327.

Pirone A, Lenzi C, Marroni P, Betti L, Mascia G, Giannaccini G, Lucacchini A, Fabiani O (2008) Neuropeptide Y in the brain and retina of the adult teleost gilthead seabream (Sparus aurata L.). Anat Histol Embryol 37:231-240.

Prod'homme T, Weber MS, Steinman L, Zamvil SS (2006) A neuropeptide in immune-mediated inflammation, Y? Trends Immunol 27:164-167.

Quigley HA, Broman AT (2006) The number of people with glaucoma worldwide in 2010 and 2020. Br J Ophthalmol 90:262-267.

Quigley HA, Addicks EM, Green WR, Maumenee AE (1981) Optic nerve damage in human glaucoma. II. The site of injury and susceptibility to damage. Arch Ophthalmol 99:635-649.

Rose JB, Crews L, Rockenstein E, Adame A, Mante M, Hersh LB, Gage FH, Spencer B, Potkar R, Marr RA, Masliah E (2009) Neuropeptide Y fragments derived from neprilysin processing are neuroprotective in a transgenic model of Alzheimer's disease. J Neurosci 29:1115-1125.

Rose PM, Fernandes P, Lynch JS, Frazier ST, Fisher SM, Kodukula K, Kienzle B, Seethala R (1995) Cloning and functional expression of a cDNA encoding a human type 2 neuropeptide Y receptor. J Biol Chem 270:22661-22664.

Rosmaninho-Salgado J, Araujo IM, Alvaro AR, Duarte EP, Cavadas C (2007) Intracellular signaling mechanisms mediating catecholamine release upon activation of NPY Y1 receptors in mouse chromaffin cells. J Neurochem 103:896-903.

Rosmaninho-Salgado J, Cortez V, Estrada M, Santana MM, Goncalves A, Marques AP, Cavadas C (2012) Intracellular mechanisms coupled to NPY Y2 and Y5 receptor activation and lipid accumulation in murine adipocytes. Neuropeptides 46:359-366.

Rosmaninho-Salgado J, Araujo IM, Alvaro AR, Mendes AF, Ferreira L, Grouzmann E, Mota A, Duarte EP, Cavadas C (2009) Regulation of catecholamine release and tyrosine hydroxylase in human adrenal chromaffin cells by interleukin-1beta: role of neuropeptide Y and nitric oxide. J Neurochem 109:911-922.

Rosolen SG, Rigaudiere F, Le Gargasson JF, Brigell MG (2005) Recommendations for a toxicological screening ERG procedure in laboratory animals. Doc Ophthalmol 110:57-66.

Rosolen SG, Kolomiets B, Varela O, Picaud S (2008) Retinal electrophysiology for toxicology studies: applications and limits of ERG in animals and ex vivo recordings. Exp Toxicol Pathol 60:17-32.

Ruan GX, Zhang DQ, Zhou T, Yamazaki S, McMahon DG (2006) Circadian organization of the mammalian retina. Proc Natl Acad Sci U S A 103:9703-9708.

Salonia A, Rigatti P, Montorsi F (2003) Sildenafil in erectile dysfunction: a critical review. Curr Med Res Opin 19:241-262.

Santos-Carvalho A, Aveleira CA, Elvas F, Ambrosio AF, Cavadas C (2013a) Neuropeptide Y receptors Y1 and Y2 are present in neurons and glial cells in rat retinal cells in culture. Invest Ophthalmol Vis Sci 54:429-443.

Santos-Carvalho A, Elvas F, Alvaro AR, Ambrosio AF, Cavadas C (2013b) Neuropeptide Y receptors activation protects rat retinal neural cells against necrotic and apoptotic cell death induced by glutamate. Cell Death Dis 4:e636.

Santos-Carvalho A, Alvaro AR, Martins J, Ambrosio AF, Cavadas C (2014) Emerging novel roles of neuropeptide Y in the retina: from neuromodulation to neuroprotection. Prog Neurobiol 112:70-79.

Sappington RM, Chan M, Calkins DJ (2006) Interleukin-6 protects retinal ganglion cells from pressure-induced death. Invest Ophthalmol Vis Sci 47:2932-2942.

Sappington RM, Carlson BJ, Crish SD, Calkins DJ (2010) The microbead occlusion model: a paradigm for induced ocular hypertension in rats and mice. Invest Ophthalmol Vis Sci 51:207-216.

Schuettauf F, Naskar R, Vorwerk CK, Zurakowski D, Dreyer EB (2000) Ganglion cell loss after optic nerve crush mediated through AMPA-kainate and NMDA receptors. Invest Ophthalmol Vis Sci 41:4313-4316.

Shareef SR, Garcia-Valenzuela E, Salierno A, Walsh J, Sharma SC (1995) Chronic ocular hypertension following episcleral venous occlusion in rats. Exp Eye Res 61:379-382.

Shaw JL, Gackenheimer SL, Gehlert DR (2003) Functional autoradiography of neuropeptide Y Y1 and Y2 receptor subtypes in rat brain using agonist stimulated [35S]GTPgammaS binding. J Chem Neuroanat 26:179-193.

Shen Y, Liu XL, Yang XL (2006) N-methyl-D-aspartate receptors in the retina. Mol Neurobiol 34:163-179.

Shimada K, Ohno Y, Okamatsu-Ogura Y, Suzuki M, Kamikawa A, Terao A, Kimura K (2012) Neuropeptide Y activates phosphorylation of ERK and STAT3 in stromal vascular cells from brown adipose tissue, but fails to affect thermogenic function of brown adipocytes. Peptides 34:336-342.

Silva AP, Cavadas C, Grouzmann E (2002) Neuropeptide Y and its receptors as potential therapeutic drug targets. Clin Chim Acta 326:3-25.

Silva AP, Carvalho AP, Carvalho CM, Malva JO (2001) Modulation of intracellular calcium changes and glutamate release by neuropeptide Y1 and Y2 receptors in the rat hippocampus: differential effects in CA1, CA3 and dentate gyrus. J Neurochem 79:286-296.

Silva AP, Xapelli S, Grouzmann E, Cavadas C (2005) The putative neuroprotective role of neuropeptide Y in the central nervous system. Curr Drug Targets CNS Neurol Disord 4:331-347.

Silva AP, Pinheiro PS, Carvalho AP, Carvalho CM, Jakobsen B, Zimmer J, Malva JO (2003) Activation of neuropeptide Y receptors is neuroprotective against excitotoxicity in organotypic hippocampal slice cultures. FASEB J 17:1118-1120.

Simon A, Barabas P, Kardos J (2006) Structural determinants of phosphodiesterase 6 response on binding catalytic site inhibitors. Neurochem Int 49:215-222.

Sinclair JR, Nirenberg S (2001) Characterization of neuropeptide Y-expressing cells in the mouse retina using immunohistochemical and transgenic techniques. J Comp Neurol 432:296-306.

Sinclair JR, Jacobs AL, Nirenberg S (2004) Selective ablation of a class of amacrine cells alters spatial processing in the retina. J Neurosci 24:1459-1467.

Siu TL, Morley JW, Coroneo MT (2008) Toxicology of the retina: advances in understanding the defence mechanisms and pathogenesis of drug- and light-induced retinopathy. Clin Experiment Ophthalmol 36:176-185.

Smialowska M, Wieronska JM, Szewczyk B (2003) Neuroprotective effect of NPY on kainate neurotoxicity in the hippocampus. Pol J Pharmacol 55:979-986.

Smialowska M, Domin H, Zieba B, Kozniewska E, Michalik R, Piotrowski P, Kajta M (2009) Neuroprotective effects of neuropeptide Y-Y2 and Y5 receptor agonists in vitro and in vivo. Neuropeptides 43:235-249.

Sohn JW, Elmquist JK, Williams KW (2013) Neuronal circuits that regulate feeding behavior and metabolism. Trends Neurosci 36:504-512.

Sosulina L, Schwesig G, Seifert G, Pape HC (2008) Neuropeptide Y activates a G-protein-coupled inwardly rectifying potassium current and dampens excitability in the lateral amygdala. Mol Cell Neurosci 39:491-498.

Soucy E, Wang Y, Nirenberg S, Nathans J, Meister M (1998) A novel signaling pathway from rod photoreceptors to ganglion cells in mammalian retina. Neuron 21:481-493.

Sperk G, Hamilton T, Colmers WF (2007) Neuropeptide Y in the dentate gyrus. Prog Brain Res 163:285-297.

Stockman A, Sharpe LT, Tufail A, Kell PD, Ripamonti C, Jeffery G (2007) The effect of sildenafil citrate (Viagra) on visual sensitivity. J Vis 7:4.

Storch KF, Paz C, Signorovitch J, Raviola E, Pawlyk B, Li T, Weitz CJ (2007) Intrinsic circadian clock of the mammalian retina: importance for retinal processing of visual information. Cell 130:730-741.

Straznicky C, Hiscock J (1989) Neuropeptide Y-like immunoreactivity in neurons of the human retina. Vision Res 29:1041-1048.

Subhedar N, Cerda J, Wallace RA (1996) Neuropeptide Y in the forebrain and retina of the killifish, Fundulus heteroclitus. Cell Tissue Res 283:313-323.

Sun L, Miller RJ (1999) Multiple neuropeptide Y receptors regulate K+ and Ca2+ channels in acutely isolated neurons from the rat arcuate nucleus. J Neurophysiol 81:1391-1403.

Sun QQ, Huguenard JR, Prince DA (2001) Neuropeptide Y receptors differentially modulate G-protein-activated inwardly rectifying K+ channels and high-voltage-activated Ca2+ channels in rat thalamic neurons. J Physiol 531:67-79.

Sun QQ, Baraban SC, Prince DA, Huguenard JR (2003) Target-specific neuropeptide Y-ergic synaptic inhibition and its network consequences within the mammalian thalamus. J Neurosci 23:9639-9649.

Tatemoto K (1982) Neuropeptide Y: complete amino acid sequence of the brain peptide. Proc Natl Acad Sci U S A 79:5485-5489.

Tatemoto K, Carlquist M, Mutt V (1982) Neuropeptide Y--a novel brain peptide with structural similarities to peptide YY and pancreatic polypeptide. Nature 296:659-660.

Thoreson WB, Witkovsky P (1999) Glutamate receptors and circuits in the vertebrate retina. Prog Retin Eye Res 18:765-810.

Tornqvist K, Ehinger B (1988) Peptide immunoreactive neurons in the human retina. Invest Ophthalmol Vis Sci 29:680-686.

Tosini G, Pozdeyev N, Sakamoto K, Iuvone PM (2008) The circadian clock system in the mammalian retina. Bioessays 30:624-633.

Toth PT, Bindokas VP, Bleakman D, Colmers WF, Miller RJ (1993) Mechanism of presynaptic inhibition by neuropeptide Y at sympathetic nerve terminals. Nature 364:635-639.

Tu B, Jiao Y, Herzog H, Nadler JV (2006) Neuropeptide Y regulates recurrent mossy fiber synaptic transmission less effectively in mice than in rats: Correlation with Y2 receptor plasticity. Neuroscience 143:1085-1094.

Twig G, Levy H, Perlman I (2003) Color opponency in horizontal cells of the vertebrate retina. Prog Retin Eye Res 22:31-68.

Uckermann O, Wolf A, Kutzera F, Kalisch F, Beck-Sickinger AG, Wiedemann P, Reichenbach A, Bringmann A (2006) Glutamate release by neurons evokes a purinergic inhibitory mechanism of osmotic glial cell swelling in the rat retina: activation by neuropeptide Y. J Neurosci Res 83:538-550.

Vallazza-Deschamps G, Cia D, Gong J, Jellali A, Duboc A, Forster V, Sahel JA, Tessier LH, Picaud S (2005) Excessive activation of cyclic nucleotide-gated channels contributes to neuronal degeneration of photoreceptors. Eur J Neurosci 22:1013-1022.

Vatansever HS, Kayikcioglu O, Gumus B (2003) Histopathologic effect of chronic use of sildenafil citrate on the choroid & retina in male rats. Indian J Med Res 117:211-215.

Verstappen A, Van Reeth O, Vaudry H, Pelletier G, Vanderhaeghen JJ (1986) Demonstration of a neuropeptide Y (NPY)-like immunoreactivity in the pigeon retina. Neurosci Lett 70:193-197.

Vezzani A, Sperk G (2004) Overexpression of NPY and Y2 receptors in epileptic brain tissue: an endogenous neuroprotective mechanism in temporal lobe epilepsy? Neuropeptides 38:245-252.

Vobig MA, Klotz T, Staak M, Bartz-Schmidt KU, Engelmann U, Walter P (1999) Retinal side-effects of sildenafil. Lancet 353:375.

Walther C, Morl K, Beck-Sickinger AG (2011) Neuropeptide Y receptors: ligand binding and trafficking suggest novel approaches in drug development. J Pept Sci 17:233-246.

Wang SJ (2005) Activation of neuropeptide Y Y1 receptors inhibits glutamate release through reduction of voltage-dependent Ca2+ entry in the rat cerebral cortex nerve terminals: suppression of this inhibitory effect by the protein kinase C-dependent facilitatory pathway. Neuroscience 134:987-1000.

Wassle H (2004) Parallel processing in the mammalian retina. Nat Rev Neurosci 5:747-757.

Wassle H, Boycott BB (1991) Functional architecture of the mammalian retina. Physiol Rev 71:447-480.

Weinberg DH, Sirinathsinghji DJ, Tan CP, Shiao LL, Morin N, Rigby MR, Heavens RH, Rapoport DR, Bayne ML, Cascieri MA, Strader CD, Linemeyer DL, MacNeil DJ (1996) Cloning and expression of a novel neuropeptide Y receptor. J Biol Chem 271:16435-16438.

Westheimer G (2007) The ON-OFF dichotomy in visual processing: from receptors to perception. Prog Retin Eye Res 26:636-648.

Wheway J, Herzog H, Mackay F (2007) The Y1 receptor for NPY: a key modulator of the adaptive immune system. Peptides 28:453-458.

Whitaker CM, Cooper NG (2009) The novel distribution of phosphodiesterase-4 subtypes within the rat retina. Neuroscience 163:1277-1291.

Widmaier EP, Raff H, Strang KT (2004) Vander, Sherman, Luciano's Human physiology: the mechanisms of body function. 9th edition. McGraw-Hill:825 pp.

Wier WG, Zang WJ, Lamont C, Raina H (2009) Sympathetic neurogenic Ca2+ signalling in rat arteries: ATP, noradrenaline and neuropeptide Y. Exp Physiol 94:31-37.

Winterdahl M, Audrain H, Landau AM, Smith DF, Bonaventure P, Shoblock JR, Carruthers N, Swanson D, Bender D (2014) PET brain imaging of neuropeptide Y2 receptors using N-11C-methyl-JNJ-31020028 in pigs. J Nucl Med 55:635-639.

Winzeler A, Wang JT (2013) Purification and culture of retinal ganglion cells from rodents. Cold Spring Harb Protoc 2013:643-652.

Wirostko BM, Tressler C, Hwang LJ, Burgess G, Laties AM (2012) Ocular safety of sildenafil citrate when administered chronically for pulmonary arterial hypertension: results from phase III, randomised, double masked, placebo controlled trial and open label extension. BMJ 344:e554.

Wolak ML, DeJoseph MR, Cator AD, Mokashi AS, Brownfield MS, Urban JH (2003) Comparative distribution of neuropeptide Y Y1 and Y5 receptors in the rat brain by using immunohistochemistry. J Comp Neurol 464:285-311.

Woldbye DP, Kokaia M (2004) Neuropeptide Y and seizures: effects of exogenously applied ligands. Neuropeptides 38:253-260.

Wu YF, Li SB (2005) Neuropeptide Y expression in mouse hippocampus and its role in neuronal excitotoxicity. Acta Pharmacol Sin 26:63-68.

Xapelli S, Silva AP, Ferreira R, Malva JO (2007) Neuropeptide Y can rescue neurons from cell death following the application of an excitotoxic insult with kainate in rat organotypic hippocampal slice cultures. Peptides 28:288-294.

Xapelli S, Agasse F, Ferreira R, Silva AP, Malva JO (2006) Neuropeptide Y as an endogenous antiepileptic, neuroprotective and pro-neurogenic peptide. Recent Pat CNS Drug Discov 1:315-324.

Xapelli S, Bernardino L, Ferreira R, Grade S, Silva AP, Salgado JR, Cavadas C, Grouzmann E, Poulsen FR, Jakobsen B, Oliveira CR, Zimmer J, Malva JO (2008) Interaction between neuropeptide Y (NPY) and brain-derived neurotrophic factor in NPY-mediated neuroprotection against excitotoxicity: a role for microglia. Eur J Neurosci 27:2089-2102.

Xiong Z, Cheung DW (1995) ATP-Dependent inhibition of Ca2+-activated K+ channels in vascular smooth muscle cells by neuropeptide Y. Pflugers Arch 431:110-116.

Yannielli P, Harrington ME (2004) Let there be "more" light: enhancement of light actions on the circadian system through non-photic pathways. Prog Neurobiol 74:59-76.

Yoon HZ, Yan Y, Geng Y, Higgins RD (2002) Neuropeptide Y expression in a mouse model of oxygen-induced retinopathy. Clin Experiment Ophthalmol 30:424-429.

Zhang X, Feng Q, Cote RH (2005) Efficacy and selectivity of phosphodiesterase-targeted drugs in inhibiting photoreceptor phosphodiesterase (PDE6) in retinal photoreceptors. Invest Ophthalmol Vis Sci 46:3060-3066.

Zhang Z, Qin X, Zhao X, Tong N, Gong Y, Zhang W, Wu X (2012) Valproic acid regulates antioxidant enzymes and prevents ischemia/reperfusion injury in the rat retina. Curr Eye Res 37:429-437.

Zhu BS, Gibbins I (1995) Synaptic circuitry of neuropeptide-containing amacrine cells in the retina of the cane toad, Bufo marinus. Vis Neurosci 12:919-927.

Zhu BS, Gibbins I (1996) Muller cells in the retina of the cane toad, Bufo marinus, express neuropeptide Y-like immunoreactivity. Vis Neurosci 13:501-508.

Zoumalan CI, Zamanian RT, Doyle RL, Marmor MF (2009) ERG evaluation of daily, high-dose sildenafil usage. Doc Ophthalmol 118:225-231.